Putative Biomarkers of Neuro-restoration in the CNS

by

Sharmilee Gnanapavan

2013

A thesis submitted to University College London for the degree of

Doctor of Philosophy

Department of Neuroimmunology

Institute of Neurology

Queen Square

London WC1N 3BG

Abstract

The aim of this work was to investigate putative biomarkers of neuronal plasticity and repair in the central nervous system. The effects of different disease processes, such as inflammation, demyelination and neurodegeneration were explored.

We developed and validated ELISA-based assays for the quantification of neural cell adhesion molecule (NCAM) and growth-associated protein (GAP)-43, two known facilitators of neuronal outgrowth in the nervous system. NCAM isoforms in biological samples were characterised using mass spectrometry. Soluble NCAM was measured in *in-vitro* and *in-vivo* models of inflammation/demyelination and neurodegeneration, and across different neurological disorders in the CSF to understand the impact of inflammation and axonal loss on its levels. Recombinant GAP-43 was produced using baculovirus technology and purified in appreciable amounts for use in a new ELISA. Soluble GAP-43 levels were quantified across different neurological disorders in the CSF. Values for CSF NCAM and GAP-43 were correlated with clinical outcome measures.

CSF NCAM demonstrated a restricted pattern of expression compared to that of serum whilst GAP-43 is almost exclusively expressed in the CSF, indicating that these biomarkers are intrathecally synthesised. CSF NCAM and GAP-43 levels were lower in neurological disorders with prominent axonal injury; multiple sclerosis, movement disorders, motor neurone disease, Alzheimer's disease and meningitis. In vitro neuronal cell culture model and in vivo experimental

autoimmune encephalomyelitis studies demonstrate that CSF NCAM correlates well with disease progression in multiple sclerosis. A similar relationship was not found with CSF GAP-43.

In conclusion, the adult CNS may possess the intrinsic capacity to repair, but this capacity may be dramatically reduced in disease states. Measuring this process may be important in understanding neuronal repair and plasticity.

Table of contents

List of Figures

List of Tables

Abbreviations

ACN	- Acetonitrile
AD	- Alzheimer’s disease
ALB	- Albumin
ANOVA	- Analysis of variance
BBB	- Blood brain barrier
BDNF	- Brain-derived neurotrophic factor
BDWG	- Biomarkers Definition Working Group
BIH	- Benign intracranial hypertension
BionMS-*eu*	- European biomarkers in multiple sclerosis consortium
CAMs	- Cell adhesion molecules
CI	- Cognitive impairement
CNS	- Central nervous system
CONSORT	- Consolidated standards of reporting trials
CSF	- Cerebrospinal fluid
CSPGs	- Chondroitin sulfate proteoglycans
CST	- Corticospinal tract
CV	- Coefficient of variation
DCX	- Doublecortin
DTT	- Dithiothreitol
EAE	- Experimental autoimmune encephalomyelitis
ECM	- Extracellular matrix
EDSS	- Expanded disability status scale
ELISA	- Enzyme linked immunosorbent assay
ESI-QTOF MS	- Electrospray ionisation time-of-flight mass spectrometry
FDA	- Food and drug administration
FK506	- Tacrolimus
GAP-43	- Growth associated protein-43
GDNF	- Glial-derived neurotrophic factor
GPI	- Glycosyl-phospatidylinositol
HRP	- Horseradish peroxidase
HSPGs	- Heparan sulfate proteoglycans
IgG	- Immunoglobulin G
KCL	- Potassium chloride

LDS	- Lithium dodecyl sulfate
MAG	- Myelin-associated glycoprotein
MND	- Motorneurone disease
MOG	- Myelin oligodendrocyte protein
MRI	- Magnetic resonance imaging
MS	- Multiple sclerosis
NaCl	- Sodium chloride
NCAM	- Neural cell adhesion molecule
NG2	- Neuron-glia antigen
NGF	- Nerve growth factor
NT	- Neurotrophin
OMgp	- Oligodendrocyte-myelin glycoprotein
PNS	- Phosphate buffered saline
PD	- Parkinson's disease
PLGS	- Proteinlynx global server
PNS	- Peripheral nervous system
PPMS	- Primary progressive MS
PSA-NCAM	- Polysialylated-NCAM
REMARK	- Reporting recommendations for tumour marker prognostic studies
RRMS	- Relapsing remitting MS
SD	- Standard deviation
SDS-PAGE	- Sodium dodecyl sulfate polyacrylamide gel electrophoresis
SELDI-TOF MS	- Surface-enhanced laser desorption/ionization mass spectrometry
SGZ	- Subgranular zone
SPA	- Sinapinic acid
SPMS	- Secondary progressive MS
STARD	- Standards for the reporting of diagnostic accuracy studies
SVX	- Subventricular zone
TMB	- 3, 3', 5, 5'-Tetramethylbenzidine
TFA	- Trifluoroacetic acid
TNFα	- Tumour necrosis factor α
VASE	- Variable alternative spliced exon

Acknowledgments

I would like to express my sincere gratitude to all those who gave me the opportunity and support to complete this thesis. I am deeply indebted to my supervisors Professor Gavin Giovannoni and Dr Geoff Keir who gave me the confidence and freedom to try out new ideas without losing sight of the end, whose stimulating suggestions and encouragement have helped me in the research and writing of this thesis.

Parts of the thesis were carried out under the direction of Professor Yuti Chernajovsy and Dr Nasim Yousaf (baculovirus expression and purification of recombinant GAP-43, QMUL), Dr Kevin Mills and Dr Wendy Heywood (proteomic studies of NCAM and recombinant GAP-43, ICH), Professor Lawrence Steinmann and Dr Peggy Ho (animal models SJL and C57BL/6 for NCAM, Stanford), Professor David Baker and Dr Sam Jackson (neuronal culture model for NCAM, QMUL) and the BioMS-*eu* consortium (reporting guidelines), without their help none of this would have been possible.

Special thanks to my friends and colleagues from the Neuroimmunology Department, Queen Square (Drs Miles Chapman, Andrew Church, Viki Worthington and Ms Donna Grant and Jan Alsop) who have been invaluable in all their comments and insights, encouragement and camaraderie.

The Promise 2010 campaign: nervous system repair and protection, an initiative of the National Multiple Sclerosis Society (USA), was the principal sponsor of this project providing salary and equipment costs. Their commitment allowed

me meet others of like minds, learn more about the world and reach the conclusion that research is more than simply a sum of its parts or our powers of scientific reasoning.

And last but not least I would like to thank Dr Mailvaganam Gnanapavan and Mrs Vasanthi Gnanapavan, for always being my parents, supporting me in my career path and helping me find my way through its challenges.

1 General Introduction

1.1 Neurodegenerative diseases: a failure of plasticity and repair?

The mechanisms of how physiological regulation of neuronal death and repair or plasticity is maintained in the central nervous system (CNS) and importantly the transition to pathological neurodegeneration, represent central questions in neuroscience. Evidence suggests that neurodegeneration occurs in two ways: 1) primary degenerative events caused for example by a failure in neuroaxonal health owing to a variety of contributory factors, such as extracellular accumulation of amyloid-beta protein in Alzheimer's disease (AD) [1; 2] and intracellular alpha-synuclein inclusions in Parkinson's disease (PD) [3; 4], or 2) secondary neurodegeneration following trauma or chronic inflammation resulting in axonal transection and Wallerian degeneration, when compensatory mechanisms fail, classically observed in conditions such as multiple sclerosis (MS) [5] and spinal cord injury [6]. In both paradigms the problem remains that neurones which are lost in this manner in the adult CNS are unlikely to be replaced and recovery is largely dependent on the redundancy in the system as well as its capacity for repair [7; 8], posing the question whether neurodegeneration is in fact a failure of plasticity and repair?

In fact neuronal death and survival represent one of the fundamental facets of brain homeostasis, and although continued neuronal loss is a hallmark of neurodegenerative disorders and senescence the extent to which functional

impairments correlate directly with neuronal loss is controversial. For instance, T2 lesion load on MRI correlate poorly with disability in MS [9]. Furthermore, pre-clinical AD cases resemble mild AD cases pathologically but do not manifest cognitive impairment or decline on standard neuropsychometric testing [10]. Granted, peak clinical performance at later stages of disease is capped by the loss of neurones, but there remain striking fluctuations in functional abilities that patients experience over time during their illnesses [11]. Whether this perceived neurological impairment is in fact neurological dysfunction rather than neuronal loss or modified by plasticity is difficult to establish, and it is this inability to reconcile the myriad of factors involved in disease pathophysiology that has prevented the formulation of a unified theory on disease progression which remains speculative at present [8; 12].

Neuronal damage almost always triggers compensatory mechanisms and neuroplasticity is a generic term referring to processes involved in the structural and functional adaptation of the organism to the environment, experience, attrition and injury [13]. At a molecular level this comprises of alterations in dendritic ramifications, axonal sprouting, synaptic remodelling, synaptogensis and neurogenesis [14]. Barriers to neuroplasticity, loss of plasticity and maladaptive plasticity-related cellular events have been postulated as initiators of neurodegeneration in both AD [15] and MS [8]. In MS the damaging inflammatory pathways also triggers regulatory mechanisms that promote tissue repair. For instance, pro-inflammatory cytokines interleukin 1β and interferon γ promote *in-situ* apoptosis of encephalitogenic T cells, while TNFα (via TNFRII) stimulates remyelination by directing the differentiation and proliferation of myelin-forming cells. Encephalitogenic CD4 T cells produce neurotrophic factors including

BDNF, neurotrophins 3 and 4/5, while antimyelin antibodies stimulate oligodendrocyte proliferation, and macrophages/microglia phagocytise myelin debris thereby promoting remyelination [8; 16; 17]. However, these counter regulatory anti-inflammatory mechanisms become blunted over time, which may be due to a decrease in neuroplasticity due to ageing of the repair mechanisms themselves. It is postulated that the efficiency of remyelination decreases with age; Sim *et al*. [18] demonstrate a delay in oligodendrocyte precursor recruitment and differentiation in old mice compared to young mice. Following axotomy, pronounced axonal sprouting proximal to the injury was found only in young mice lacking Nogo A/B (myelin-derived axon growth inhibitor) with a restriction at the older ages [19]. Whilst older growth cones of axons are repelled during regrowth compared to their younger counterparts owing to a decline in growth cone responsiveness to external stimuli [20]. Clinical presentations of neurodegenerative disorders parallel that of experimental data with most neurodegenerative disorders becoming apparent in adult life, for example AD, MS and PD, likely explaining why age is the single most important risk factor for AD. In AD the magnitude and rate of compensatory synaptogenesis following injury and the ability to sustain the effects of long-term potentiation (LTP) are all slowed or decline progressively with age [21; 22]. It is therefore conceivable that the physiological cellular plasticity is responsible for alleviating or altering symptoms, but may also contribute to the symptoms of neurodegeneration through an inability to stimulate repair effectively in an aged environment.

This argument does not hold true if you are a stroke patient, however, who despite their advanced age, show recovery in function up to a year after the event. Analysis of human stroke tissue demonstrated evidence of early

neuronal markers doublecortin (DCX) and β-III tubulin in the ischaemic penumbra indicating at least in stroke there is a viable endogenous repair mechanism [23]. Equally, rodent models in stroke show proliferation of cells within the known neurogenic zones, the subgranular zone (SGZ) and the subventricular zone (SVZ) and migration of newborn neurones into the ischaemic brain regions [24; 25]. The acute nature of the insult may be relevant, whereas neurodegenerative disease processes normally gather momentum over time heightening the burden on neuroplasticity. So again, the idea that neurodegeneration may in fact be a counterpart of neuroplasticity warrants consideration.

1.1.1 The CNS axon and its response to injury

Spontaneous repair in the adult CNS, in comparison with the peripheral nervous system (PNS) or the embryonic nervous system, does not occur as a rule [26; 27]. In addition, the glial environment of the adult CNS is more likely to be an additional barrier to axonal regrowth than to provide assistance [28; 29]. Despite this permanency in regeneration failure, it has long been recognised that there are also variable degrees of compensatory plasticity within lesioned pathways. Three distinct types of axonal sprouting have been described following injury; regenerative sprouting, collateral sprouting and compensatory sprouting, which may occasionally lead to partial recovery of the original function (Figure 1-1) [30]. Regenerative sprouting refers to the formation of new axonal processes at the site of injury shortly after transaction; this has always been an abortive process owing to the inhibitory CNS environment and a lack of guidance cues involved in axonal pathfinding. Collateral sprouting is sprouting from unlesioned

neighbouring fibres into the synaptic space formerly occupied by the transected axon. Whereas, compensatory sprouting is the formation of new axonal sprouts from the injured axon proximal to the lesion towards neurones neighbouring the denervated area.

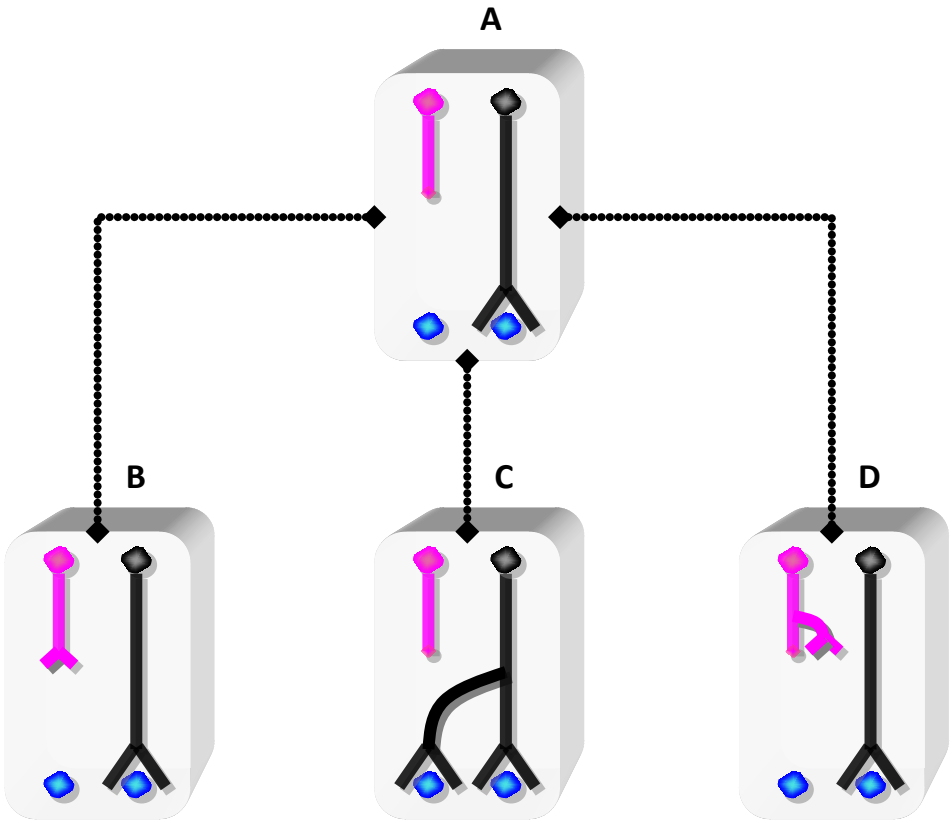

Figure 1-1 Modes of control of axonal regneration following injury to the adult CNS. A) A lesioned axon is separated from its original target (on the left). B) Regenerative sprouting involves the growth of an axon that has been interrupted but does not lead to reconnection with the original target. C) Collateral sprouting involves growth of additional presynaptic arbors from somewhere along an existing undamaged axon. D) Compensatory sprouting involves the formation of additional collaterals above the level of lesioned axon that acts to increase the density of innervations targets rostral to the site of injury.

Axonal sprouting and pathfinding is mediated by the growth cone, the motile tip of the growing axon, and is known to be guided by at least four mechanisms: 1) contact-mediated attraction, 2) chemo-attraction, 3) contact-mediated repulsion,

and 4) chemorepulsion (Figure 1-2) [31]. A relatively limited set of guidance molecules exist, including the neural cell adhesion molecule immunoglobulin

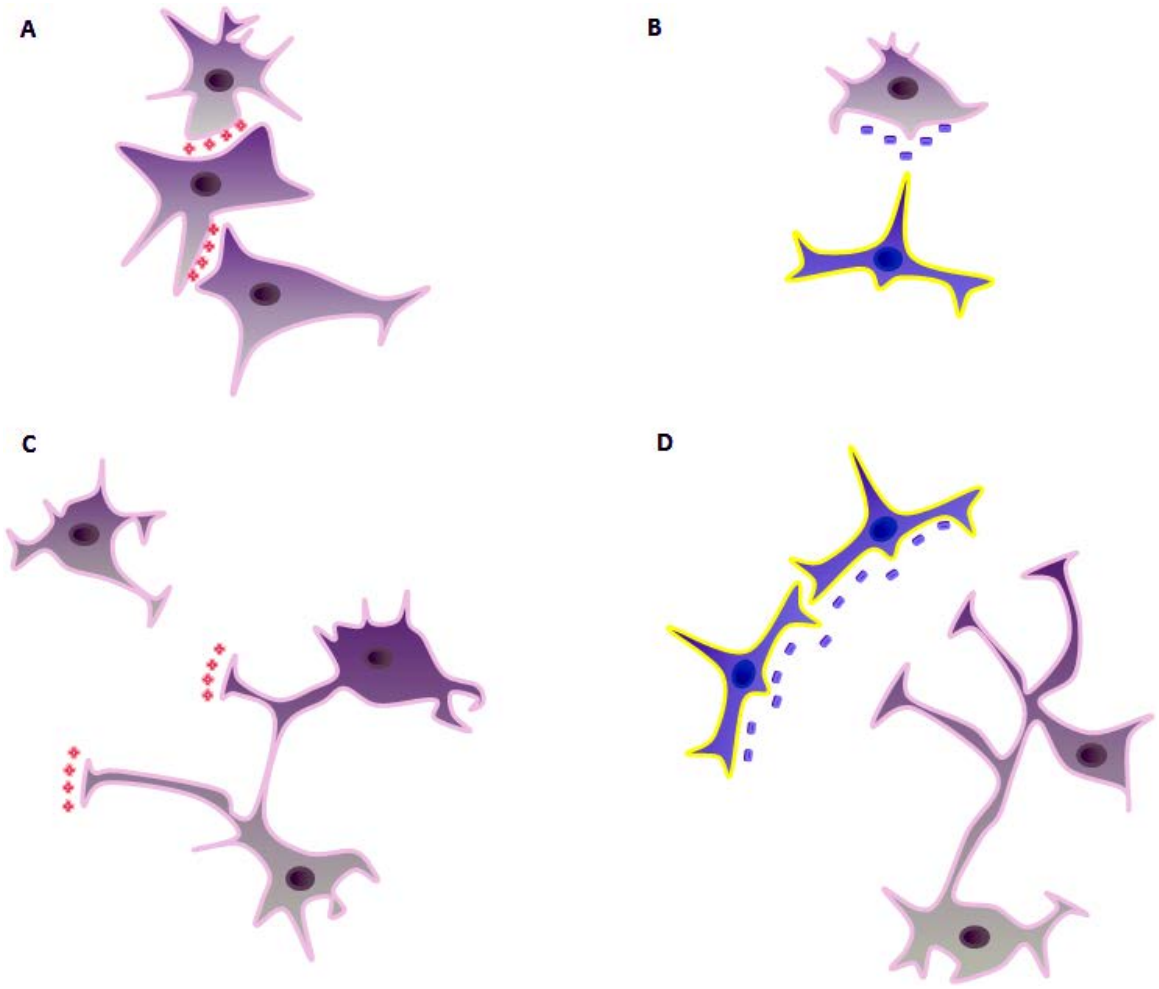

Figure 1-2 Proposed roles of neural recognition molecules in growth cone guidance. A) Contact-mediated attraction over short-range requiring direct cell-cell or cell-substratum contact. B) Contact-mediated repulsion over short-range requiring direct cell-cell or cell-substratum contact. C) Chemo-attraction over long-range as a result of diffusible factors. D) Chemorepulsion over long-range as a result of diffusible factors.

superfamily (CAMs), the netrins, semaphorins, SLIT family, and the ephrins, all of which are highly conserved phylogenetically [32; 33]. Most of these guidance cues are expressed in the adult CNS, whilst some may be further up-regulated

following injury [34]. In addition to these classical guidance molecules, another class of growth-guidance cues, the growth-associated proteins later characterised as one and the same protein: GAP-43 is equally interesting. A large body of supportive evidence from in vitro and in vivo work suggests that GAP-43 plays an important role in neurite outgrowth by greatly potentiating neurite adhesion, sprouting and terminal arborisation, and can therefore be considered an intrinsic determinant of nerve growth [35; 36; 37]. Trophic influence from neurotrophins brain-derived neurotrophic factor (BDNF), nerve growth factor (NGF), and neurotrophin (NT)-3,-4, have also been demonstrated to stimulate regeneration, remyelination and increase neuronal survival when applied exogenously [38; 39; 40; 41; 42]. In the PNS following peripheral nerve injury, Schwann cells as well as actively phagocytosing myelin debris produce neurotrophic factors that support axonal growth. In the CNS, the lack of growth factor support may be one of the factors contributing to poor recovery. This and the inhospitable milieu of the injured environment strongly perturb axonal regrowth. CNS myelin-associated proteins, Nogo-A, myelin-associated glycoprotein (MAG), oligodendrocyte-myelin glycoprotein (OMgp) and ephrin-B3, which normally provide inhibitory guidance cues to axonal pathfinding during development, become an additional barrier to axonal regrowth following injury [43; 44].

1.1.2 Measuring neuroplasticity: looking to neurodevelopment for the answers

One of the major challenges facing contemporary neurobiology has been to find procedures for measuring neuronal self-protection, plasticity and restoration. The adult human brain contains anywhere between 80-90 billion neurones [45], which, during development have been carefully guided along specific pathways to their intended goals [46]. During such migration the growth cone explores the surrounding extracellular matrix (ECM) and other cells responding to a wide variety of attractive and repelling cues [47]. The expression of most guidance cues is developmentally regulated but some of them are present in the adult nervous system and, or recapitulated following injury (see Figure 1-3). Understanding the developmental processes; molecular events underlying the differentiation, migration and integration of neuronal connections in the brain, may provide insight into neuro-restorative capacity of the adult brain and tangible ways of measuring this neurogenic potential.

During development, both NCAM and GAP-43 are abundantly expressed in the CNS [35; 48]. The spatiotemporal expression of NCAM in the developing brain is regulated in manner to suggest involvement in morphogenesis, in establishing the precision and topography of neural patterns [49; 50; 51; 52; 53]. NCAM is found throughout the rat corticospinal axons as they grow from the cortex to the spinal cord, with PSA-NCAM becoming evident only later restricted to the distal segments coinciding with delayed onset of branching by these axons [54]. Retinotectal neurones display high levels of PSA-NCAM at periods of high plasticity thought to be involved in targeting corrections by these axons, evidence from antibodies directed against NCAM support this with

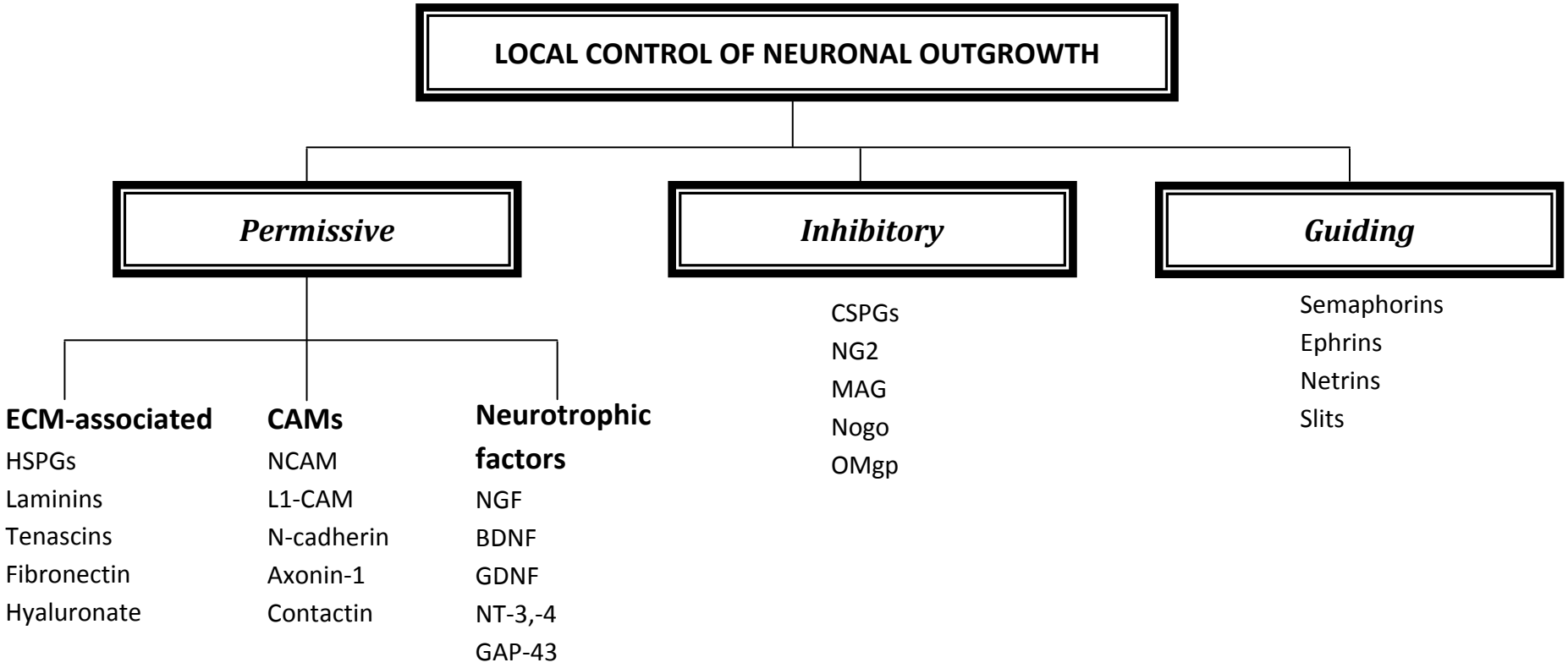

Figure 1-3 Classification of factors regulating neuronal outgrowth in the mammalian nervous system. This list represents a subset of permissive, inhibitory and guiding (affecting the advance of the growth cone) environmental cues that direct axons via interactions with the growth cone. BDNF=brain-derived neurotrophic factor; CAMs=cell adhesion molecules; CSPGs=chondroitin sulfate proteoglycans; GAP-43=growth associated protein-43; GDNF=glial-derived neurotrophic factor; HSPGs=heparan sulfate proteoglycans; MAG=myelin-associated glycoprotein; NCAM=neural cell adhesion molecule; NG2=neuron-glia antigen 2; NT=neurotrophin; OMgp=oligodendrocyte-myelin glycoprotein (adapted from Kiryushko *et al.* [47]).

the finding that these antibodies distort the retinotectal projection patterns greatly reducing their precision [55; 56; 57]. NCAM also appears to play a critical role in the formation and function of synaptic terminals, in particular the mechanisms of recycling synaptic vesicles, wherein high-frequency synaptic transmission at neuromuscular junctions is impaired resulting in locomotor defects [58]. GAP-43 has also been well-researched in the rodent and mammalian brain and shown to be present specifically in areas undergoing axonal elongation and synapse formation associated with growth cones and immature synapses, respectively [59]. Convergent data from different sources indicate that GAP-43 plays an important role in the maintenance of a functional growth cone and its induction may be a pre-requisite for axon growth, whilst also modulating the formation of new connections and structural plasticity [35; 59; 60]. At a molecular level, GAP-43 comprises of 1% of the total protein of growth cone membranes in the developing brain and the time course of GAP-43 expression coincides with, or slightly precedes initiation of axon growth in regenerating fish and amphibian neurones, consistent with the proteins' involvement in axon elongation [37]. Elevated GAP-43 expression continues for the duration of axon elongation and synaptogenesis in all developing and regenerating systems during the 'critical period' for plasticity which is anywhere between 2-10 weeks after nerve injury [36; 61]. Overexpression experiments indicate that GAP-43 greatly promotes spontaneous sprouting of nerves in their terminal fields [62], whilst a lack of GAP-43 leads to defects in neuronal pathfinding during early development [63]. Considering the effects of these molecules on plasticity during development, it would be tempting to speculate that in the mature nervous system their re-expression is necessary for structural remodelling of neuronal

networks. The ageing brain is characterised by a reduction in brain weight, cortical atrophy and neuronal cell loss [64]. To avoid functional decline, regenerative processes may have to be activated. However, the profound neuronal loss and cognitive decline occurring in advanced age imply that these mechanisms of plasticity may be particularly vulnerable during the ageing process. NCAM converts from the embroyonic PSA-NCAM to the distinct adult forms NCAM-180, NCAM-140 and NCAM-120 which carry one third of the sialic acid content of the embryonic form and therefore more adhesive with tendency toward homophilic binding during maturation [53; 65]. In rats, the total NCAM content in whole brain remains unchanged from postnatal day 40 to old age, but drops during early postnatal development [66]. The subunit composition of the adult form of NCAM are also known to change with neural cell differentiation with the selective expression of NCAM-180 whose lateral mobility within the membrane is reduced by the longer cytoplasmic domain and its interaction with cytoskeletal-associated proteins [67]. NCAM-180 is accumulated in post-synaptic densities determining the stability of contacts between pre- and post-synaptic membranes and the state of synaptic activity [68]. In ageing rodent brains, NCAM-180 and NCAM-140 (expressed on both pre- and post-synaptic membranes) are selectively down-regulated, thus indicating a general decline in remodelling capacity during ageing [66; 68]. An age-associated decline in GAP-43 expression has not been found in experimental models [69; 70], however, regional changes in GAP-43 expression have been observed. In the rat hippocampus, an area linked with continual synaptic turnover or plasticity, there is an overall reduction in GAP-43 mRNA with age, especially in the CA3 region [71]. Following seizure activity, young and middle-aged rats retain the ability to upregulate GAP-43

expression in the hippocampus, while in the old rats this response was markedly weakened, suggesting a reduced potential for plasticity here [71].

1.1.3 An approach to quantifying neuroplasticity in the adult CNS

Due to the unavailability of living human brain for biochemical analysis considerable efforts have been devoted to the study of cerebrospinal fluid (CSF) as a tool for assessing the production of molecules and compounds by the CNS. CSF is produced at a rate of 500 ml/day, containing approximately 0.2 g/l [72] of plasma protein constituting 60% of CSF total protein, with the remainder comprising mainly CNS-synthesised proteins [73]. These non-plasma proteins are largely cytoskeletal components expressed predominantly in neurones and glial cells and released into the CSF through destruction or changes in membrane permeability, or as by-products of metabolism. Several brain specific proteins have been described to date, and include soluble versions of all three major isoforms of NCAM as well as GAP-43. CSF NCAM is thought either to arise from spontaneous release from the plasma membrane, particularly in the case of NCAM-120 following extracellular cleavage by phosphatidylinositol-specific phospholipase C [74], or possibly by degradation of the extracellular matrix or active secretion [75]. The synaptic protein GAP-43 has been shown to be preferentially released from damaged brain tissue during neuronal necrosis [76]. Their functional role in the CSF remains a mystery, with claims for a regulatory role or simply waste products from the nervous system. Alterations in CSF NCAM and GAP-43 have been described in various neurological disorders (Table 1-1), whether their CSF profile can become representative of neuroplasticity is yet to be demonstrated.

1.2 Multiple Sclerosis: a model for the study of neuroplasticity

MS is an autoimmune disorder where characteristically both inflammation and neurodegeneration coexist to greater and lesser degrees creating heterogeneity. Activated immune cells enter the brain via the blood brain barrier (BBB), facilitated by the disruption of the BBB by inflammatory cytokines and chemokines [77]. Once inside, these activated immune cells react to putative autoantigens, which include myelin basic protein (MBP) and myelin oligodendrocyte protein (MOG) leading to demyelination [78]. Over time, a self-sustaining autoimmune reaction to these putative autoantigens may ultimately be established despite attempts to mitigate this by local regulatory factors. Both, T-cells and B-cells have been found in MS brain lesions and CSF of MS patients and felt to be directly involved in the pathogenesis of the disease, but only recently the discovery of meningeal B-cell follicles proffers a way to understanding the maintenance of lymphoid activity in the chronic stages of the disease [79].

Amidst all the chronic inflammation, there are suggestions of the existence of a repair phenomenon as evidenced by the formation of fully-differentiated interneurones in chronically demyelinated plaques and shadow-plaques (areas of remyelination), which are a consistent feature in the early stages of MS [80]. Remyelination within active plaques appears to be accomplished by oligodendrocyte progenitor cells recruited to sites of demyelination. The presence of clinically silent MRI lesions paints a picture of a silent conflict between pathological processes and repair or adaptation (plasticity). Moreover, a comparison of MRI with histophathological findings found signs of

remyelination in 42% of areas investigated, confirming that remyelination is a frequent occurrence in MS [81]. Previously held belief that repair is scarce in the adult CNS may have misled us to believe that it is absent altogether.

In the later stages of the disease atrophy appears to be the predominant feature and neuroplasticity the exception, not the rule. Remyelination, whilst rapid and extensive in new plaques and in the gray matter, evidence from chronic plaques suggest that remyelination may be less conspicuous here and mostly restricted to plaque edges [82; 83]. Halting the inflammatory response leading to relapses in mouse model of MS (chronic relapsing EAE) does not prevent disease progression based on deterioration in mobility and the development of spasticity [84]. Similarly evidence from Campath-1H, a humanised monoclonal antibody that causes prolonged T lymphocyte depletion, suggests that halting lymphoid cell inflammation does not appear to curb the accumulation of disability in secondary progressive MS patients [85]. The continuation of axonal loss in non-relapsing progressive MS is poorly understood. It has been suggested that inflammation in early disease primes the damaged axons for degeneration in the future [85], and also it is likely that persistent demyelination [86] and loss of homeostasis of ionic gradients in axons [87] are other necessary mechanisms leading to axonal loss. In EAE, damage to the corticospinal tract (CST) is a predictor of clinical paralysis, with almost two-thirds of axons displaying substantial degeneration [88]. CST cells are noted for their lack of regenerative capacity [89] and may explain some of the limited recovery observed after injury or axotomy.

The MS model can therefore be used to study the molecular and cellular mechanisms that contribute to neuro-restoration or lack thereof. There is a plethora of knowledge on axonal loss and neurodegeneration, but little is known about the mechanisms sustaining neuroplasticity and the consequences of chronic damage.

1.3 Biomarkers

Depending on the subject area the word ‘biomarker’ has a specific meaning as well as application, which has understandably lead to some confusion on the subject. The official National Institute of Health (NIH) definition of a biomarker in biological sciences is: ‘a characteristic that is objectively measured and evaluated as an indicator of normal biological processes, pathogenic processes, or pharmacological responses to a therapeutic intervention’ [90; 91]. A biomarker is different from that of a ‘clinical endpoint’ which applies primarily to an outcome in a therapeutic intervention trial that provides the most compelling evidence in support of a therapeutic effect or lack of, an example of this is mortality [90; 92]. Biomarkers are also mistakenly referred to as ‘surrogate endpoints’ which are measures that can be used in substitution of a clinically meaningful endpoint [93]. A surrogate marker requires a long list of characteristics to be established, including technical validation, biological feasibility, be translational across species, and not least to correlate with other measures of a similar nature, such as MRI or neurophysiology, to mention an important few. Consequently, it comes as no surprise that only a subset of biomarkers ever reach the status of surrogate endpoints and remain as only “candidate” surrogate markers [94].

Due to the complex nature of nerve regeneration it is unlikely that a single biomarker will be representative of the whole process. The majority of biomarkers are from secondary biological processes and their relationship to the primary pathological event is not directly causal but due to bystander or associated effects [94]. Therefore in order to exemplify what takes place during nerve regeneration a multifactorial all-inclusive approach to selecting biomarkers is needed comprising of markers that are both disease-specific and process-specific, but also to be practically useful they should not be remote from the clinical endpoint. Moreover, they should compare favourably with other well-established clinical and laboratory parameters already in use. This will require the translation of biomarkers from *in-vitro* experiments and animal models, into well-controlled clinical trials (Figure 1-4). Occasionally as in regenerative work, the biomarkers may be so novel that there may be no relevant comparisons, in which case they will require qualification at a later stage.

In neuroprotection studies, one of the major hurdles to success has been insufficient appreciation of the complexities of the human central nervous system. It therefore stands to reason that, a better understanding of nerve regeneration and repair will go a long way to help researchers develop and test neuroprotective strategies where, biomarkers may have a key role to play. So far in neuroscience, imaging in particular MRI has established a precedent in diagnosing and monitoring disease process [95]. However, MRI is unable to image directly remyelination and neurogenesis. Magnetization transfer ratio (MTR) has been shown to be a reliable marker of myelin content in demyelinated lesions and normal appearing white matter (NAWM) based on

DISEASE	ISOFORMS	CONC.	SAMPLE	TECHNIQUE	REFERENCES
Neural Cell Adhesion Molecule (NCAM)					
Alzheimer's disease	Total NCAM	↑/↔	CSF	ELISA	[97; 98]
	Total NCAM	↑	Plasma	ELISA	[97]
	100-130 kDa (low), >130 kDa (high)	↑	Serum	Western blotting	[99]
Multiple Sclerosis	Total NCAM	↓/↔	CSF	ELISA	[98; 100; 101]
Schizophrenia	Total NCAM	↑	CSF	Western blotting	[102; 103]
	120 kDa	↑	CSF	Western blotting	[104]
	105-115 kDa cleaved NCAM	↑ /↓ in FE-NN*	CSF	Western blotting	[105; 106]
	165 kDa (heavy), 155 kDa (medium) VASE	↑	CSF	Western blotting	[107]
	140 kDa (low) VASE	↔	CSF	Western blotting	[107]
Bipolar disorder (BPD)	165 kDa (heavy), 155 kDa (medium), 140 kDa (low) VASE	↔	CSF	Western blotting	[107]
	120 kDa	↑ in BPD type I not II	CSF	Western blotting	[108]
Growth Associated Protein (GAP)-43					
Alzheimer's disease	N/A	↑/↔	CSF	ELISA	[109; 110]
Parkinson's disease	N/A	↓	CSF	ELISA	[110]
Multiple Sclerosis	N/A	↔	CSF	ELISA	[111]

Table 1-1 Levels of soluble NCAM and GAP-43 observed in blood and CSF of neurological disorders.

* First-episode neuroleptic-naïve patients.

Figure 1-4 A flow chart of fit-for-purpose validation of biomarkers for application in clinical trials. Incorporation of biomarkers into clinical trials as predictive indices of patient response entails biomarkers demonstrating their efficacy in preclinical and early and late phase trials or equivalent.

histopathological correlations, but can be confounded by the effects of inflammation [96]. By comparison molecular research into the CNS has been vast, with a large body of work primarily devoted to that of disease pathophysiology. Studies focused on neuroregeneration and plasticity, however, have been few in number as well as conflicting in their messages [112; 113; 114], making it difficult to draw tangible conclusions. Much of the research into nervous system regeneration and repair relies heavily on knowledge from non-human animal studies. Information from the human CNS at different stages of development and injury are rare due to scarcity of post-mortem material. Therefore, for biomarker studies in living subjects, body fluids such as serum, plasma, urine

and CSF are a more suitable choice [91]. Urine sampling is non-invasive but susceptible to urinary tract infections which can induce certain biomarkers leading to supranormal values [115], and collection volumes may vary depending on the degree of bladder dysfunction [116]. Analysing biomarkers in blood is an alternative and although moderately invasive is relatively easy to collect. However, the existence of an active clotting system complicates analysis and the high protein content may interfere with tests in even so called “optimised” ELISA kits designed to minimize interference [117]. Conversely, the protein concentration of the CSF is much lower owing to the size restriction posed by the blood-brain-barrier, and the absence of a clotting system makes this the ideal biofluid for biomarker analysis. The CSF is also an accessible liquid extension of the CNS and a better reflection of the processes taking place within [118]. In addition, some proteins are present in very low concentrations in the blood but their relative concentration is far more significant in the CSF as they are exclusively synthesised in astrocytes or in neurones – for example Beta-2-transferrin which generally used in the determination of the aetiology of nasal discharge to represent CSF leak [119]. As a last remark, the procedure of obtaining CSF is invasive requiring considerable expertise and the total volume of CSF is far lower than the total volume of blood (150-270 ml of CSF [120] compared to 5 l of blood in humans), limiting the amount that can be sampled for analysis at any one time.

1.4 Hypothesis and aims

The goal of this study was to investigate and validate potential biomarkers of neuro-restoration, specifically those involved in neuronal pathfinding, which can be used to measure plasticity in the adult CNS following injury, and to discuss emerging ideas regarding how these molecules are regulated in disease. My hypothesis is that the nervous system has an intrinsic capacity or potential for regeneration, but this capability may be dramatically reduced by disease.

NCAM and GAP-43 were selected as candidate biomarkers for further study based on existing supportive evidence for their role as surrogate markers of neuroplasticity, as they are predominantly expressed in the brain and may be preferentially released after neuronal damage, and their protein sequences are conserved across different species considered necessary for the translation of biomarkers from animal to human models (see Table 1-2).

The specific aims of the thesis are detailed below:

1) To develop sensitive enzyme-linked immunosorbent assays (ELISA) to quantify levels of NCAM and GAP-43 in cerebrospinal fluid.

2) To generate recombinant GAP-43 suitable for use in ELISA.

3) Characterise the soluble isoforms of NCAM in CSF using mass spectrometry.

4) Using *in-vitro* and *in vivo* models of MS track the expression of NCAM through the disease state in order to understand the effects of disease progression on neuronal plasticity.

5) Compare the levels of CSF NCAM and GAP-43 in control subjects and in patients suffering from MS and other neurological disorders, and to correlate this with patient outcome measures.

6) Establish guidelines for biomarker validation and reporting.

Accession	Entry name	Protein name	Length & mass	Species	Identity
P13591	NCAM1 HUMAN	Neural cell adhesion molecule 1 (NCAM-1)	858 aa, 94,574 Da	Rhesus macaque	*99%*
				Rat	*95%*
				Mouse	*93%*
P17677	NEUM HUMAN	Growth associated protein 43 (GAP-43)	238 aa, 24,803 Da	Rhesus macaque	*98%*
				Rat	*73%*
				Mouse	*76%*

Table 1-2 Sequence alignment scores for human NCAM and GAP-43 by species (generated using NCBI Blastp suite). Percentage sequence homology with other species is given; this has practical issues for biomarker experiments in animal models and translating this work across to humans.

2 NEURAL CELL ADHESION MOLECULE (NCAM):

A novel method for analyzing NCAM isoforms using mass spectrometry combined with protein retrieval and the development of a sensitive quantitative ELISA for NCAM

2.1 Introduction

The neural cell adhesion molecule (NCAM) constructed from domains of the immunoglobulin superfamily plays an integral role in neuronal repair and regeneration and has been implicated in such diverse processes as neuronal cell-cell/cell-substratum adhesion, axonal outgrowth, guidance and fasciculation, myelination, synaptic plasticity and myogenesis (see reviews by [51; 121; 122; 123; 124]). NCAM was originally described by Jorgensen and Bock as "D2" protein [125]. It is transcribed from a single gene on chromosome 11, but because of alternative splicing of the protein it exists in many isoforms [126; 127]. The three major isoforms are NCAM-120, NCAM-140 and NCAM-180, corresponding to their respective molecular weights when separated by sodium dodecyl sulfate polyacrylamide gel electrophoresis (SDS-PAGE). They differ primarily in their *C*-termini with NCAM-180 having the longest intracellular component, whereas NCAM-120 is linked to the plasma membrane via a glycosyl-phospatidylinositol (GPI) anchor with no intracellular component (Figure 2-1). The *N*-termini of all three isoforms is identical, comprising of five Ig-like domains and two fibronectin type III repeats. The expression of NCAM isoforms takes place in a tissue (NCAM-120 is found in glia, NCAM-140 in neurons and glia, and NCAM-180 in neurons) and developmental stage specific manner [128; 129], although their individual contributions to the overall plasticity-promoting role of the protein is less well understood.

Occasionally, NCAM polypeptides with differing sizes from the major isoforms have been described [130; 131; 132]. These contain minor variations in the length of the extracellular domain of NCAM, and it is possible that a single band

observed by immunoblotting may therefore contain many different isoforms. In pathology, a selective increase in 105-115kDa NCAM and VASE (variable alternative spliced exon), a 10 amino acid insert into the fourth NCAM domain, have been described in patients with schizophrenia [107; 133; 134]. In bipolar mood disorder patients a preferential rise in the 120kDa NCAM and 140kDa VASE isoform has been found [108; 135]. Altered or over-expression of NCAM isoforms has been observed in a variety of tumours, including gliomas, breast, colon, small cell lung carcinoma, and melanoma [136; 137; 138; 139; 140; 141].

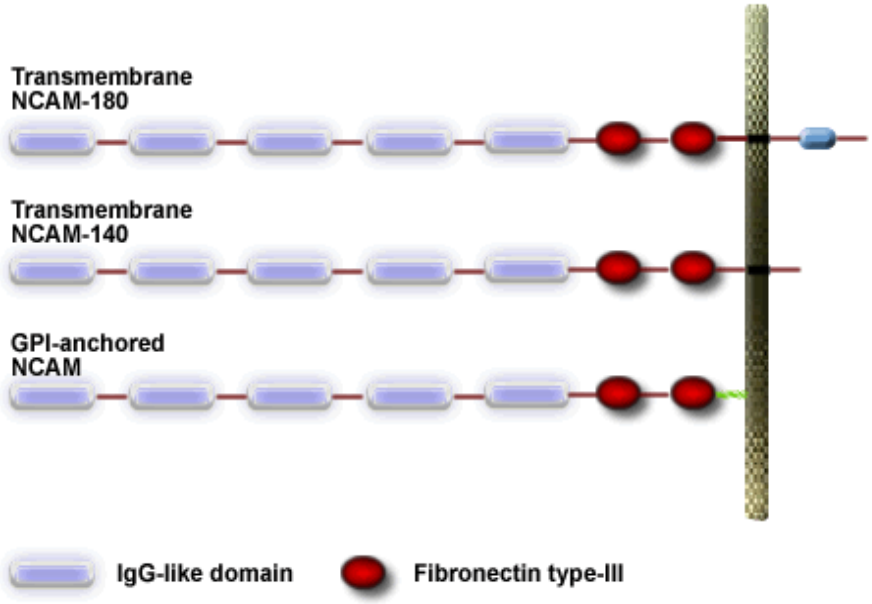

Figure 2-1 Schematic diagram of three main classes of NCAM. They vary only in their cytoplasmic domain: NCAM-120 kDa (GPI anchored), NCAM-140 kDa (short cytoplasmic domain), NCAM-180 kDa (long cytoplasmic domain). While the extracellular domain consists of five immunoglobulin (IgG)-like domains followed by two fibronectin type-III domains.

In addition to membrane-bound isoforms of NCAM soluble versions of all three major isoforms exist in the blood, CSF, amniotic fluid and cell culture supernatants [131; 142; 143; 144]. They are thought to arise from spontaneous release from the membrane following extracellular cleavage by phosphatidylinositol-specific phospholipase C (PI-PLC), as in the case of NCAM-120, or possibly by

the degradation of the extracellular matrix in the transmembrane isoforms or active secretiion [142; 145]. Biologically, their role is somewhat mysterious, with one description of them being regulatory molecules by interfering with NCAM-mediated cell adhesion or modulating other extracellular matrix components by binding to them [142], or simply waste products of the nervous system.

Serum levels of NCAM are higher than in the CSF, although in paired samples there appears to be no correlation between the two [146]. Recently, Massaro *et al.* reported that CSF NCAM is also unsialylated, whilst the sera are PSA (polysialic acid) – positive, further highlighting differences between the two compartments [147]. Despite the extent to which NCAM has been explored in the research field we have yet to find an analytical use for it. In MS, whilst reduced levels have been noted in non-acute MS, following an acute exacerbation NCAM levels rose steadily in the CSF in patients treated with steroids, suggesting possible involvement in nervous system recovery after an inflammatory insult [148].

2.2 Aims

The aims of the work presented in this chapter were firstly to study the distribution of NCAM isoforms in blood and CSF space to determine whether they were comparable, and then to determine which isoforms were present in the CSF.

Secondly, to determine whether NCAM quantification in CSF could serve as an indicator (biomarker) of plasticity and repair in neurological disorders.

2.2.1 The detection of NCAM isoforms: past and future

Previously NCAM isoforms have been inferred indirectly from NCAM protein isoform sizes determined by western blotting techniques. The serum matrix is complex, requiring sample dilution and loss of sensitivity whilst dealing with low abundant proteins. One way of overcoming these limitations is to combine immunoaffinity protein capture with mass spectrometric methods of detection, which provides targeted assessment of isoforms present in biological fluids, and also permit their characterization through peptide sequencing.

Using a monoclonal antibody specific for the N-terminal portion of NCAM which is able to identify the common molecular forms (-120, -140, -180kDa isoforms) as well as any additional variations in the extracellular isoforms of NCAM, I have developed a SELDI-based expression profiling method for studying the NCAM isoforms in matched serum and CSF samples. Bound NCAM was eluted directly without intervening fractionation steps and analysed using ESI (electrospray ionization)-Q-TOF (tandem quadrupole/orthogonal-acceleration time-of-flight) sequencer.

2.2.2 Quantitative NCAM analysis

An ELISA allows rapid quantitation of a large number of samples for the presence of an analyte, allowing high throughput quantitation. The resulting quantitative signal is dependent on the sensitivity and specificity of the assay, which is largely antibody dependent, but is also determined by the ELISA format (direct *vs.* indirect). Several groups, including our own have previously attempted to produce NCAM ELISAs but a few simple or robust assays exist owing to difficulties in obtaining reagents, since antibodies are often produced in-house, or that only look at a specified form of NCAM, for example PSA-NCAM. Using a monoclonal NCAM antibody specific for an epitope on the N-terminus of NCAM, an ELISA that could potentially summate signals from all NCAM isoforms was developed, thereby providing a quantitative signature of neuronal plasticity. The levels of total NCAM in the CSF of different neurological conditions were subsequently determined.

2.3 Materials and methods

2.3.1 Patients

2.3.1.1 Mass spectrometry and western blot patient material

Paired CSF and serum samples were from secondary progressive MS patients within the placebo arm of the Lamotrigine trial (NCT00257855) [149]. The study was approved by the Joint University College London and University College London Hospitals Committee on the Ethics of Human Research. All participants

gave informed consent for blood and lumbar puncture procedures. Clinical diagnosis of MS was supported by the presence of intrathecal oligoclonal band patterns on gel electrophoresis and an intercurrent infection was excluded bacteriologically. Samples were frozen and kept at -70^{o}C until analysis.

2.3.1.2 CSF samples for NCAM ELISA

CSF samples used in this part of the study were obtained from the CSF laboratory, National Hospital for Neurology and Neurosurgery, Queen Square, U.K. There was local research ethics committee approval for use of these samples in the development of new investigations. CSF samples had been centrifuged at receipt and stored at -20^{o}C.

NCAM analysis was performed blind to clinical data. The final clinical diagnoses on the samples were obtained from clinical notes retrospectively; those in whom the diagnosis was unclear were not included in the final analysis. CSF NCAM was measured in a total of 225 samples. Their underlying diagnoses were benign-intracranial hypertension (BIH), multiple sclerosis (MS), neuropathy, Alzheimer's disease (AD), cognitive impairment (CI), motorneurone disease (MND), meningitis and viral encephalitis. The control population consisted of headache and back pain with normal imaging and CSF profile. Their characteristics is summarised in Table 2-1.

Table 2-1 Clinical characteristics of patients used to measure CSF NCAM (N=225).

Diagnosis	N	Gender (M:F)	Age (years)
BIH	36	4:32	31 (18-51)
MS	51	15:36	44 (17-74)
Neuropathy	27	13:14	50 (23-75)
AD	37	19:18	60 (47-74)
CI	12	7:5	61 (51-78)
MND	15	8:7	60 (37-81)
Meningitis	13	6:7	46 (21-62)
Viral encephalitis	17	13:4	54 (22-79)
Controls	17	9:8	61 (31-81)

All age values are expressed as means (range). *N* = number of individuals; M = male; F = female; BIH = Benign Intracranial Hypertension; MS = Multiple Sclerosis; AD = Alzheimer's Disease; CI = Cognitive Impairment; MND = Motor Neurone Disease.

2.4 Buffers and Solutions

Buffers and solutions used in this Chapter are given in the Appendix to Chapter 2.

2.5 Methods

2.5.1 Overview

An overview of the methods used for NCAM isoform analysis and total NCAM level quantification is given in Figure 2-2.

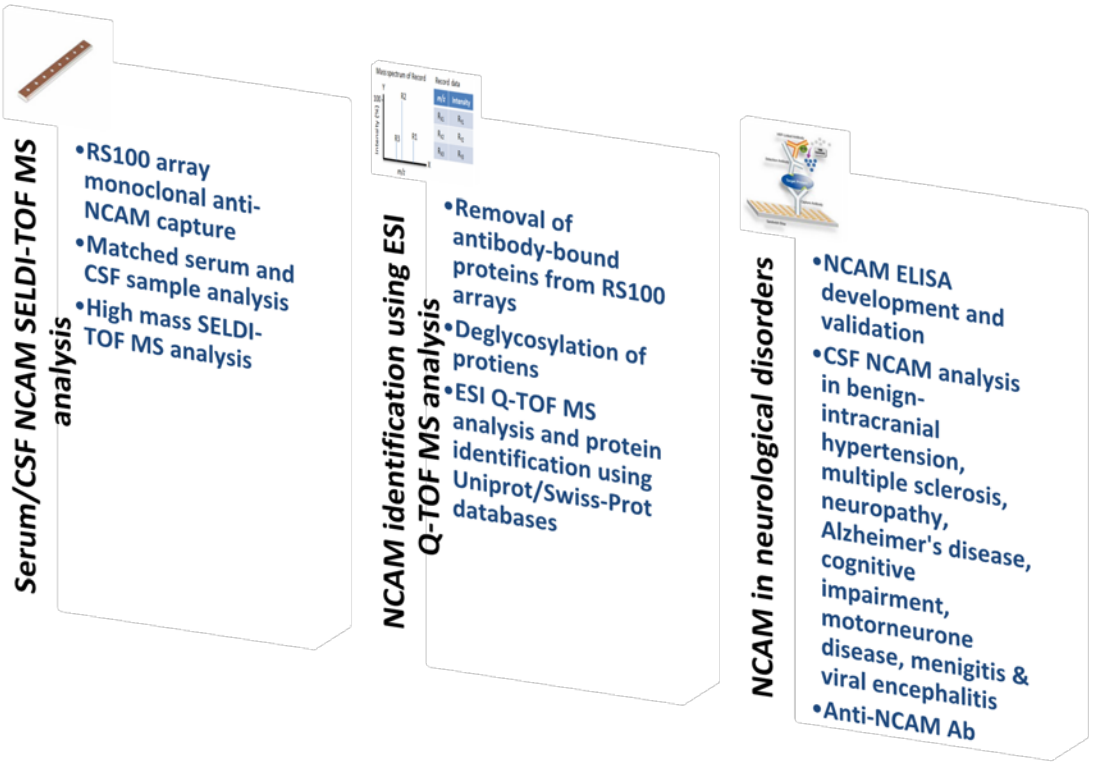

Figure 2-2 An outline of NCAM mass spectrometry and quantification experiments. *Serum/CSSF NCAM SELDI-TOF MS* analysis: to characterise NCAM found in the CSF *versus* sera using anti-NCAM antibody bound to RS100 array using SELDI-TOF-MS which permits on-spot segregation of native NCAM from other protein populations in the samples. *NCAM identification using ESI Q-TOF MS* analysis: a technique of dissociating NCAM from the array was developed in order to permit direct ESI Q-TOF peptide analysis. *NCAM in neurological* disorders: the development and validation of a new NCAM ELISA for protein quantification, including exploratory study of endogenous anti-NCAM antibodies which may have the potential to intefere with the analysis and quantification of NCAM in neurological disorders.

2.5.2 Sample preparation

Blood samples were collected in 10mL sterile collection tubes (BD vacutainer®, #367820) containing no anticoagulant and allowed to clot spontaneously over a period of 10-15mins. Serum was then collected after centrifugation at 2,000 g x 10min at room temperature, and stored in aliquots until analysis.

All CSF samples were collected in sterile polypropylene tubes as they exhibited low peptide binding. They were then centrifuged at 750 g x 5min at room temperature. The cell-free supernatants were aliquoted and stored until analysis. Only CSF samples without macroscopic blood contamination were included in the analysis.

2.5.3 Antibodies

Anti-NCAM mouse monoclonal antibody (BD Biosciences, #559043) used as a capture antibody in the ELISA and for immunoaffinity capture in SELDI experiments recognises the third extracellular immunoglobulin-like domain at the amino-terminus that is shared by NCAM-120, -140, and -180. The *rabbit polyclonal anti-NCAM antibody* (Chemicon, #AB5032) raised against purified chicken NCAM was used as the detector antibody in the ELISA. Whilst, *HRP-coupled goat anti-rabbit IgG* (DAKO, #P0217) was used as the reporter antibody.

Rabbit polyclonal anti-NCAM antibody (Chemicon, #AB5032) was used as the detector antibody in the positive control and omitted for the negative control in the anti-NCAM antibody immunoblot. *Polyclonal swine anti-rabbit IgG conjugated with HRP* (Dako, #P0217) and *Polyclonal rabbit anti-human IgG conjugated with HRP* (Dako, #P0214) were used as reporter antibodies.

2.5.4 Western blot analysis of NCAM in CSF

CSF samples were prepared by mixing 19.5 µl of CSF, 7.5 µl LDS sample buffer (Invitrogen) and reducing agent, 3 µl 0.5 M dithiothreitol (DTT or Clelands reagent, Sigma) and boiling for 15 min. Samples were electrophoresed on a NuPage 4-12% Bis-Tris 10 well 1.0 mm precast gel (Invitrogen) at 200 V, 120 mA and 25 W for 35 minutes in 2-{N-Morpholino]ethanesulphonic acid (MES) running buffer (Invitrogen) in a buffer tank and power pack (Invitrogen). The gel was then electroblotted to nitrocellulose (BioRad) using a semi-dry electroblotting system (Novex®, Invitrogen) in transfer buffer (Invitrogen) plus 10% methanol (VWR) for transfer of one gel (20% methanol when transferring two gels) for two hours at 25 V, 160 mA and 17 W. Non-specific binding was blocked using 2% w/v semi-skimmed milk (Marvel, Premier Brands Ltd.) in 0.9% saline for at least 1 h on a slow rocker and rinsed off with two changes of saline. The blot was then incubated overnight at 4^{o}C in primary antibody; anti-NCAM mouse monoclonal antibody diluted 1:500 in 0.2% w/v milk. After washing with 0.2% semi-skimmed milk in 0.9% saline containing 0.05% Tween 20 five times at 5 min intervals, the blot was incubated in the second antibody; swine anti-rabbit-HRP diluted 1/200 in 0.2% w/v milk for 2 hours. The washing step was repeated and the HRP activity detected using enhanced chemiluminescence (ECL). 5 ml of SuperSignal® West Pico Luminol enhancer solution and SuperSignal® West Pico stable peroxide solution (Thermo Scientific) were mixed together prior to immersing the membrane in this for approximately three minutes with agitation and then transferred to FluroChem SP chemiluminescence system (Alpha Innotech) for imaging exposure and interpreted on the accompanying AlphaEase® v4.0 Image Analysis software.

2.5.5 Western blot analysis of endogenous antibodies against NCAM in serum/CSF

A random selection of serum/CSF samples from MS subjects were tested for reactivity with recombinant NCAM by western immunoblotting looking for endogenous antibodies to NCAM potentially leading to antibody-associated interference in ELISA. MS subjects were selected as the elevated humoural response present in this disorder makes it more likely that some of these are formed against NCAM.

In brief, 50 µg of protein (R&D Systems, #2408-NC) was solubilised in LDS sample buffer (Invitrogen) and reducing agent DTT (Sigma), boiled for 10 min as described earlier and separated on NuPage 4-12% Bis-Tris 2D well precast gel (Invitrogen). The gel was then electroblotted onto nitrocellulose membrane (BioRad) using the Novex® semi-dry transfer system (Invitrogen). The membrane was blocked for 1 h at room temperature in 2% w/v semi-skimmed milk (Marvel) in 0.9% saline. Afterwards, the membrane was placed in an incubation manifold (Amersham Pharmacia) which allowed different samples to be tested against the same separated protein. The rabbit polyclonal anti-NCAM was used as a positive control diluted 1:500 in 2% w/v semi-skimmed milk in saline (saline was used as the negative control), and MS sera and CSF were diluted 1:500 dilution or neat, respectively. Each chamber contained 0.5 ml of sample. The entire manifold was placed on a rocker so that the sample followed back and forth from one end of the chamber to the other and left overnight at $+4^{o}$C. Afterwards the samples were discarded and the nitrocellulose was washed with 0.2% semi-skimmed milk in saline containing 0.05% Tween

(Sigma) 10 times at 10 min intervals between washes to remove unbound antibody. Anti-rabbit IgG/HRP for the positive control and anti-human IgG/HRP for the MS samples at 1 in 1000 dilution, were added and incubated with gentle rocking for 2 h at room temperature. The nitrocellulose was washed as previously described and removed from the manifold. Identification of antibody reactivity was carried out using ECL.

2.5.6 Surface-enhanced laser desorption/ionization mass spectrometry (SELDI-TOF MS) and protein retrieval

Immunoaffinity capture of NCAM from MS CSF and sera were performed using the eight-spot format RS100 ProteinChip arrays (BioRad).

Monoclonal anti-NCAM antibody (BD Biosciences, #559043) containing 1.0 mg/ml of protein in PBS (phosphate buffered saline, Sigma) was coupled to a single spot on the array (x8) and incubated overnight at 4^{o}C in a humidity chamber. Following this, the residual sites were blocked using 0.1% BSA/PBS and incubated for 30min at room temperature. Unbound antibodies were removed by washing once with 0.1% (v/v) Triton-X (Sigma) PBS wash buffer on an agitator, and twice in PBS (containing no Triton) for 15min each. The arrays were then placed in parallel in a 96-well format Bioprocessor (Ciphergen Biosystems, Fremont, CA, U.S.A.) and 30µl of paired crude CSF/serum was added to each spot alternatively with the last two containing recombinant NCAM (R&D Systems, #2408-NC) and PBS/BSA only as positive and negative controls, respectively. Using the Bioprocessor maximised antibody exposure to

NCAM in the sample. The Bioprocessor was then placed in a humidity chamber at 4^{o}C and incubated overnight with gentle agitation to again facilitate antibody-antigen capture. After incubation, the sample was removed from each array and washed twice for 15min in wash buffer and once in PBS for 15min on the agitator. Lastly, to remove the salts, the arrays were rinsed thrice in 5mM ammonium acetate, pH7 for 10s each. The arrays were then air-dried at room temperature. Prior to SELDI-TOF MS analysis, 2 x 1µl saturated sinapinic acid (SPA) matrix in 50% acetonitrile (ACN) and 0.1% trifluoroacetic acid (TFA) was applied to one of the spots as well as the control spot and air-dried.

Mass analysis was performed using the SELDI-TOF ProteinChip System with integrated ProteinChip software (Ciphergen Biosystems, Fremont, CA, U.S.A.) collecting the data. Each array was read at high mass with laser intensity set at 288 U, detector sensitivity of 9 and the focus mass optimized from 120-180kDa. Retrieval of antibody-bound protein was carried out on the CSF spots without the addition of SPA. Using an up-and-down motion each CSF spot was rinsed with 3 µl of 70% ACN and 0.2% TFA, followed by 3µL of 50% formic acid: 25% ACN: 15% isopropanol: 10% water. Eluate was transferred to an Eppendorf tube and freeze-dried.

2.5.7 ESI Q-TOF MS analysis

This portion of the analysis was performed by Dr Wendy Heywood, Proteomics department, Institute of Child Health, London, U.K.

20 µl of 100mM Tris, pH 7.8 containing 6M urea was added to the freeze dried sample protein and left to shake at room temperature for 1hr. Deglycosylation was performed using PNGase F (#P7367, Sigma) to increase protein coverage since NCAM has a lot of glycans that can hinder trypsin digestion and mass spectrometry detection. Disulphide bridges were reduced by the addition of 3µl of 100mM Tris-HCL, pH 7.8 containing 5M DTE and incubation at room temperature for 60min. Free thiol groups were carboamidomethylated followed by incubation with 6µL of 100mM Tris-HCL, pH 7.8 containing 5M iodoacetamide. The solution was then diluted with 155 µl H_2O, vortexed and 2 µg of sequence grade trypsin was added to the solution. Samples were incubated overnight at 37^{o}C in a water bath. Proteins were identified by direct analysis of the reaction mixture described above. All analyses were performed using a nanoAcuity HPLC and QTOF Premier mass spectrometer (Waters Corporation, Manchester, U.K.). Peptides were trapped and desalted prior to reverse phase separation using a Symmetry C18 5µm, 5mm x 300µm pre-column. Peptides were then separated prior to mass spectral analysis using a 15cm x 75 µm C18 reverse phase analytical column. Peptides were loaded onto the pre-column at a flow rate of 4 µl/min in 0.1% formic acid for a total of 4 mins. They were eluted off the pre-column and separated on the analytical column using a gradient of 3-40% acetonitrile [0.1% formic acid] over a period of 120 min and at a flow rate of 250 nl/min. The column was washed and re-generated at 300 nl/min for 10 min using a 99% acetonitrile [0.1% formic acid] rinse. After all non-polar and non-peptide material were removed, the column was re-equilibrated at the initial starting conditions for 20 min. Column temperature was maintained at 35^{o}C. Mass accuracy was maintained during the run using a lock spray of the peptide [glu1]-fibrinopeptide B delivered through the auxiliary pump

of the nanoAquity at a concentration of 300 fmol/l and at a flow rate of 300 nl/min.

Peptides were analysed in positive ion mode using a Q-Tof Premier mass spectrometer (Waters Corporation, Manchester, U.K.) and was operated in v-mode with a typical resolving power of 10,000 FWHM. Prior to analyses, the TOF analyser was calibrated using [glu1]-fibrinopeptide B (785.8426 m/z) with a sampling frequency of 30 sec. Accurate mass LC-MS data were collected in a data independent and alternating, low and high collision energy mode. Each low/high acquisition was 1.5 sec with 0.1 sec interscan delay. Low energy data collections were performed at constant collision energy of 4 V, high collision energy acquisitions were performed using a 15-40 V ramp over a 1.5 sec time period and a complete low/high energy acquisition achieved every 3.2 sec.

ProteinLynx GlobalServer version 2.3 was used to process all data acquired. Protein identifications were obtained by searching UniProt/Swiss-Prot. Protein identification form the low/high collision spectra for each sample was processed using a hierarchical approach where more than three fragment ions per peptide, seven fragment ions per protein and more than two peptides per protein had to be matched.

2.5.8 Establishment of a two-site sandwich ELISA for quantification of NCAM

2.5.8.1 The two-site ELISA

I specifically choose the two-site ELISA design as binding of the protein by two different antibodies has the obvious advantage of increasing the specificity of the assay. The format was a monoclonal-polyclonal sandwich assay using a single epitope specific monoclonal antibody as the capture antibody and a polyclonal detector antibody which recognises other epitopes of the protein. A third enzyme labeled antibody was used to generate colour which could be measured by an optical reader (Figure 2-3).

2.5.8.2 Calibration

The assay was calibrated using *recombinant human NCAM* (R&D Systems, #2408-NC). The vial was reconstituted in 0.1% BSA/1M PBS, pH 7.4 and subsequently diluted to give a standard curve ranging from 500 ng/ml to 0 ng/ml in a solution of 5% semi-skimmed milk/1M PBS, pH 7.4 as diluent.

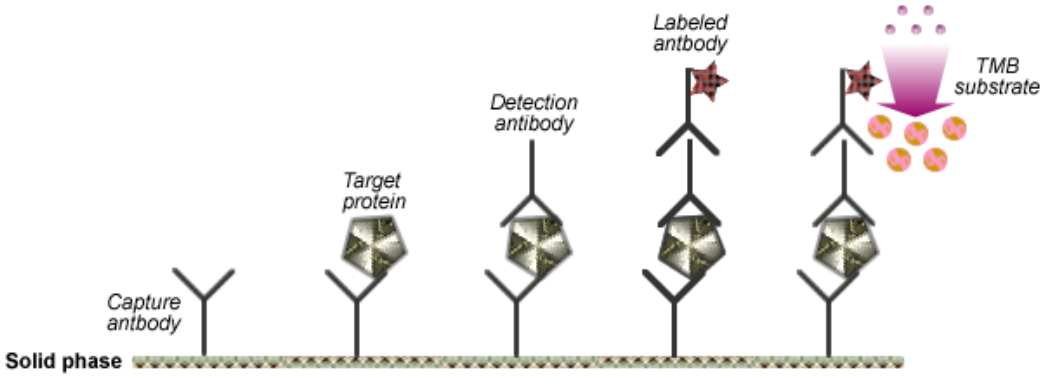

Figure 2-3 Schematic representation of the two-site ELISA. A 96-well microtitre plate was coated with the capture antibody. Samples are then added to the wells and any antigen present bind to the antibody. A detection antibody is added, followed by an enzyme-labeled antibody.TMB substrate is added as a final step and is converted by the enzyme into a detectable form.

2.5.8.3 Assay protocol

96-well microtitre plates (Nunc MaxiSorp, Nunc, Roskilde, Denmark) were coated overnight at 4^{o}C with 100 µl 2.5 µg/ml of mouse monoclonal anti-NCAM (capture antibody) in 1M PBS, pH 7.4 (Sigma). The wells were then washed once with 0.05% Tween-20/1M PBS solution (0.05% Tween/PBS), and subsequently blocked at room temperature for 1 h with 5% semi-skimmed milk in PBS (5% milk/PBS) solution. The wells were then rinsed once with 0.05% Tween/PBS leaving the plate to stand for 5 min before decanting. Aliquots of 25 µl of standards, controls and CSF samples and 75 µl of 5% PBS/milk solution were added to the plate wells in duplicate and incubated overnight at 4^{o}C with shaking. Wash step was repeated five times leaving to stand for 5 min per wash, and incubated for 1 h 30 min with 100 µl polyclonal rabbit anti-NCAM (detector antibody) at 1/1000 dilution with shaking. Again after washing 100 µl conjugated HRP goat anti-rabbit (reporter antibody) at 1/1000 dilution were added to each well and incubated at room temperature for 1 h worth of shaking.

Lastly, after a final wash step 100 µl of TMB (Supersensitive 3,3',5,5' tetramethylbenzidine, Sigma) was added and the colour development allowed to develop and then stopped using 50 µl 1M HCL (Sigma). Absorbencies were determined photometrically at 450 nm (test) and 700 nm (blank) using an ELISA plate reader (FLUOstar Omega, BMG Labtech) and the concentrations of NCAM interpolated using the standard curve generated.

2.5.8.4 CSF albumin quotient and blood-brain barrier dysfunction

The albumin quotient [1] and IgG index [2], indicators of blood-brain barrier permeability and intrathecal IgG production, respectively, were calculated. Albumin concentrations in serum (g/l) and CSF (mg/l) and similarly, IgG were quantified by nephelometry (BN *ProSpec*, Siemens).

$$\frac{ALB_{CSF}}{ALB_{SERUM}} \times 100 \qquad [1]$$

$$\left[\frac{IgG_{CSF}}{IgG_{SERUM}}\right] \times \left[\frac{ALB_{SERUM}}{ALB_{CSF}}\right] \qquad [2]$$

Spearman-rank correlations were calculated to assess if there was relationship between albumin quotients, IgG index and NCAM levels.

2.5.8.5 Statistical analysis

All analysis was performed using SPSS version 16. Comparisons between the different diagnostic categories were performed using ANOVA after establishing normality using the one-sample Kolmogrov-Smirnov test. The level of statistical significance was set at 0.05. Multiple comparisons were adjusted using Bonferroni correction. Further sub-group analyses were performed in the MS and neuropathy categories. The effects of age and gender on NCAM values were tested using regression analysis with age as a covariate and gender as a factor. Spearman-rank correlation was performed between CSF NCAM, albumin quotient and IgG index to assess whether NCAM values rose with blood-brain barrier dysfunction or intrathecal IgG synthesis.

2.6 Results

2.6.1 Optimisation of antibody capture in SELDI-TOF MS

Optimisation steps are typically required to evaluate antibody-antigen interactions, but I found using CSF specimens particularly difficult since they were more likely to be negative or yield low intensity peaks at the final analysis (Figure 2-4). A similar problem was not encountered when using serum samples. This may be a reflection of the lower concentrations of protein normally found in cerebrospinal fluid. I therefore inserted the arrays into an eight-well Bioprocessor (Ciphergen Biosystems) for sample incubation, using which much larger volumes of CSF could be loaded, akin to a 96 ELISA well

plate. Samples were then incubated overnight at 4^{o}C to allow additional binding. This produced better peak definition with CSF samples than previously (Figure 2-5).

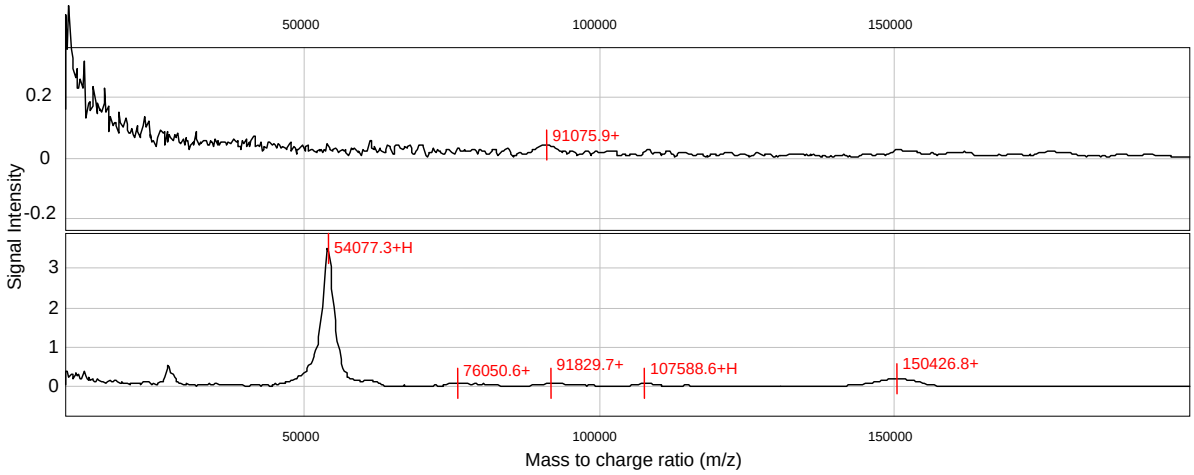

Figure 2-4 SELDI peaks in CSF (top) and serum (bottom) prior to optimisation. This generated small m/z peaks corresponding to molecular weights in the CSF; the same problem was not encountered with serum samples.

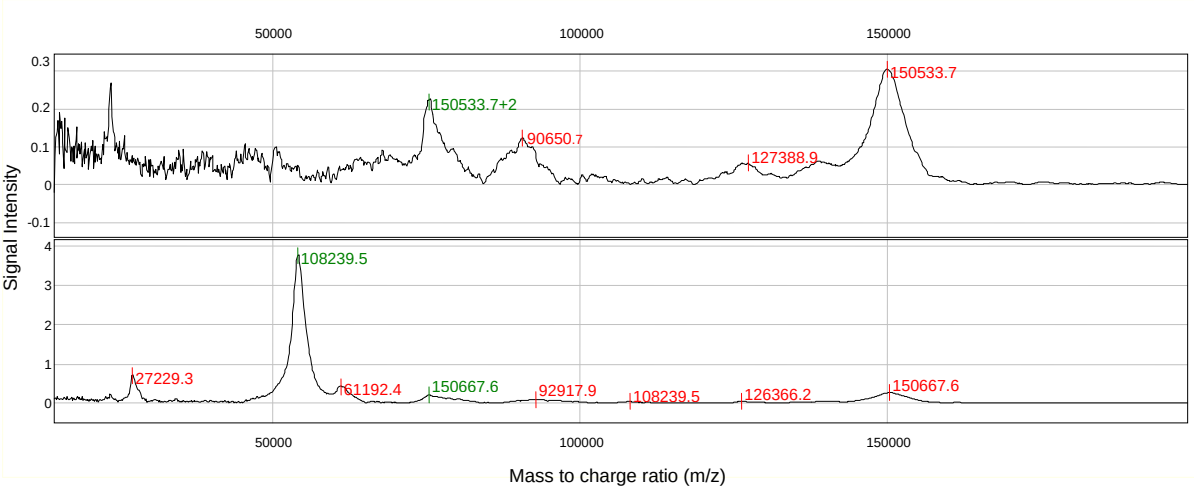

Figure 2-5 SELDI peaks in CSF (top) and serum (bottom) after optimisation. This generated m/z peaks with better definition in the CSF samples. The peak at about 75 kDa in the CSF and 54 kDa in the serum are the double-charged proteins.

2.6.2 Identification of soluble NCAM by SELDI-TOF MS reveals differences and similarities between MS patient sera and CSF

Protein profiling experiments by antibody pull down and SELDI MS revealed distinct cluster of peaks at mass to charge ratio (*m/z*) of approximately 75 kDa, 91 kDa, 127 kDa, and 150 kDa in MS CSF. Figure 2-6 shows representative profiles from five MS patients showing matching signatures suggesting identical protein compositions. Control run using recombinant NCAM (molecular weight 120 kDa, under reducing conditions) produced peaks at *m/z* approximately 46 kDa, 92 kDa, 150 kDa and 184 kDa, and the negative control identified a peak at *m/z* of approximately 67 kDa corresponding to albumin which used as the blocking agent. Paired serum analysis demonstrated shared peaks at *m/z* of approximately 75 kDa, 91 kDa, and 150 kDa similar to the CSF but also a distinctly large peak at *m/z* of approximately 54 kDa which has been highlighted as the doubly ionized form of the original protein fragment at 108 kDa, i.e. same mass but twice the charge. The intensities of the shared peaks were comparable between the two compartments. The protein composition was elucidated using shotgun sequencing which confirmed the presence of NCAM in both the CSF and serum samples, as well as few other proteins including the mouse antibody (see Table 2-2).

Accession	Entry	Description	mW (Da)
		CSF	
NCAM1_HUMAN	P13591	Neural cell adhesion molecule 1 *Homo sapiens*	94515
CLUS_HUMAN	P10909	Clusterin *Homo sapiens*	52461
FIBB_HUMAN	P02675	Fibrinogen beta chain *Homo sapiens*	55892
FIBG_HUMAN	P02679	Fibrinogen gamma chain *Homo sapiens*	51478
IGKC_MOUSE	P01837	Ig kappa chain C *Mus musculus*	11770
IGG2B_MOUSE	P01867	Ig gamma 2B chain C *Mus musculus*	44231
KV4A1_MOUSE	P01680	Ig kappa chain V IV *Mus musculus*	13825
		SERUM	
NCAM1_HUMAN	P13591	Neural cell adhesion molecule *Homo sapiens*	94515
CO3_HUMAN	P01024	Complement C3 *Homo sapiens*	187029
CO4A_HUMAN	P0C0L4	Complement C4 A *Homo sapiens*	192649
C1QC_HUMAN	P02747	Complement C1q subcomponent subunit C *Homo sapiens*	25757
CLUS_HUMAN	P10909	Clusterin *Homo sapiens*	52461
VTNC_HUMAN	P04004	Vitronectin *Homo sapiens*	54271
APOA1_HUMAN	P02647	Apolipoprotein A I *Homo sapiens*	30758
PLF4_HUMAN	P02776	Platelet factor 4 *Homo sapiens*	10837
ANT3_HUMAN	P01008	Antithrombin III *Homo sapiens*	52568
IGG2B_MOUSE	P01867	Ig gamma 2B chain C *Mus musculus*	44231
IGKC_MOUSE	P01837	Ig kappa chain C *Mus musculus*	11770
KV4A1_MOUSE	P01680	Ig kappa chain V IV *Mus musculus*	13825
IGHA2_HUMAN	P01877	Ig alpha 2 chain C *Homo sapiens*	36503
IGKC_HUMAN	P01834	Ig kappa chain C *Homo sapiens*	11601

Table 2-2 Shotgun sequencing results from SELDI MS analysis of paired MS sera and CSF. The technique of antigen retrieval from the chip not only removed NCAM off the array surface but also some of the mouse antibody. As these were MS samples there were also proteins characteristically found in inflammation, such as complement, clusterin, fibrinogen, anti-thrombin III, platelet factor 4 and human IgG which may have been bound to NCAM. The extent of protein binding was more in the serum.

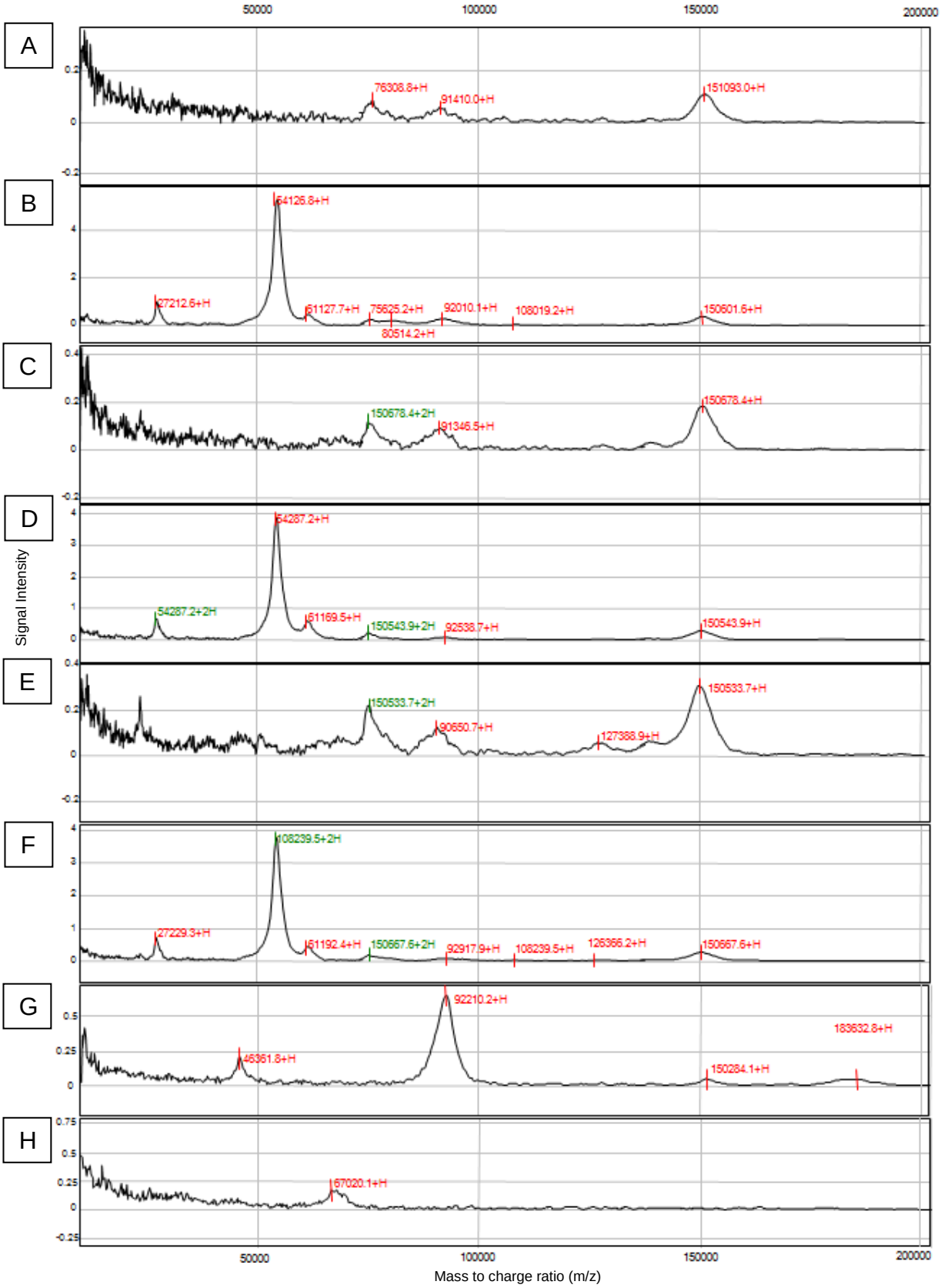

Figure 2-6 SELDI-TOF NCAM mass spectra in paired CSF and sera. Paired CSF (A, C, and E) and serum (B, D, and F) samples, G recombinant NCAM (positive control), H BSA only (negative control) were applied to RS100 arrays. Representative high mass spectra are shown. Doubly-charged proteins are in green.

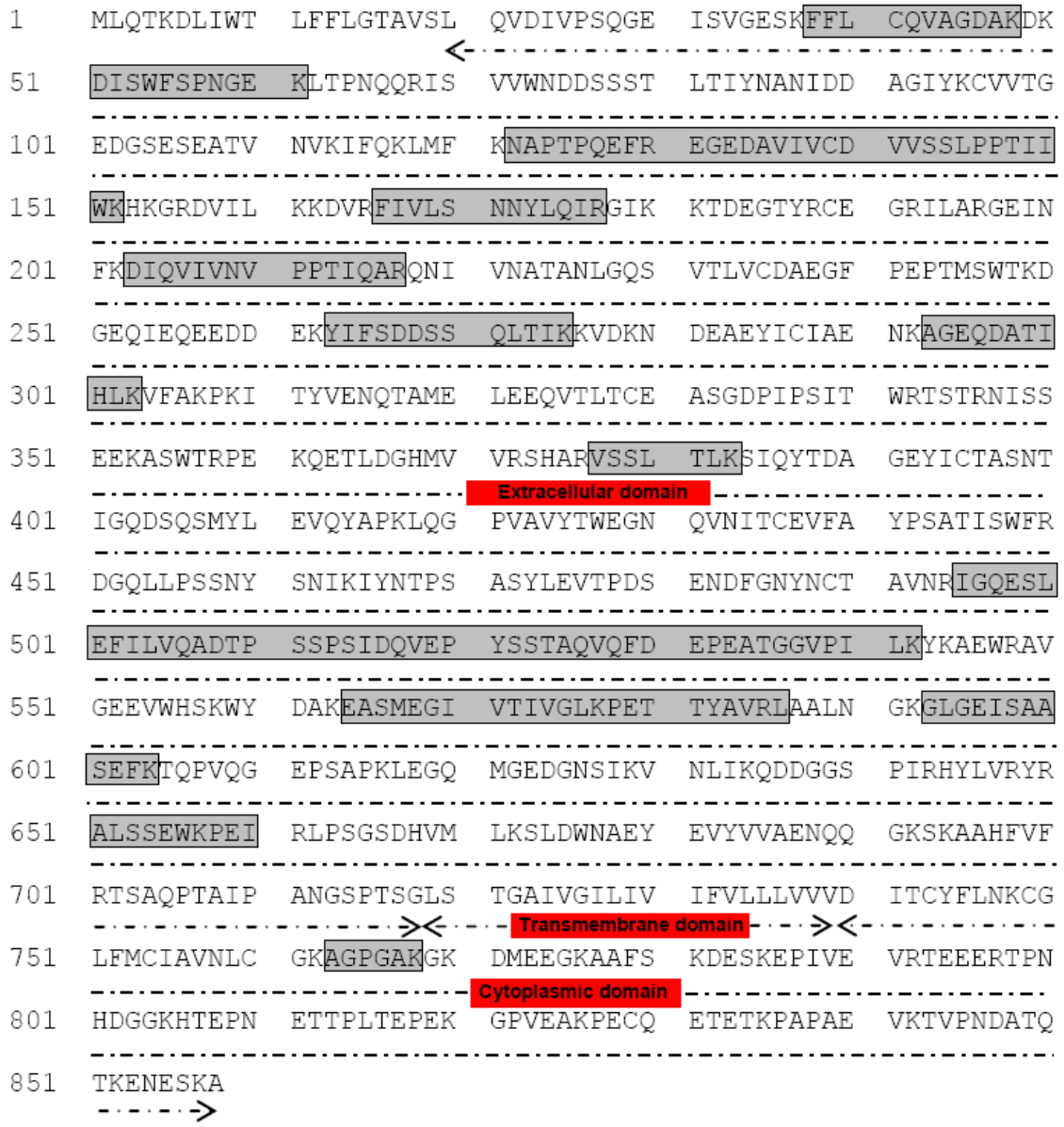

Figure 2-7 A map of NCAM sequence coverage generated using ESI-QTOF analysis. Regions of the proteinsequence that match peptides are highlighted in grey with their corresponding domains marked in red.

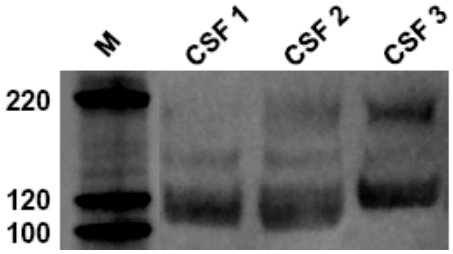

Figure 2-8 Western blot analysis of CSF NCAM (3 samples). A pattern of bands between 100 and 200 kDa was observed.

2.6.3 ESI Q-TOF MS analysis

Characterization of protein retrieved from the chips by ESI Q-TOF MS corresponded to sequence motifs from the extracellular Ig-like C2-type 1-5 domains, fibronectin type-III 1, 2 domains, and the intracellular cytoplasmic domain of NCAM (Figure 2-7). This suggests that it is possible to have the entire length of the NCAM polypeptide in the CSF. Further analysis by western blot showed three polypeptide bands with an apparent molecular weight range of 100 to 220 kDa in line with earlier findings. The 120 kDa band was the predominant band visualized but was also diffuse. Their relative proximity to each other suggests that they are isoforms of NCAM (Figure 2-8).

2.6.4 Development of the NCAM ELISA

Optimisation of the NCAM ELISA to provide a very sensitive signal involved manipulation of reagent concentrations, blocking agents and incubation period. The working concentrations of the rNCAM and monoclonal capture antibody reagents in the assay were optimised through the use of checkerboard titrations (CBT) [150]. The process of CBT involves a series of experiments in which the concentrations of two reagents are varied against each other in order to examine the activity ensuing from all resulting combinations. Final concentrations of the two reagents were then selected based on the combination(s) which provided the best signal: noise ratio. The CBT results for rNCAM and capture antibody are presented in tabulated format (Table 2-3). The titration results show the levels of binding of the serially-diluted rNCAM to the

serially diluted immobilised anti-NCAM. The optimal values of antibody and rNCAM dilutions are in blue, optical readings of 2.5 and greater were above the photometric accuracy for the FLUOstar Omega plate reader used for this study and were therefore excluded. A working dilution of rNCAM of 500 ng/ml and monoclonal anti-NCAM antibody of 2.5 µg/ml were chosen as this combination allowed for a lower capture antibody concentration. For the polyclonal anti-NCAM antibody and anti-species antibody a working dilution of 1:1000 was accepted (Figures 2-9, 2-10). Also, a variety of blocking buffers were compared in the ELISA: 2% BSA, 2% gelatin and 5% dried skimmed milk, in order to reduce non-specific binding and increase sensitivity. The colour development was faster with the BSA and gelatin as blocking buffers, but the background signal was lower with the 5% dried skimmed milk, which was therefore selected for use in the assay (Figure 2-11). To complete the assay, optimal incubation times were determined: coating performed overnight at 4^{o}C, antigen incubation performed overnight at 4^{o}C, whilst the incubation with the detector antibody was for 1 h at room temperature and the anti-species reporter antibody was for 1.5 h at room temperature.

		Capture Antibody (µg/ml)							
		20	10	5.0	2.5	1.25	0.63	0.31	0.16
rNCAM (ng/ml)	2000	3.434	3.302	3.212	2.317	0.510	0.087	0.050	0.045
	1000	3.370	3.245	3.280	2.422	0.572	0.077	0.054	0.043
	500	3.424	3.279	3.218	2.074	0.421	0.096	0.056	0.053
	250	3.447	3.290	3.105	1.605	0.289	0.079	0.061	0.046
	125	3.193	2.654	2.087	1.455	0.207	0.078	0.049	0.054
	62.5	2.559	2.116	1.864	0.736	0.162	0.070	0.050	0.046
	31.3	1.948	1.397	1.199	0.428	0.137	0.087	0.076	0.059
	Blank	1.183	1.007	0.541	0.189	0.115	0.064	0.051	0.053

Table 2-3 Double-checkerboard titration experiments carried outwith anti-NCAM and rNCAM. The optimal combinations of rNCAM and capture antibody are highlighted in blue.

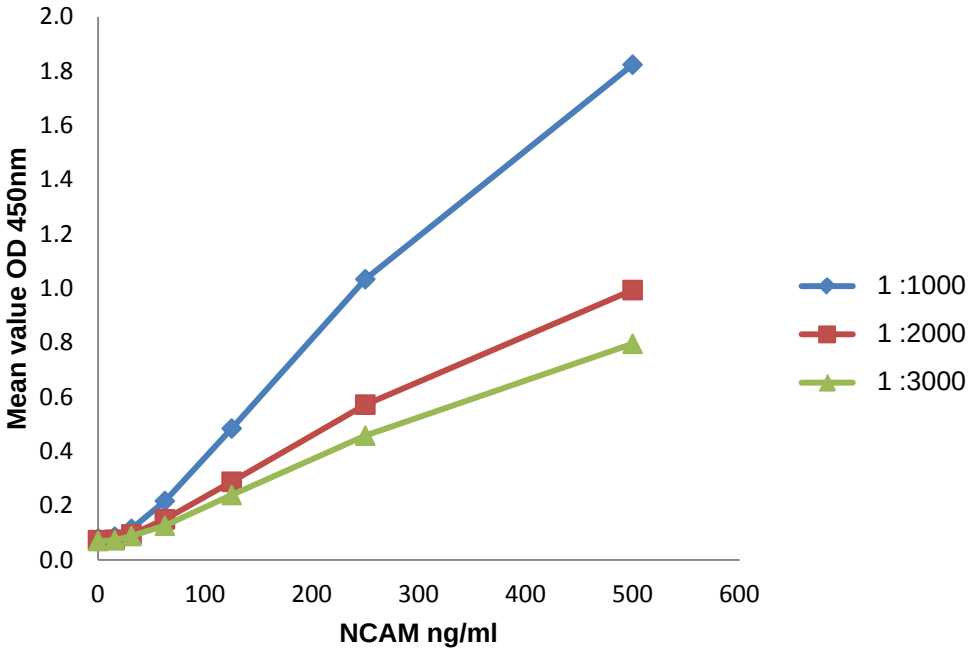

Figure 2-9 NCAM standard curves at varying concentrations of detector antibody. Polyclonal detector antibody at 1:1000, 1:1500 and 1:2000 dilutions were used with 1:1000 dilution being best.

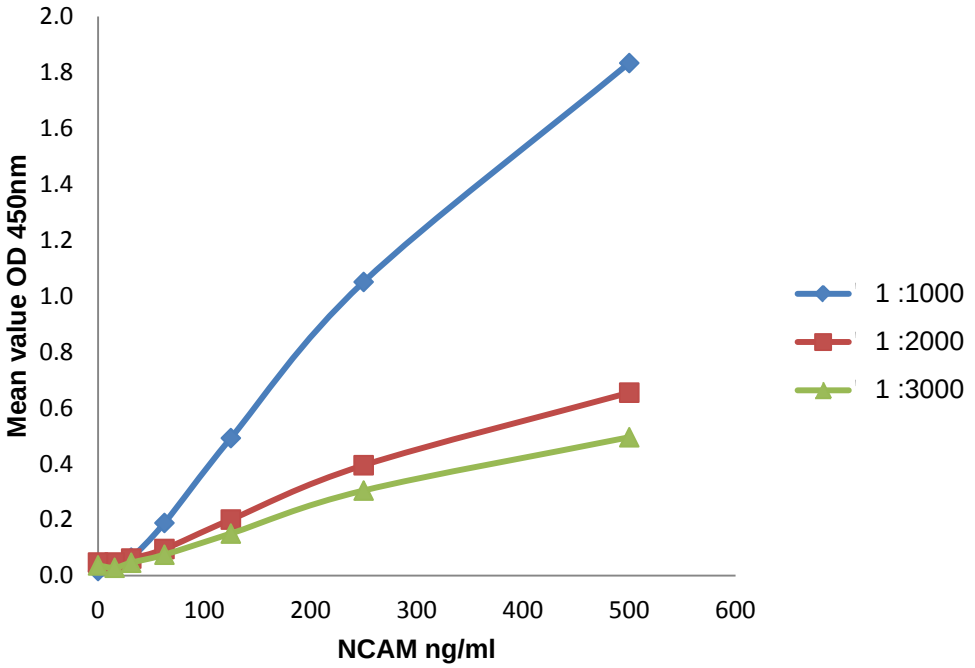

Figure 2-10 NCAM standard curves at varying concentrations of anti-species labeled antibody. Antibody was used at dilutions of 1:1000, 1:2000 and 1:3000.

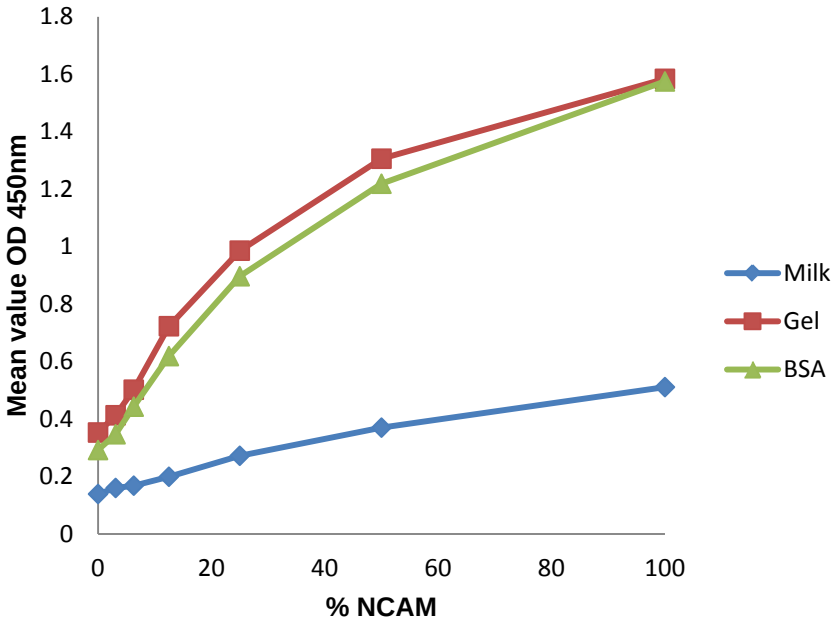

Figure 2-11 NCAM standard curves using different blocking solutions. Semi-skimmed milk (5%) gave the lowest assay background.

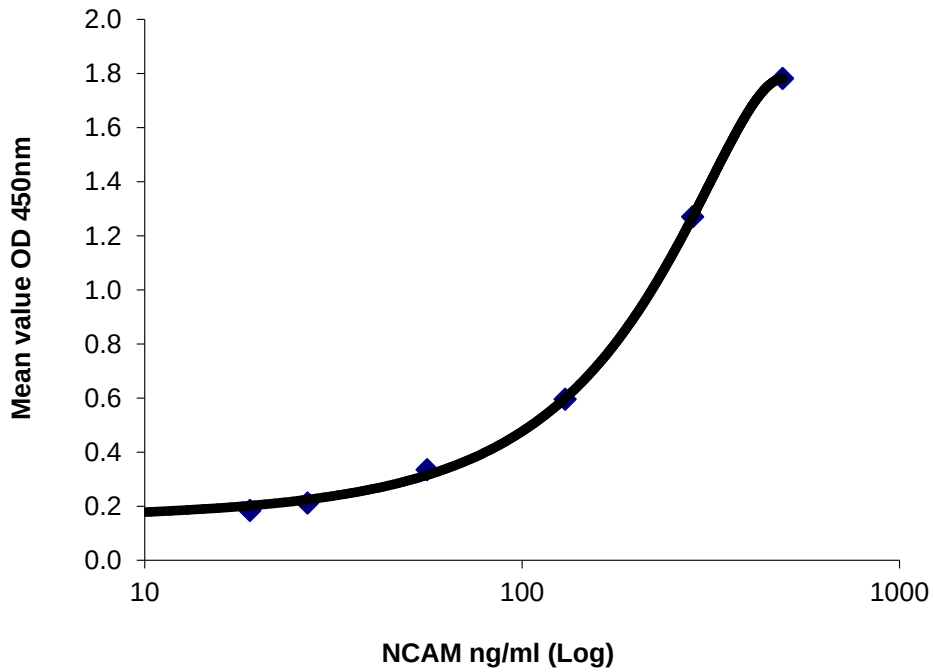

Figure 2-12 Typical NCAM calibration curve.

2.6.5 NCAM immunoassay characteristics

A typical calibration curve for the NCAM assay is shown in Figure 2-12, the minimum detectable concentration was 14.86 ng/ml (this was derived from twenty replicates of the zero concentration sample and the apparent concentration at two standard deviations from the mean was determined). Precision of the NCAM assay was assessed throughout its working range. Table 4 shows the intra-assay and inter-assay precision expressed as coefficient-of-variation (CV%) at each concentration level and the variability of observations for the quality control performed over twenty days was found to be within two standard deviations (SD) of the expected concentration for all but two of the readings performed on days 4 and 11 (Figure 2-13).

I found the concentration-response relationship of NCAM in the CSF matrix to be similar to that in the substitute standard curve matrix to allow extrapolation of sample concentrations in the range of the standard curve (Figure 2-14).

Table 2-4 Precision profile for the NCAM ELISA (SD, CV%). Table shows the intra-assay (repeatability) and inter-assay (within laboratory) precision in standard deviation (SD) and coefficient of variation (CV, %) of the ELISA over the range of concentrations analysed.

NCAM concentration (ng/ml)	n	Intra-assay		Inter-assay	
		SD	CV	SD	CV
15.6	5	0.5	3.3%	1.4	9.2%
31.3	5	1.0	3.1%	1.5	4.6%
62.5	5	1.7	2.7%	2.8	4.5%
125	5	3.7	2.9%	4.3	3.5%
250	5	11.4	4.5%	14.2	5.7%
500	5	14.2	2.8%	18.9	3.8%

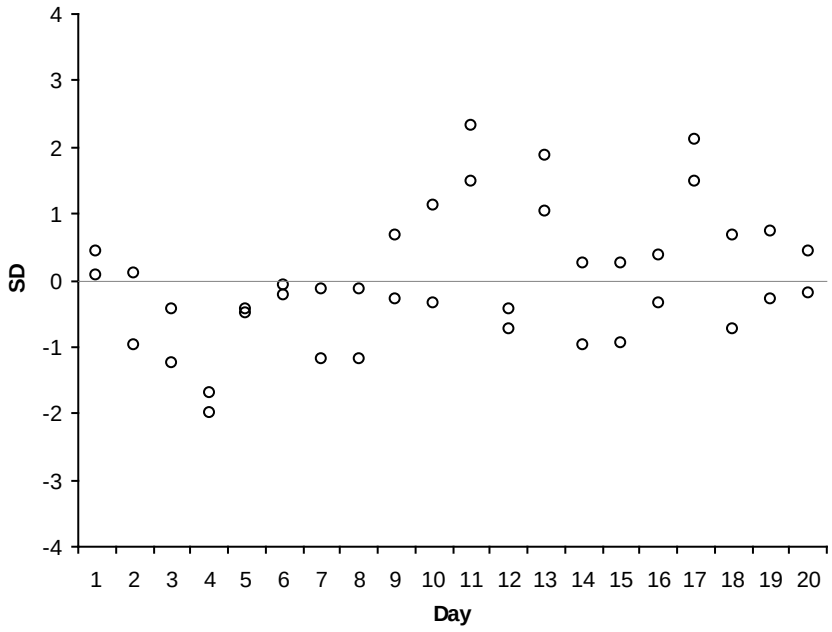

Figure 2-13 Levey-Jennings precision plot of variability in NCAM values by day. QC limits were set at mean ± 2SD. The plot demonstrates that there are no systematic errors in analytical runs.

The stability of NCAM in CSF after freeze-thaw, bench-top and freezer storage was examined. Triplicate aliquots of study CSF were frozen at -80^{o}C and then taken through five repeated freeze/thaw cycles, and also stored at ambient temperature, refrigerator (+4^{o}C), and -20^{o}C for a seven-day period. Analysis revealed a good freeze/thaw and storage stability of CSF NCAM under these conditions (Figure 2-15). Lastly, four CSF samples were spiked with the 500 ng/ml top standard in a 1:1 ratio, and the recovery calculated as a ratio between the measured and expected values (Table 2-5). The mean recovery was 100.6% (range 88-104%).

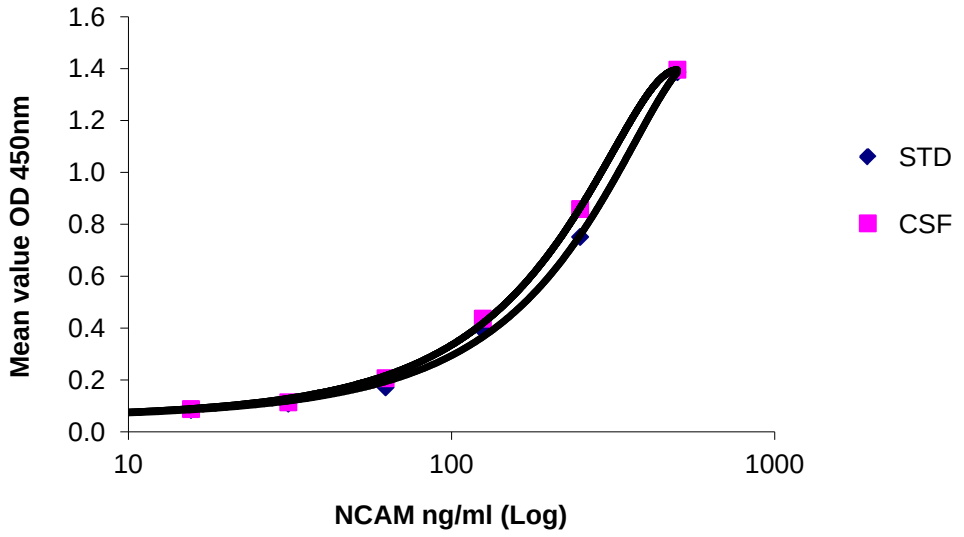

Figure 2-14 Parallelism between NCAM in the reference calibrator and the CSF. Serial dilutions of CSF across the working range of the assay shows good parallelism with the reference standard suggesting that CSF NCAM corresponds exactly with those in the assay calibrators.

Figure 2-15 NCAM freeze/thaw and storage stability (below).

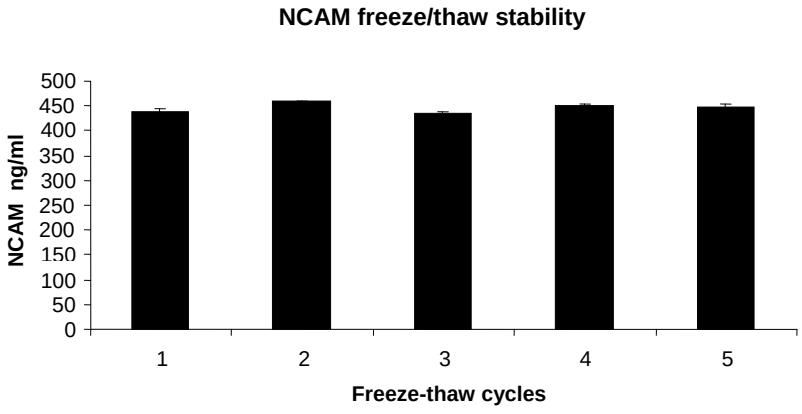

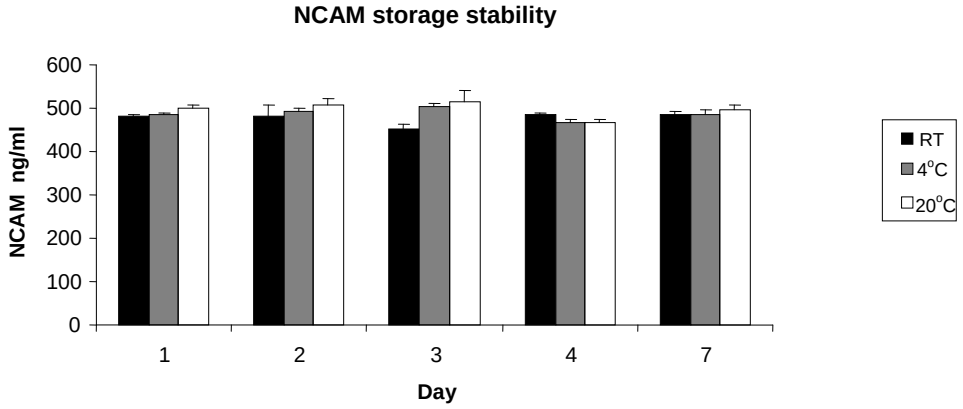

CSF sample	NCAM values			
	Unspiked (ng/ml)	Spiked observed (ng/ml)	Spiked expected (ng/ml)	Observed/Expected (%)
1	**569.4**	**470.8**	**534.7**	**88.0**
2	**645.7**	**560.9**	**572.8**	**97.9**
3	**511.3**	**502.4**	**505.6**	**99.4**
4	**262.1**	**397.96**	**381.0**	**104.4**

Table 2-5 Spike and recovery of NCAM in CSF samples. Expected values were calculated by adding endogenous NCAM values, from unspiked samples to those of spiked diluent control (i.e. standard). Percentage recovery was determined by dividing observed by expected values.

2.6.6 CSF NCAM values in neurological disorders are a potential prognostic indicator of neuronal plasticity

The mean NCAM values ± SD (ng/ml) were 308 ± 101 (BIH), 250 ± 107 (MS), 307 ± 109 (neuropathy), 250 ± 98 (AD), 293 ± 83 (CI), 357 ± 140 (MND), 170 ± 127 (meningitis), 515 ± 193 (viral encephalitis), and 412 ± 109 (controls) (Figure 2-16). The differences in mean NCAM values among the different categories were statistically significant (p<0.001) by one-way ANOVA. There were significant differences between the control and MS, AD and meningitis categories which had the lowest mean NCAM values. The viral encephalitis category were also found to be significantly different from all other diagnostic

categories examined except for controls; with HIV encephalitis/cryptococcal co-infection contributing to the very high levels (757-886 ng/ml), followed by HSV encephalitis (495-749 ng/ml). No significant differences were found regarding mean age (p=0.06), or sex (p=0.113). The mean albumin quotient and IgG index were 0.68 mg/l (range 0.12 – 3.35 mg/L) and 1.01 mg/l (range 0.26 – 6.84 mg/L), respectively. There was no correlation between the albumin quotient measures (r=0.20, p=0.13) and IgG index (r=-0.17, p=0.21) and CSF NCAM levels.

Further sub-group analysis of neuropathies into Guillain-Barré Syndrome (GBS), polyneuropathy, hereditary motor and sensory neuropathy (HMSN) gave mean NCAM values of 286 ± 80 ng/ml, 285 ± 117 ng/ml, 384 ± 99 ng/ml, respectively. Polyneuropathy was found to be significantly lower than controls (p=0.01) but did not differ from either GBS or HMSN. MS was sub-divided into clinically isolated syndrome (CIS), relapsing-remitting MS (RRMS), secondary progressive MS (SPMS) and primary progressive MS (PPMS) with mean NCAM values of 393 ± 83 ng/ml, 259 ± 87 ng/ml, 193 ± 97 ng/ml, 284 ± 32 ng/ml, respectively. Both RRMS (p<0.001) and SPMS (p<0.001) had NCAM values significantly lower than controls, whilst CIS was found to have higher values than RRMS (p=0.03) and SPMS (p<0.001). No inter-category differences were found between PPMS and the rest.

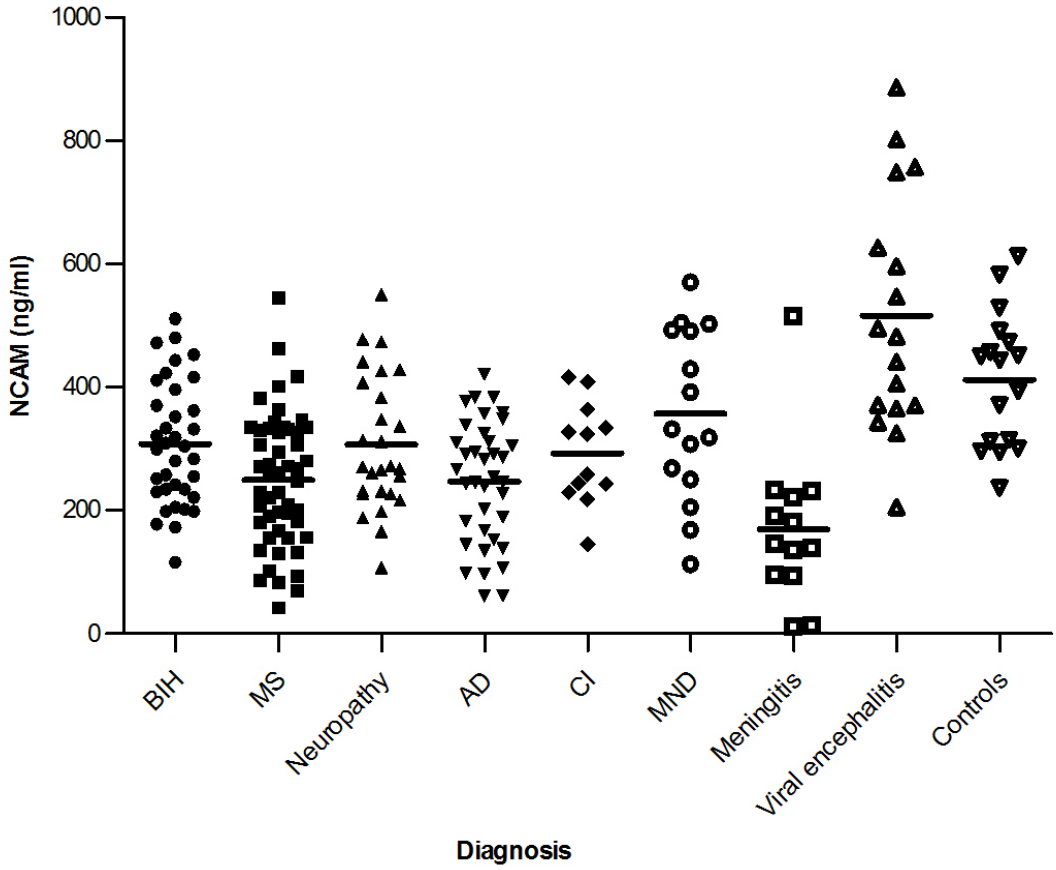

Figure 2-16 Quantification of NCAM in selected neurological disorders. Low NCAM values were measured in MS, AD and meningitis ($P<0.001$) when compared to controls. Viral encephalitis was significantly different from other neurological disorders but not controls.

2.6.7 NCAM antigen-specific antibodies in serum/CSF

NCAM antigen-specific antibodies were present in some of the MS serum samples tested but not all (Figure 2-17A). Conversely, out of the 50 CSF samples tested only one sample gave rise to a weakly positive result (marked by * in Figure 2-17B).

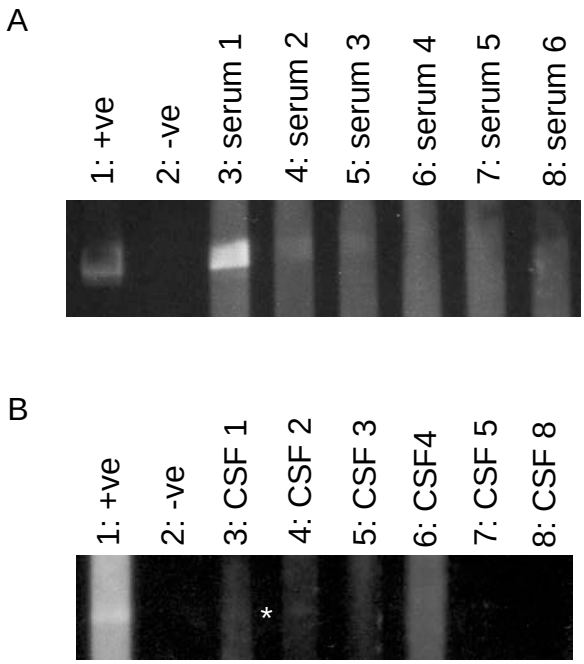

Figure 2-17 Western blots of NCAM antigen-specific antisera in MS and control samples. A) Serums. A strongly positive band was seen with serum 1 (lane 3), whilst serums 2, 3 (lanes 4, 5) displayed weakly positive bands. Serums 4-6 (lanes 6-8) were negative. B) CSFs. A weakly positive band was visible with CSF 2 (lane 4, marked by *), the remaining CSF samples were negative (lanes 3, 5-8).

2.7 Discussion

Immunocapture protein profiling by SELDI-MS has shown similarities and differences in NCAM in CSF compared to serum. In the CSF at least there is a restricted pattern of expression, indicating that the CSF composition of NCAM is intrathecal-specific. Under physiological conditions proteins within the CSF circulate into the vascular system, and as the CSF contains less protein compared to serum, any local differences are likely to be reduced in the serum. This was not evident in our paired CSF samples suggesting that other non-

neuronal tissues probably also contribute to serum NCAM composition. NCAM is predominantly expressed in the CNS in neurons and glial cells; however, it is also present in skeletal muscle, adrenal medulla, developing kidney, pancreatic islet cells and CD56 NK cells and may explain the soluble NCAM in the sera [144; 151; 152; 153; 154; 155]. The spectra of mass-to-charge ratios generated from a sample by SELDI-TOF MS do not infact identify proteins in that sample; however, by shotgun protein sequencing I was able to confirm the presence of NCAM within them. Subsequent ESI Q-TOF MS analysis of the CSF protein digest, however, was able to advance this further by providing information on potential NCAM isoforms candidates in the CSF through assessment of peptide sequence coverage. The extracellular segment as well as the intracellular cytoplasmic portion of NCAM was identified indicating that it is possible for all three isoforms of NCAM to be present in the CSF. A concept further supported by the western blot data where bands ranged from 115 – 220 kDa supporting the shedding of intact transmembrane isoforms. NCAM-120 has been described as the predominant size in the CSF using approximate sizing against molecular weight markers and owing to its largely extracellular configuration [104; 108]. Cox *et al*. provide evidence of ectodomain shedding of an extracellular 105-115 kDa fragment (NCAM-EC) and a smaller 30 kDa intracellular fragment (NCAM-IC) thought to be derived from the cytoplasmic domain of NCAM-140 [52]. Whilst Olsen *et al.* demonstrated shedding of the transmembrane NCAM in intact soluble form from membranes of cells transfected with this isoform [142]. Furthermore secretion studies timing the secretion of NCAM into neuronal cell culture medium demonstrated that this occurred 15-20 min before the accumulation of NCAM on the cell surface suggesting that soluble NCAM contains a secreted component [75].

I have chosen to look at CSF NCAM as it is most closely related to the brain and likely to be representative of brain pathology. Although soluble forms of NCAM have been observed in culture media and body fluids, it is unclear whether they have any biological role [131; 142; 143; 144]. It is postulated that soluble NCAM interferes with homophilic adhesion between membrane bound NCAM resulting in de-adhesion and thereby modulating NCAM-dependent neuronal growth. *In vitro* evidence from Olsen *et al.* [142] demonstrated that soluble NCAM inhibited cell binding to an immobilised NCAM substratum. Specific inhibition of NCAM release from the membrane by blocking metalloproteinase cleavage (using inhibitors BB-3103 or GM 6001) resulted in aggregation of neurons in primary hippocampal neurons in culture and NCAM-140 expressing B35 neuroblastoma cells [156; 157].

In this chapter, I have reported on an ELISA method for measuring NCAM levels in the CSF using readily obtainable commercial reagents. The ELISA was able to detect NCAM levels in a sensitive and reproducible manner. I also provide results on the distribution of NCAM levels in a variety of neurological disorders that suggest that NCAM measurements may be useful in quantifying capacity for repair in the nervous system. Previous groups have published work using NCAM ELISA [98; 137], however, without reference to assay validation and to my knowledge this is the first description of an ELISA using commercially available reagents.

Using this ELISA I found low NCAM levels in the CSF of MS, Alzheimer's disease and meningitis patients. We found the levels were independent of age and gender. It is possible that the low NCAM levels represent extensive

neuronal damage or a lowered potential for endogenous repair in these disorders due to chronicity or neurodegenerative aetiology. This is further substantiated by the sub-category analysis where low levels of NCAM were found in polyneuropathy compared to GBS and HMSN, and also SPMS (the progressive form of MS), in particular, and RRMS compared to CIS (early MS). Others have similarly demonstrated reduced NCAM levels in the CSF of MS patients, but not AD [98; 148]. Work by Thomaidou *et al*. [158] indicated involvement of soluble NCAM in Schwann cell migration and a lack there of in chronic MS and may be an important factor to take into account when looking at remyelination strategies. Conditions where no significant differences were noted from controls were BIH, CI, MND and viral encephalitis. However, the latter was the only category where very high levels were recorded, a few much higher than the control range. More extensive analysis using a larger sample size is required to investigate this further. Little in fact is understood about neuronal turnover in CNS infections, previous work in rabies have shown that the virus mediates entry at the neuromuscular junction via the NCAM receptor and that cells susceptible to rabies infection also express NCAM on their surface [159]. Whether other viruses are capable of a similar mode of entry is not known. Another possibility is that high NCAM levels are an indication of natural killer cell activity, as NCAM in neuronal surfaces is virtually identical to the CD56 leukocyte antigen found on the surface of Natural Killer (NK) cells and I may be indirectly measuring this in the CSF.

I found no correlation between CSF NCAM levels and CSF/serum albumin ratios suggesting that CSF NCAM was not the result of passive transfer of NCAM from serum to CSF following blood-brain barrier dysfunction. The

evaluation of local IgG production (IgG index) in these samples showed no relationship with CSF NCAM levels indicating that a rise in NCAM (a member of the immunoglobulin superfamily) levels was not a phenomenon similar to the local increase in the IgG index observed in the CSF of patients with multiple sclerosis [160]. In this study, I found anti-NCAM antibodies in some of the MS patient sera which have the potential to interfere with the detection of NCAM in ELISAs. In the samples tested, only one of the CSF samples tested gave rise to a weakly positive band. One possible explanation might be that there is a dilutional effect of antibodies in the CSF and if present at small quantities, may not be visible by western blotting. However, more work is needed to determine whether the anti-NCAM antibodies present in serum have the ability to inhibit the detection of NCAM in an ELISA system; this may depend on the affinity of the antibodies involved, the sharing of epitopes, and the concentration of anti-NCAM antibodies.

In conclusion, my preliminary work points to interesting findings about soluble NCAM and how it varies between different neurological conditions. Using SELDI MS and ESI Q-TOF MS analysis I was able to demonstrate that NCAM is present in similar quantities in the CSF as well as serum, the composition of isoforms is both extracellular and intracellular, and the total levels are comparatively lower than expected in MS, Alzheimer's disease and meningitis. This may be a reflection of the extent of neuronal injury or underlying neurodegenerative aetiology, or both. Therefore, low NCAM levels may not be unique to a particular disorder, they may however, have an overall prognostic significance.

3 Progression in multiple sclerosis is associated with low endogenous NCAM in models

3.1 Introduction

MS is the prototypical inflammatory demyelinating CNS disorder. It has a varied onset and disease course, but progression is the ultimate outcome in the majority of cases. New concepts in pathogenesis have emerged and include theories on axonal degeneration as a prerequisite for progression and remyelination and repair as being important for recovery [161; 162; 163]. Remyelination is a frequent finding at the edges of most chronic plaques but absent within its centres [82]. It is a consistent feature in early lesions exemplified by shadow plaques (Figure 3-1) [80]. Axonal plasticity, however, is less well documented. Many argue that adult CNS does not spontaneously regenerate after injury, a view that has been prevalent for over a century (S. Ramon Y Cajal, 1989) [26]. However, functional plasticity has been visualised in MS patients using fMRI despite a high burden of cerebral pathology [164].

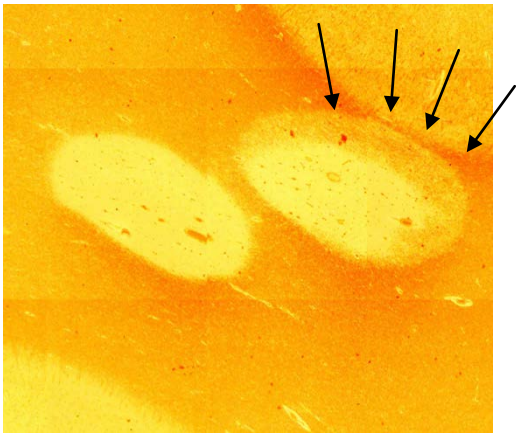

Figure 3-1 Remyelination in MS. A shadow plaque in MS demonstrating Remyelination (arrows). The histologic section was immunostained for myelin basic protein. Image courtesy of Dr K Schmierer, London, UK.

In order to be able to recapitulate developmental events for neuronal growth and to enable response to guidance cues, the regenerating axon needs to express the correct complement of cell surface molecules. A plethora of cell adhesion molecules have been identified, but the neural cell adhesion molecule (NCAM) is one of the most-widely studied and best characterised, being intimately linked to the process of axonal outgrowth, guidance and fasciculation [47; 123; 124; 165]. It not only serves as “glue” in cell-cell adhesion and contact-mediated attraction, but also interacts with a number of heterophilic binding partners such as fibroblast growth factor receptor (FGFR) [166], adhesion molecule L1[167], ATP [168], prion protein (PrP) [169], and has also been recently suggested to regulate signalling via the receptors for other growth factors; brain-derived neurotrophic factor (BDNF) [170], glial cell line-derived neurotrophic factor (GDNF) [171; 172], platelet-derived growth factor (PDGF) [173], and epidermal growth factor receptor (EGFR) [174]. This ability to interact with multiple binding partners may lead to diverse results based on the potential complexes formed.

Evidence from NCAM-null mice suggests that though NCAM is not essential for survival, they demonstrated a reduction in olfactory bulb size, abnormal fasciculation of hippocampal mossy fibres and a deficiency in long term potentiation [49; 51; 175]. More recent work, however, clearly demonstrates severe hypoplasia of the long axonal projection, the corticospinal tract [176], and pronounced alterations in the recycling of synaptic vesicles at the neuromuscular junction, with an inability to sustain high-frequency nerve transmission [58]. MS patients enter a progressive phase characterised by primarily motor deficits in walking, this is largely attributable to dysfunction in the long spinal tracts, which have lesser likelihood of instituting successful repair

and reinnervation following injury, and NCAM may have an important role to play in locomotor recovery. Moreover, NCAM has been shown to be involved in contact-mediated axon-glial signalling influencing the survival and outgrowth of oligodendrocytes following contact with the axon during myelination [122]. Whilst, double MAG (myelin-associated glycoprotein)/NCAM knockouts demonstrate pronounced axonal pathology even in the absence of overt dysmyelination, possibly by altering the function of specialised membranes such as lipid rafts, and thus disturbing the functional integrity of axons leading to axonal injury [177].

Experimental autoimmune encephalomyelitis (EAE) has long been used as an animal model of MS. It is primarily a T-cell mediated disease and is dominated by macrophage-mediated inflammation at the end stage [178]. Depending on the antigen and mode of sensitisation different aspects of MS pathology can be produced. Axonal loss occurs with each relapsing attack and probably continues into the chronic progressive phase, alluding to a causal relationship between inflammation, axonal degeneration, and irreversible neurological disability [179; 180]. In contrast, limited repair of myelin damage can be achieved [181], but structural reconnection and functional repair can only be achieved early in the disease in the presence of sufficient reserve capacity [182]. The EAE model therefore presents an opportunity for determining the impact of inflammation and axonal degeneration on means of recovery in MS. Another route to explore this aspect further is through *in-vitro* neuronal culture models; previously demyelinating mechanisms related to MS have been studied in neuronal cell cultures from foetal rat brain. Exposure to anti-myelin oligodendrocyte glycoprotein (α-MOG) has been shown to result in demyelination, and MBP synthesis resumes following removal of demyelinating agents predictably,

providing a unique model to study the effects of demyelination on axonal plasticity [183; 184].

3.2 Aims

The preliminary findings from chapter 2 point toward NCAM possibly being lowered after neuronal injury or neurodenegeration, and I wanted to test this further in models of neuronal injury in order to elucidate the molecular processes that take place in greater detail. The aim of this chapter was to investigate the impact of inflammation/demyelination and axonal injury on NCAM using *in-vitro* culture and EAE models.

In order to achieve this, NCAM was quantified by ELISA in CNS neuronal aggregates over time and under demyelinating experimental conditions to study its effect on axonal plasticity.

Further assessments of NCAM levels were carried out in acute and chronic EAE models to obtain an insight into the endogenous reserve capacity of inflammatory CNS disorders.

3.3 Materials and methods

NCAM concentrations were determined in neuronal aggregates and mice spinal cord tissues by a modification of the method for the commercial sandwich enzyme-linked immunoassay from R&D Systems (#DY2408). The assay was

suitable for the analysis of cell culture supernatants and detected NCAM concentrations in the picogram (pg)/ml range required for this portion of the work. Assay reproducibility was checked prior to use.

The rat CNS neuronal aggregate system was maintained by Dr Sam Jackson, Blizard Institute, Queen Mary University of London. Serum free, rotation-mediated neuronal aggregate cultures were prepared from foetal Sprague Dawley rat telencephalon (adult timed pregnant rats were obtained from Charles River, Margate, Kent) as previously described [183]; experiments were performed in accordance with the UK Animals (Scientific Procedures) Act 1984, under the control of the UK Government Home Office. Preparative steps are detailed below. A list of solutions used can be found in the Appendix to Chapter 3.

EAE induction in SJL/J (using active immunization with proteolipid protein-residues 139-151 peptide in Freunds complete adjuvant) and C57BL/6 mice (using active immunization with MOG-residues 35-55 peptide in Freunds complete adjuvant), representative of relapsing-remitting and chronic EAE, respectively, were performed by Dr Peggy Ho, Department of Neurology and Neurological Sciences, Stanford University School of Medicine, CA. Female SJL/J and C57BL/6 mice were obtained from The Jackson Laboratory (Bar Harbor, ME, USA). All animal protocols were approved by the Division of Comparative Medicine at Stanford University School of Medicine, in accordance with the National Institutes of Health guidelines.

3.3.1 The rat CNS aggregate cell culture system

Pregnant rats were sacrificed by decapitation at the age where their foetuses were 16 days old; the embryos were removed and placed in sterile ice-cold D1 solution (see 3.6.1). The foetal telencephalons were dissected out. After washing twice in D1 solution, brain tissue was progressively dissociated by sieving through a 200 µm pore followed by 115 µm pore nylon mesh (Nybolt, Zurich, Switzerland). The filtrates were centrifuged at 300 x *g* for 15 min at 4^{o}C and tested for viability using 0.1% trypan blue exclusion and then re-centrifuged. The remaining telencephalon cell population was seeded at 4 x 10^{7} cells per flask and incubated at 37^{o}C in a humidified 10% CO_2/ 90% O_2 atmosphere (Heraeus incubator, Philip Harris Scientific, UK) under continuous rotation (Kuhner Shaker, Philip Harris Scientific, UK). The rotation speed was increased from 0.15 to 0.18 g over the first week of incubation to enable optimal cell aggregation. The day of seeding was termed 'Day *In-Vitro*' zero (DIV 0). Cells were subsequently transferred to larger flasks on DIV 2, and the DMEM (Gibco BRL) was doubled to 8 ml. On DIV 5, 8, 11, 14 and subsequently every other day, cultures were fed by replacing 5 ml of pre-warmed DMEM in each flask (Figure 3-2).

3.3.1.1 Demyelination protocol

Z12 mouse IgG2a-MOG specific antibody (a gift from P. Smith, NL) plus complement (guinea pig serum, Serotec) was added to pre-warmed culture medium, whilst control cultures received either medium alone or IgG2a (Sigma)

as an IgG control were added at DIV 25 for 72 h. Cultures were maintained as normal, substituting medium for supplemented medium on DIV 21 and 23. Antibody was removed by medium replacement three times on DIV 29. Control flasks were also subjected to triple medium replacement.

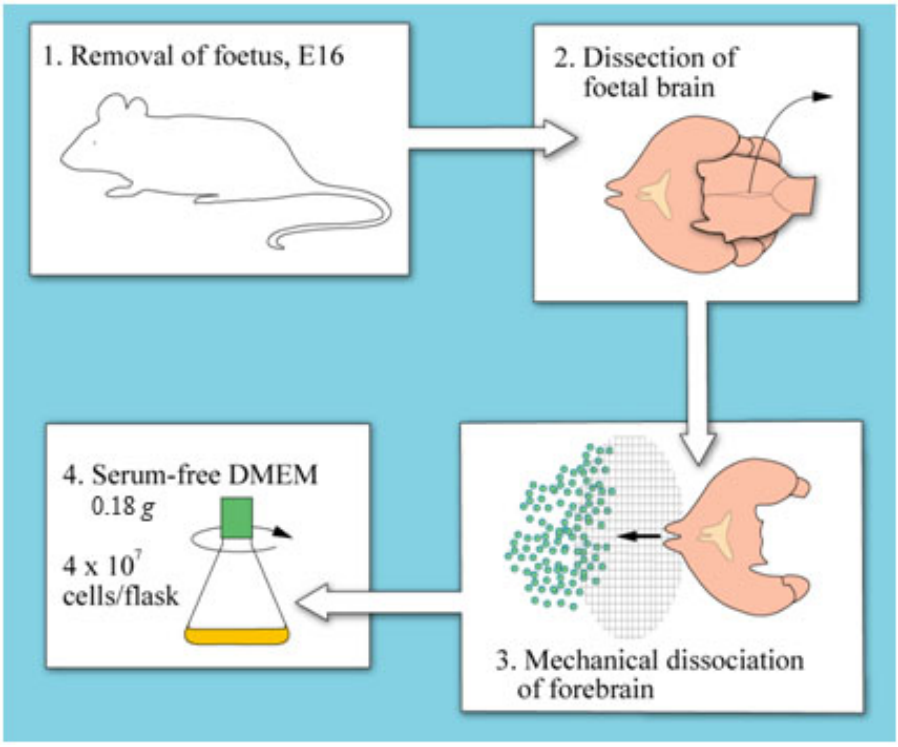

Figure 3-2 Steps detailing the preparation of rat CNS neuronal aggregate cultures. Embryonic E16 rat brain were dissected and dissociated mechanically by sieving. Dissociated cells form aggregates maintained as rotation-mediated free floating aggregate cultures.

3.3.1.2 Sampling of aggregates

For analysis by ELISA aggregates were sampled at various time points DIV 25 – 40. They were homogenised for 30 s in 1:20 (w/v) Tissue Protein Extraction Reagent (T-PER, Pierce) with protease inhibitors at 20:1 (w/v) (Protease inhibitor cocktail, Sigma). Samples were then centrifuged at 1520 x *g* to remove

particulate material, and insoluble material was discarded. Total protein content was assayed using the Bio-Rad protein assay: 25 µl of reagent A was loaded into each well of a microtitre plate, followed by 10 µl of protein standard containing 0.063 mg/ml to 2 mg/ml protein and samples, and then 200 µl reagent B. The plate was then left to stand at room temperature for 10 minutes with agitation to mix the reagents and the final absorbances were read at 750 nm. The standards were plotted and the total protein value calculated from the standards. Samples were assayed in batches and stored at -80^{o}C.

3.3.2 Induction of EAE in SJL and C56BL/6 mice

Female SJL/J and C57BL/6 mice were immunised at 8-10 weeks of age with 0.1 mg PLP 139-151 (SJL) or MOG 35-55 (C57BL/6) in PBS emulsified in Complete Freund's Adjuvant (CFA) and were boosted intravenously with 400 ng *Bordetella pertusssis* Toxin (List Biological Laboratories, Campbell, CA) on days 0 and 2. Animals were examined daily for clinical signs of EAE and scored as follows: Grade 0, healthy; Grade 1, tail paralysis; Grade 2, hind limb paraparesis; Grade 3, hind limb paralysis; Grade 4, complete paralysis (tetraplegy); and Grade 5, death. A relapse was defined as an increase in one grade or more in the EAE scale, sustained for at least two consecutive days. At the times indicated, mice were euthanized and perfused with 40 ml ice-cold 1x PBS before brains and spinal cords were dissected and snap frozen for further analysis. Spinal cords were collected at specific stages of disease (see results section Figure 3-3 & Table 3-1).

Subsequently, spinal cords were mechanically homogenised in T-PER (Pierce) at 1:20 (w/v) of tissue to reagent on ice until all visible aggregates had disappeared. Homogenates were then centrifuged at 1520 x *g* for 30 min to remove particulate material, and insoluble material was discarded. To the resulting supernatants protease inhibitors (Protease inhibitor cocktail, Sigma) were added at 20:1 (w/v). Total protein content was determined as above. Samples were stored at -80^{o}C and assayed in batches.

3.3.3 R&D NCAM ELISA Protocol (#DY2408)

3.3.3.1 Plate preparation

Capture antibody at 2.0 µg/ml concentration in PBS, pH 7.4 (Sigma) without carrier protein were coated onto polystyrene Nunc-MaxiSorp^{TM} 96-well plate overnight at 4^{o}C. Afterwards, wells were washed once with PBS containing 0.05% Tween 20 (Sigma) and blocked with 300 µl 1% bovine serum (Sigma) in PBS and left for 1 hr at room temperature on a plate shaker to saturate the wells thoroughly and prevent non-specific binding of antigen. The plate was then rinsed with PBS-Tween.

3.3.3.2 Assay procedure

200 µl of sample or standards diluted in 50 µl of reagent diluent containing 1% bovine serum in PBS were applied to each well and incubated for 2 h at room temperature on a plate shaker. The final dilutions of the standard curve ranged from a top-standard of 2500 pg/ml to 156 pg/ml using two-fold serial dilutions in reagent diluent. Again, the wells were washed three times with PBS-Tween followed by the addition of 100 µl of the detection antibody at a final concentration of 200 ng/ml diluted in reagent diluent. After 2 h incubation at room temperature with shaking, wells were re-washed three times with PBS-Tween. 100 µl of streptavidin-HRP solution at a dilution of 1/200 (R&D Systems) in reagent diluent was applied to the wells and incubated for 20 min with shaking at room temperature (plate was covered to avoid exposure to light). After washing as before, 100 µl of substrate solution (1:1 admixture of Hydrogen Peroxide and Tetramethylbenzidine) was added and incubated for 10 min in darkness. The reaction was stopped by the addition of 50 µl of 2 *N* H_2SO_4 solution per well. The optical density at 450 nm with wavelength correction at 540 nm was read with a FLUOStar Omega plate reader (BMG Labtech). Sample values were calculated from the NCAM antigen standard curve and corrected by deducting blank values from wells coated with 1% bovine serum (zero standard). NCAM values were converted to per mg of protein based on previously calculated total protein measurements for the samples.

3.3.4 Statistical analysis

Neuronal culture analyses were performed using SPSS (version 16) statistical software. Before proceeding, the data were assessed for normality using

Shapiro-Wilk test. NCAM values were log-transformed and differences in mean NCAM values were tested for significance by one-way ANOVA with post hoc comparisons conducted using Tamhane test for unequal variances (the alpha was set at 0.05). EAE analysis was performed using GraphPad Prism (version 5) software, with Kruskal-Wallis test and Dunn's post hoc evaluation.

3.4 Results

3.4.1 Differential modulation of NCAM during development and following demyelination

In neuronal aggregates, NCAM concentrations decreased in all three experimental groups over the lifespan of the aggregate cultures suggesting a developmental reduction in the protein, a finding which is consistent with its role in axonal growth and plasticity (Figure 3-3). The introduction of the demyelinating agent α-MOG mAb at the optimum age of the cultures (DIV 25) resulted in a significant reduction in NCAM afterwards (Figure 3-3). A demyelinating insult therefore also results in changes to the underlying axon. By DIV 40, NCAM levels were comparable to those of control experiments, suggesting that the effect was reversible.

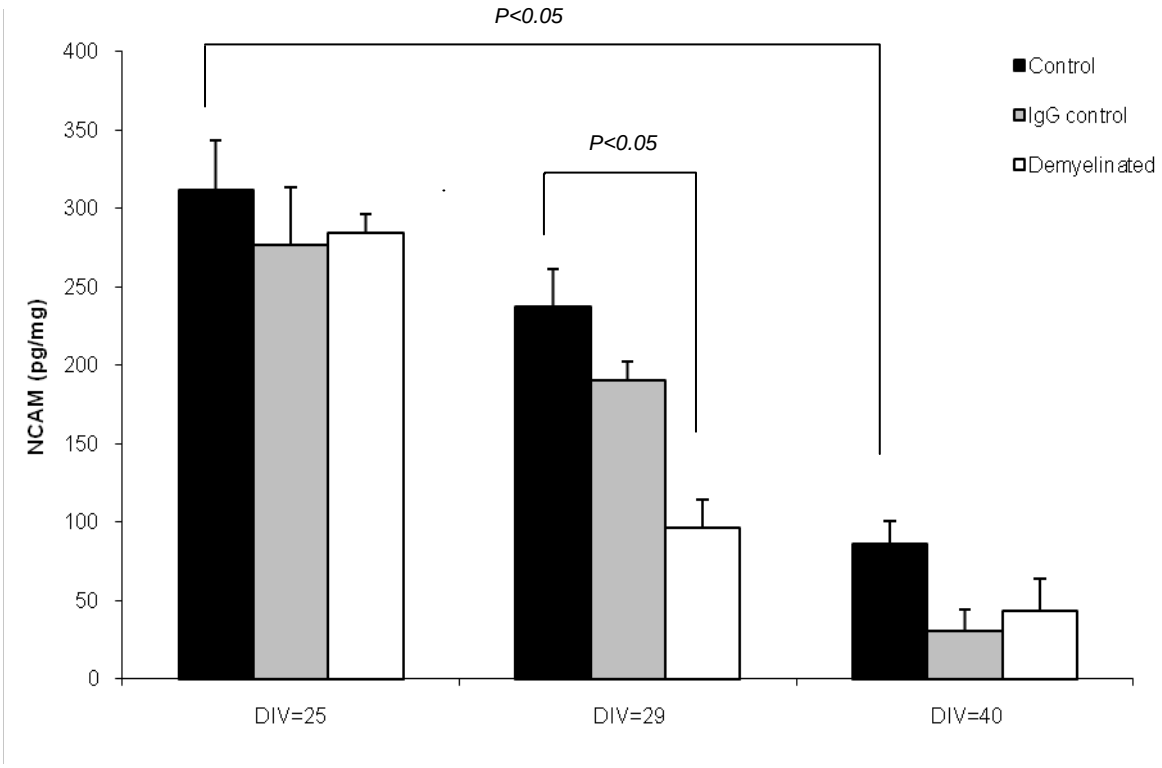

Figure 3-3 NCAM expression during demyelination and repair in 3D neuronal cultures. Neuronal aggregate cultures from rat telencephalon were grown and these were demyelinated by the addition of a MOG-specific antibody and complement or a non-binding mouse IgG2a control antibody on day. The results represent the mean NCAM (pg/mg) ± SE at day *in vitro* (DIV) 25, 29, and 40 and following demyelination with α-MOG.

3.4.2 Persistent reduction of NCAM in chronic EAE

NCAM was investigated in SJL and B6 mice that exhibit a relapsing-remitting disease course and a chronic course in EAE, respectively (Figure 3-4). There was a significant drop in NCAM levels in acute EAE at the peak of the disease in both models compared to naive animals suggesting a comparable pathophysiology. Similarly, during the chronic phase of the disease NCAM levels remained low in both models suggesting that there was no recovery in NCAM levels by this point. Although not statistically significant, during remission stages in the spinal cords of the SJL mice, an upward trend in mean NCAM

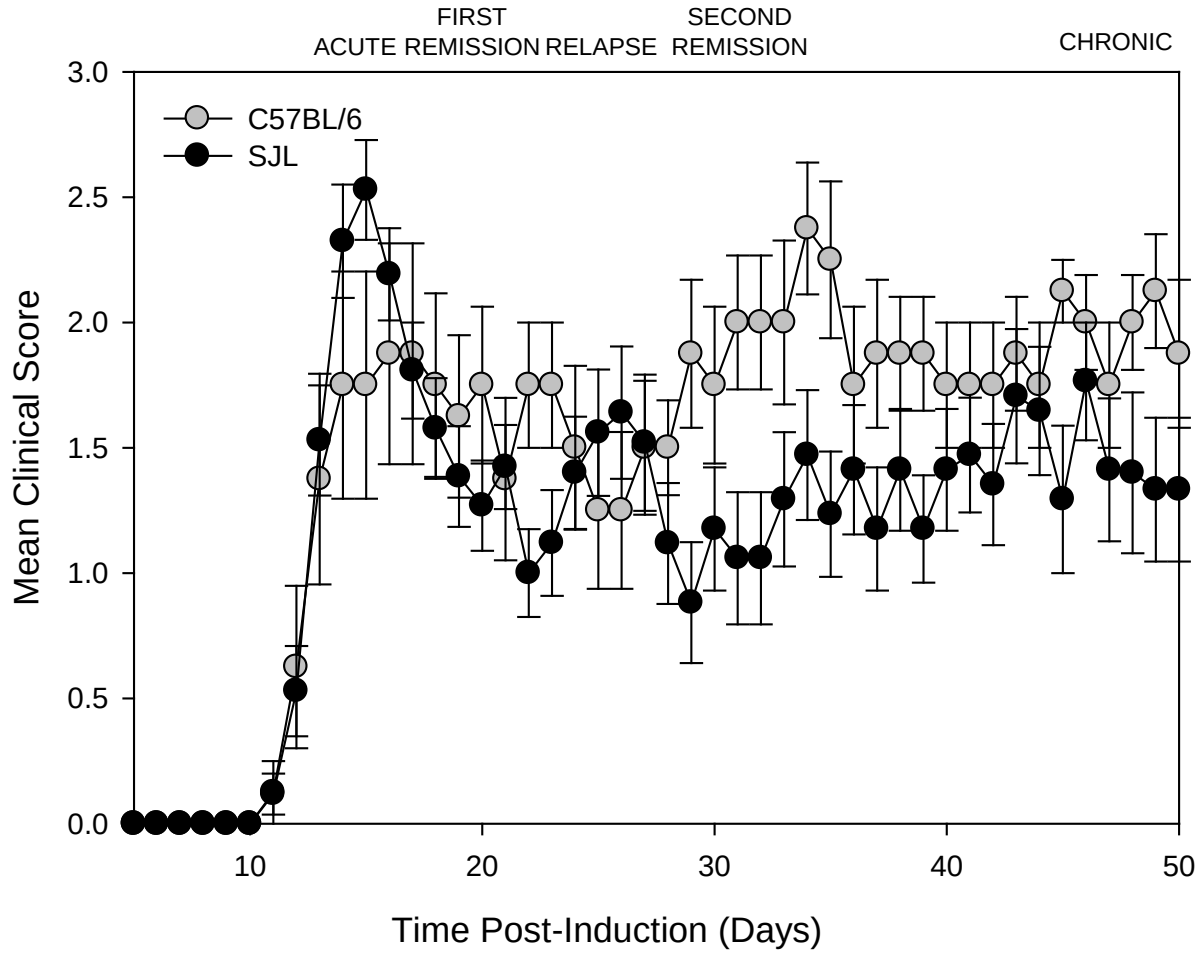

Figure 3-4 Neurological course of EAE in mice. SJL mice were sensitised with PLP peptide or C57BL/6 mice were sensitised with MOG peptide in Freunds adjuvant on day 0. The results represent the mean daily clinical score ± SEM (n ≥ 8). The approximate timing of each disease phase relative to disease in SJL mice is shown.

Table 3-1 Clinical disease scores of EAE in SJL and C57BL/6 mice during the different phases of EAE.

	Naive/CFA D21/D21	Acute D14/D18	RM1 D21/D21	Relapse D26	RM2 D52	Chronic D80/D52
SJL	0.0 ± 0.0	3.9 ± 0.1	1.1 ± 0.3	3.0 ± 0.2	1.5 ± 0.3	2.0 ± 0.0
C57BL/6	0.0 ± 0.0	2.4 ± 0.4	2.0 ± 0.0	n/a	n/a	1.9 ± 0.3

EAE was induced in mice on day 0. The results represent the mean clinical score ± SEM during active disease or the minimal score during remission when tissue were sampled for NCAM-specific ELISA (n ≥ 8). The days of sampling was indicated in white for SJL mice and grey for C57BL/6 mice. CFA=complete freund's adjuvant.

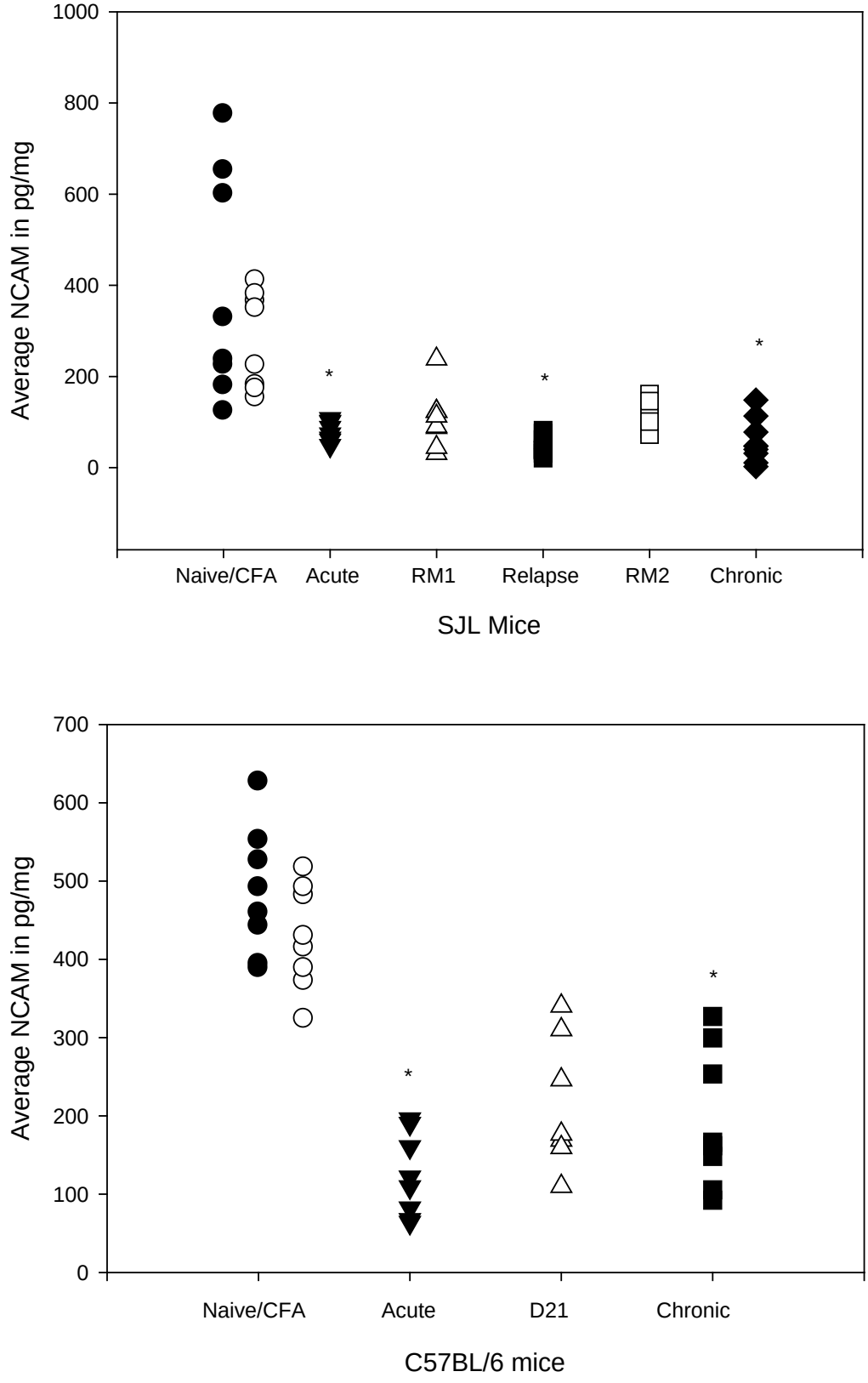

Figure 3-5 NCAM levels in spinal cords during EAE. Following the induction of EAE NCAM (pg/ml) levels were measured in SJL (top) and C57BL/6 (bottom) mice by ELISA. During EAE NCAM content reduced (*$P<0.05$).

levels was apparent (Figure 3-5). CFA also appeared to reduce NCAM content (open circles), though not statistically significant.

3.5 Discussion

Axonal recovery following inflammatory or demyelinatory injury requires the engagement of axonal signalling molecules in promoting neurite outgrowth. The cell adhesion molecule, NCAM, has long been indicated to possess this capability, through growth promoting signal transduction pathways conducive to axonal regrowth and synaptic plasticity [185]. Here *in-vitro* and *in-vivo* evidence suggesting that NCAM maybe irretrievably down regulated or damaged in the injured CNS following inflammation and demyelination is presented. Furthermore, this effect may be amplified by the temporal downregulation of NCAM with ageing.

Neuronal aggregates of dissociated rat foetal brain neuronal cells form when cells are brought in culture at concentration higher than 10^4 cells/ml, and can be used as highly reproducible alternatives to monolayer cultures of neurones [184; 186]. The analysis of NCAM concentration in these neuronal aggregates demonstrates the existence of a temporally precise modulation of NCAM concentration over time. Although the expression persists into the mature aggregates beyond that of what is considered developmental expression, it is only a fraction of the original NCAM content. This has obvious implications for enhancing repair in the ageing CNS. Antibody-mediated demyelination results in a marked reduction in NCAM suggesting acute axonal damage. This is

supported by previous work by Jackson *et al*. who demonstrated that demyelination induces immunopositivity to SMI32 antibody in aggregates, a marker of changed phosphorylation status in the axon [187]. Previous work in neuronal aggregates have only investigated the effects of demyelination induced by cytokines (TNF-α, IFN-γ and IL-1) or antibody directed against myelin (α-MOG) in this system, wherein myelin synthesis resumes following the removal of demyelinating agents. Analysis presented here provides evidence that short-term exposure to anti-MOG antibody resulting in demyelination also adversely affects neuronal plasticity in this aggregate system as well. This effect is transient with the NCAM content of aggregates being proportional to that of untreated and control cultures by DIV 40.

In EAE, a T-cell mediated inflammatory model, the drop in NCAM concentration is immediate and persists into the chronic stages suggesting that the outcome is identical despite the differences in aetiopathogenesis. The EAE findings further indicate that there is no definite recovery in NCAM levels during periods of disease remission and the precise point in the temporal decline in NCAM expression that occurs with ageing is reached much sooner than anticipated with inflammatory insults. Evidence from natural history studies in MS suggest that in patients this occurs during the sixth-decade of life and is unaffected by the initial course of MS, whether it be relapsing-remitting or progressive MS [188; 189]. These observations are supported by the results here, wherein the SJL mice which exhibit a relapsing-remitting course in EAE and the B6 mice which have a more chronic disease course, both demonstrate a similar reduction in NCAM concentrations despite their differences in disease pathophysiology. The degree and frequency of insult apparently makes little difference to the overall

outcome. Axonal injury is now considered a consistent feature of MS pathology, with evidence from EAE suggesting that axonal loss determines permanent neurological impairment [190]. Whilst, there is little information on axonal regeneration with the only evidence coming from focal spinal cord injury models but not EAE. Often the premise for regeneration is based purely on the amelioration of signs of EAE [191; 192]. By contrast, remyelination has been extensively studied and has been shown to promote functional recovery in these models [193]. It remains to be seen whether remyelination strategies alone can hold back the tide on disease progression.

In summary, demyelination and neurodegeneration characterise the course of multiple sclerosis. Although hallmarks of recovery (remyelination) have been documented in early MS, the regenerative capacity of the adult CNS remains uncertain. NCAM has been widely implicated in axonal outgrowth, guidance and fasciculation. Here, *in-vitro* and *in-vivo* models of MS were used to investigate its role in disease progression. It was evident that NCAM decreases over time with ageing in neuronal aggregate cultures and decreases acutely after demyelination and after the initial inflammatory episode in EAE, but remains reduced with subsequent relapses. This suggests that lower levels of NCAM, hence axonal plasticity may be associated with disease progression observed in MS. Alternatively, it demonstrates that NCAM was lost as EAE accumulated irreversible nerve loss that was associated with the chronic disability.

4 Growth Associated Protein (GAP-43):

Expression, purification and characterisation of recombinant GAP-43 protein tagged with V5 and poly His for the development of a sensitive quantitative ELISA for GAP-43

4.1 Introduction

The membrane protein GAP-43 (growth-associated protein of 43 kDa), also known as neuromodulin or B-50, was originally isolated in 1980 [194] and appeared to be a major protein present in synaptic plasma membranes. It is found in axons specifically associated with growth cones and immature synaptic terminals [59]. While GAP-43's precise function is not known, there are several lines of evidence to support for a role in pathfinding in axons. GAP-43 expression has been found to be greatly increased in growing [195] and regenerating axons, and in some mature axons capable of regeneration (i.e. those of fish and amphibians), axotomy resulted in a gross upregulation of the protein that coincided with, or preceded the initiation of axonal outgrowth [61]. Knock out mice lacking GAP-43 die early in the postnatal period, as well as having axons stall and then take random courses when they reach decision points such as the optic chiasm, suggesting that GAP-43 serves to amplify the response of growth cones to external cues [63; 196]. When GAP-43 is overexpressed in mice lesion-induced nerve sprouting and terminal arborisation during reinnervation were greatly potentiated [62].

GAP-43 is found exclusively in particulate fractions of brain tissue and absent from cytosolic subcellular fractions of peripheral organs [197]. Throughout life GAP-43 is found in high levels in neocortical association areas and the limbic system, presumably localised to areas rich in synaptic contacts [35; 198; 199]. Whilst in certain brain areas involved in ascending somatosensory information (e.g. cochlear nuclei, the vestibular complex or the sensory cortex) and motor control

(e.g. red nucleus, the motor nuclei of cranial nerves or the motor cortex), GAP-43 is essentially absent [200; 201].

In disease, GAP-43 was found to be reduced in a majority of white matter plaques in multiple sclerosis (MS), with the exception of remyelinated lesions where the expression was increased [111]. CSF GAP-43 levels negatively correlated with MRI measures of brain atrophy (r = -0.30), a marker of axonal injury [111]. A close study of the early stages of inflammatory lesions in the CNS in an animal model using targeted inflammatory lesions to the corticospinal tract, demonstrated that the axons remodelled in response to the lesions by recruiting local interneurones and collaterals closely associated with prolonged temporal expression of GAP-43. Moreover, behavioural studies showed that recovery was closely linked to these changes [182]. Reduced GAP-43 levels correlated with high neurofibrillary tangle density in Alzheimer's disease (AD) [202] and end-stage AD brains exhibit reduced neuronal expression of GAP-43 [203]. Positive correlation was found between CSF GAP-43 and tau, with significantly reduced levels in Parkinson's disease (PD) [110]. These observations suggest shared mechanisms in the respective cascades of neurodegeneration in these disorders. GAP-43 was reduced in bipolar disorder, the reduction correlating with disease duration, whilst in schizophrenic patients it was enriched in the visual association and frontal cortices, indicating that increased GAP-43 is associated with dysfunctional organisation of synaptic connections in schizophrenia [204]. GAP-43 plays a crucial role in axonal regeneration in avulsed motor neurones with up-regulation as early as day one accompanied by axonal regeneration [205]. In contrast, regeneration of rubrospinal tracts (CNS) into peripheral nerve grafts were detected after cervical and not after thoracic injury

with increased GAP-43 present only in the former, indicating that GAP-43 expression after injury is a prerequisite for CNS axonal regeneration and is diminished if the injury occurs farther from the cell body [206]. While there is evidence to suggest that external administration of growth factors BDNF and NT-4/5 into the vicinity of injured rubrospinal neurones stimulated GAP-43 and prevented neuronal atrophy [207]. Tacrolimus (FK506), an immunosuppressant, increased the number of GAP-43 positive neurones after spinal cord injury in the rat paralleled by significant improvement in neurological function [208].

GAP-43 can therefore serve as a growth cone marker protein, potentially advancing our understanding of regulation of neuronal growth and response to disease. CSF GAP-43 is presumably the secreted GAP-43 that is localised in presynaptic membranes, but must be permealised for it to be recognised. The GAP-43 protein is highly hydrophilic (isoelectric point of 4.3 – 4.5), except for the small membrane binding domain and entirely conceivable that it can exist as a soluble protein. Qualitative western blot analysis reveals a major band at ~ 50 kDa (molecular weight range 47 – 53 kDa) [209; 210; 211], densitometric assessment of this band is one possible approach to estimating GAP-43 protein content, although performing it is cumbersome with inconsistent measures. At the time this study was performed, ELISA protocols for GAP-43 utilised partially purified protein with the estimation of total protein or simply arbitrary values [199; 212] or recombinant protein gifted from another source without the details of production [109; 110; 111]. There was no commercially available recombinant protein as it is technically difficult to secrete via a vector expression system since it attaches to the inner membrane surface preventing its release [35].

4.2 Aims

The aims of the work presented in this chapter were to develop a method for producing and purifying recombinant GAP-43, in preparative quantities for use in an ELISA system. The GAP-43 was to be as pure as possible, retaining the folding and post-translational modifications of authentic GAP-43 and therefore maintaining its antigenicity towards anti-GAP-43 antibodies. It would then be used as the standard in a quantitative ELISA for detecting CSF GAP-43 in neurological disorders. The chapter also describes the validation steps in the development of CSF GAP-43 ELISA.

4.3 Materials and methods

4.3.1 The construction of GAP-43 recombinant protein

All reagents used for the expression of GAP-43, including the baculovirus expression system and cell culture reagents were from Invitrogen (Paisley, UK) unless otherwise stated.

The amino acid sequence for GAP-43 (UniProt #P17677) is illustrated in Figure 4-1. Its membrane localisation is primarily due to a short amino terminal sequence comprising of the first ten amino acids of the N-terminus. Cysteines 3 and 4 are crucial for the membrane association [213; 214]. Therefore, when producing the soluble recombinant fusion GAP-43 protein we omitted the membrane binding area and used only amino acids 11 – 238 (Val – Ala) of GAP-43 to allow for its secretion during the expression phase of protein

production. The final construct generated encodes 287 amino acids long sequence which also contains an IL-2 signal peptide sequence at the N-terminus and a linker sequence plus V5 epitope and polyhistidine tag (V5-His tag) at the C-terminus (Figure 4-2, 4-3).

```
        10         20         30         40         50         60
MLCCMRRTKQ VEKNDDDQKI EQDGIKPEDK AHKAATKIQA SFRGHITRKK LKGEKKDDVQ

        70         80         90        100        110        120
AAEAEANKKD EAPVADGVEK KGEGTTTAEA APATGSKPDE PGKAGETPSE EKKGEGDAAT

       130        140        150        160        170        180
EQAAPQAPAS SEEKAGSAET ESATKASTDN SPSSKAEDAP AKEEPKQADV PAAVTAAAAT

       190        200        210        220        230
TPAAEDAAAK ATAQPPTETG ESSQAEENIE AVDETKPKES ARQDEGKEEE PEADQEHA
```

Figure 4-1 The amino acid sequence for GAP-43. We used the mRNA transcript 'GAP-43, Accession no. NM_002045' to generate this protein.

M Y R M Q L L S C I A L S L A L V T N S V E K N D D D Q K I E Q D G I
K P E D K A H K A A T K I Q A S F R G H I T R K K L K G E K K D D V Q
A A E A E A N K K D E A P V A D G V E K K G E G T T T A E A A P A T G
S K P D E P G K A G E T P S E E K K G E G D A A T E Q A A P Q A P A S
S E E K A G S A E T E S A T K A S T D N S P S S K A E D A P A K E E P
K Q A D V P A A V T A A A A T T P A A E D A A A K A T A Q P P T E T G
E S S Q A E E N I E A V D E T K P K E S A R Q D E G K E E E P E A D Q
E H A I Q H S G G R S S L E G P R F E G K P I P N P L L G L D S T R T
G H H H H H H

Figure 4-2 The amino acid sequence of the recombinant GAP-43 protein. The IL-2ss-GAP43-V5-poly(His) construct has an IL-2 secretion sequence at the N-terminus (in pink) and a linker sequence plus a V5-poly(His) tag at the C-terminus (in blue). The GAP-43 sequence is in black.

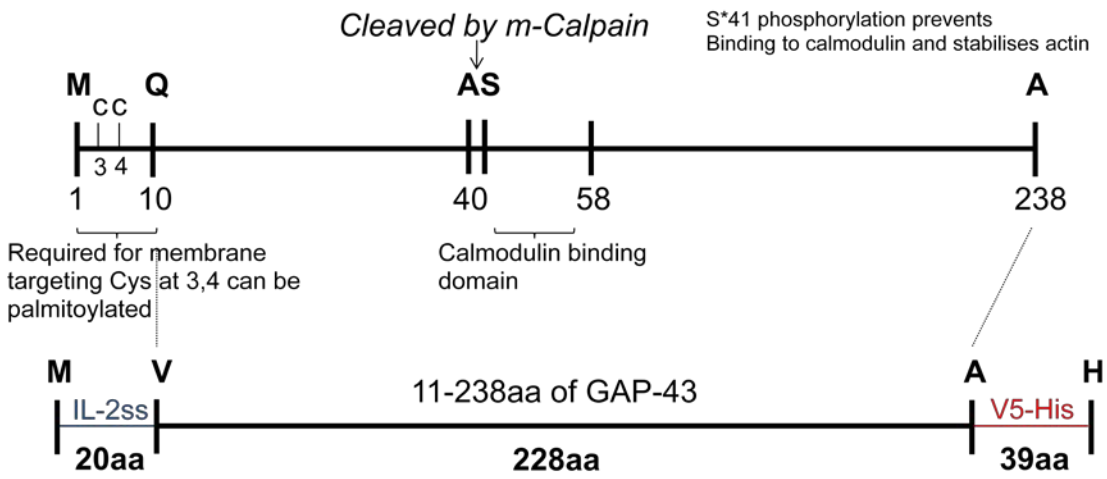

Figure 4-3 Attributes of the recombinant GAP-43 protein. A) native protein and B) engineered IL2ss-GAP43-V5-poly(His) tag protein. The engineered protein is 287 amino acids long compared to the native 238 amino acid GAP-43 and lacks the N-terminus membrane-binding region (amino acids 1-10) which has been replaced by the 20 amino acid IL-2ss at the N-terminus and the 39 amino acid linker sequence plus V5-His tag at the C-terminus. Palmitoylation of Cys 3, 4 is required for plasma membrane association. The calmodulin binding domain (amino acids 43-58) and several phosporylation sites, including serine 41 remain unchanged. Phosphorylation at serine 41 by protein kinase C (PKC) regulates calmodulin binding and modulates the ability of GAP-43 to facilitate neuronal growth. M-calpain mediated GAP-43 proteolysis creates a truncated GAP-43, which is believed to activate G_o-mediated growth cone collapse.

The IL-2 signal peptide improves the level of secretion of recombinant proteins in the baculovirus expression system by directing the GAP-43 propeptide to the endoplasmic reticulum and through the secretory pathway [215]. GAP-43 is expressed as a fusion to the V5-His tag via a peptide linker to facilitate immunodetection and protein purification. The recombinant GAP-43 protein was designed by Dr Nasim Yousaf at the Bone and Joint Research Unit, Barts and The London, Queen Mary's School of Medicine and Dentistry, London.

4.3.2 Experimental outline of the baculovirus expression system

The figure 4-4 below illustrates the steps required to express the GAP-43 gene using the baculovirus expression system.

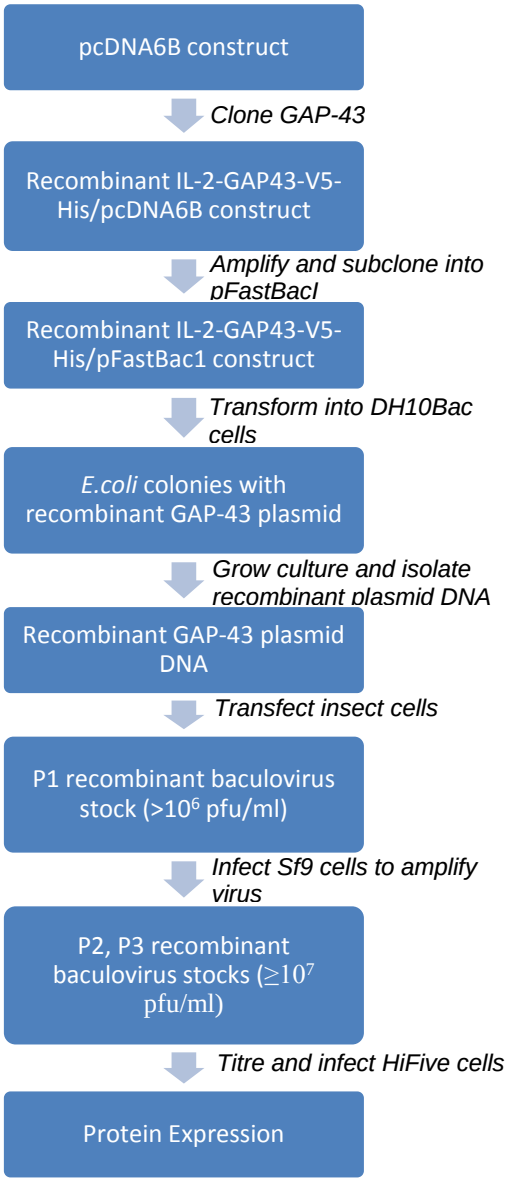

Figure 4-4 The flow chart demonstrates the experimental outline of the steps used to express GAP-43 gene using pcDNA6B and pFastBacI vectors and generate recombinant baculovirus used in protein expression. Initially GAP-43 gene was cloned into pcDNA6B vector and the construct was amplified by PCR. The PCR product was recovered and subcloned into the pFastBacI vector. The final recombinant vector was used to transform recipient *E.coli* cells and the plasmid DNA was harvested. The final steps of transfection of

GAP-43 recombinant DNA into insect cells lead to the generation of baculovirus particles that were scaled up in successive rounds of infection and later used for protein expression.

4.3.2.1 Recombinant GAP-43 protein (IL-2-GAP43-V5-His) construct

The complementary DNA encoding amino acids 11-238 of GAP-43 was cloned in-frame downstream of the secretion signal from IL-2 gene, which had previously been subcloned into mammalian pcDNA6/V5-HisB vector (Invitrogen, Figure 4-5). The cloning strategy allowed the generation of V5 and 6xHis tags at the C-terminus of the GAP-43 protein (Figure 4-3), and these tags were used for immunodetection and purification, respectively. Using this construct as a template, the IL-2ss-GAP43-V5-His was amplified by PCR using the forward primer (5'- ACGAATTCGGTTGAAAAAAATGATGACGACC –3') and the reverse primer (5'- GGCATGTTCTTGGTCAGCCTC –3'). The PCR product was then recovered from the PCR reaction by ethanol precipitation, digested with BamH*I/PmeI* and subcloned in frame into the baculovirus vector pFastBac1 (Invitrogen, Figure 4-6) cut with *BamHI/StuI*. The final construct generated encodes IL-2ss-GAP43-V5-His. The IL-2ss-GAP43-V5-His/pFastBacI construct was transformed into Competent DH10Bac cells (*Escherichia coli*) for amplification. Subsequently, the recombinant plasmid was prepared from this and later transfected into Sf9 insect cells (*Spodoptera frugiperda*) to produce the first P1 baculovirus stock.

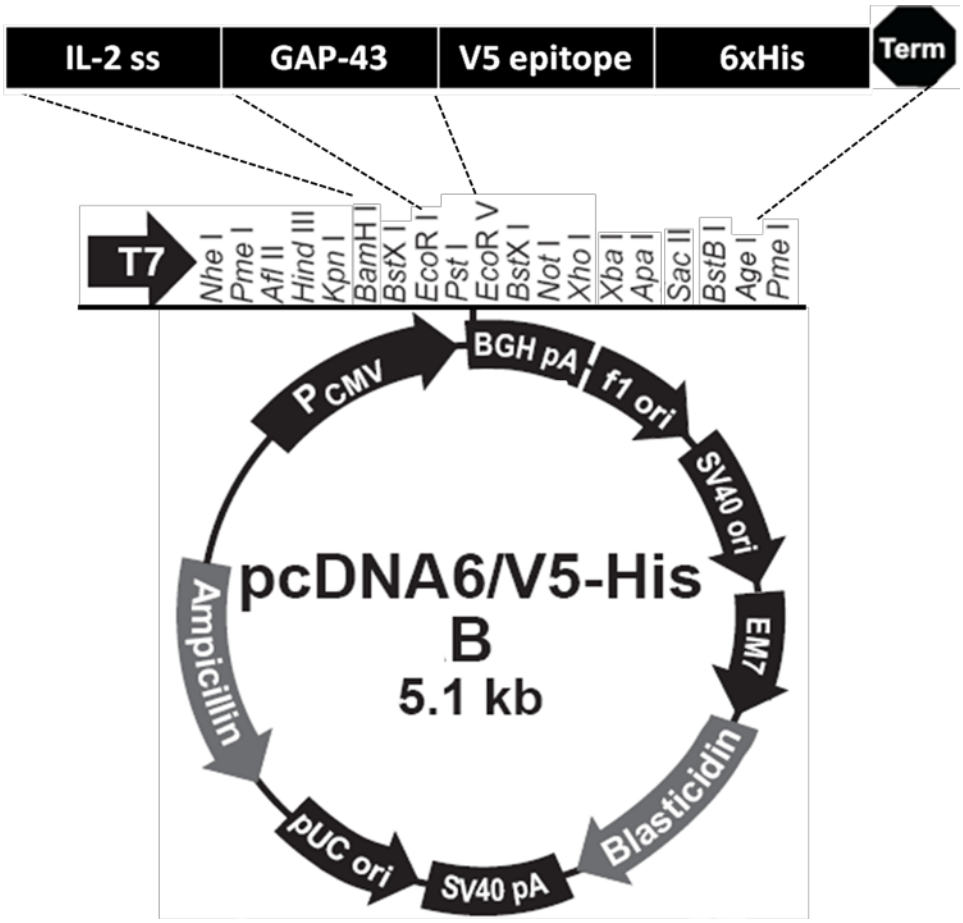

Figure 4-5 The restriction enzyme and genetic map of the commercial vector pcDNA6/V5-His B (Invitrogen). The coding sequences of the GAP-43 gene were cloned immediately downstream of the secretion signal IL-2ss. The vector was digested at *BamHI/PmeI* with the appropriate enzymes.

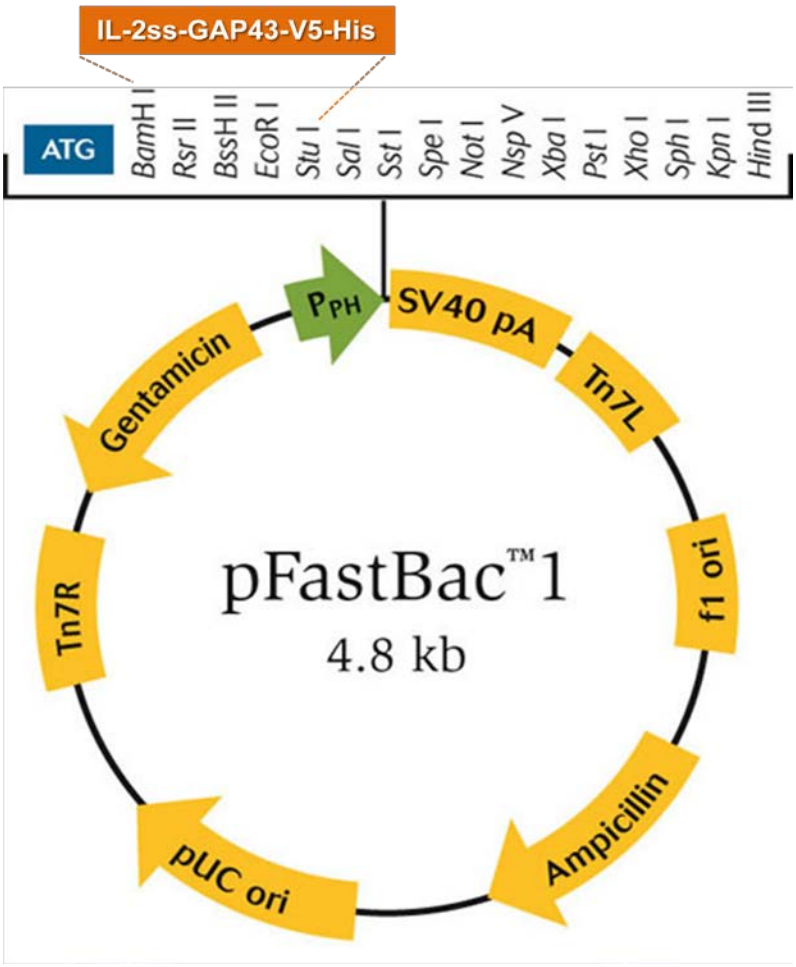

Figure 4-6 The restriction enzyme and genetic map of the commercial vector pFastBac1 (Invitrogen). The coding sequence of IL-2ss-GAP43-V5-His was cloned into pFastBac1 digested at *BamHI/StuI* with the appropriate enzymes.

At all stages of cloning, the plasmids were analyzed by restriction enzyme digestion and by sequencing both DNA strands using the ABI Prism BigDye terminator sequencing kit and an ABI automated DNA analyzer at the Genome Centre of The William Harvey Research Institute. The analyses of both the nucleotide and the putative translated amino acid sequences were performed by DNA and protein databases (www.ncbi.nlm.nih.gov and http://us.expasy.org).

4.3.2.2 Isolating P1, P2 and P3 viral stocks

The Sf9 cell line (*S frugiperda*) was maintained in Sf-900 II SFM media (Gibco) supplemented with 2mM of L-glutamine, 100 U/ml of penicillin and 100 µg/ml of streptomycin. For transfection, Sf9 cells (9×10^5) were seeded in each 6-well (35 mm) tissue culture plate with 2 ml of growth medium and transfection carried out with 1 µg of GAP-43 recombinant DNA. The cells were incubated in a 27^{o}C humidified incubator for approximately 72 hours until there were signs of viral infection (a 25-50% increase in cell diameter and increase in size of cell nuclei in the first 24 hours, followed by cessation of cell growth and signs of viral budding and granular appearance to the cells in the late 24-72 hours). The media were then collected to harvest the virus and centrifuged at 500 x *g* for 5 min at room temperature to remove cell debris. The resultant clarified supernatant was passed through a 0.45 µm filter (Sartorius) to remove further particulate material from the concentrated P1 GAP-43 viral stock. Subsequently using the P1 viral stock, higher titre P2 and P3 stocks were generated. The numbers of Sf9 cells required for the transfections were calculated beforehand and the cells expanded accordingly. They had to have greater than 95% viability and to be growing in the logarithmic phase with a density of 1.5-2.5 x 10^6 cells/ml before proceeding to transfection. 2 x 10^6 Sf9 cells/small flask (Sartorius) were plated in a monolayer culture transfected with 0.4 ml P1 viral stock and incubating cells at 27^{o}C for 72 h or until signs of viral infection, to generate the P2 viral stock. Using 200 µl of the P2 stock, I transfected 8 x 10^6 Sf9 cells/medium flask (Sartorius) to generate an even higher-titre P3 stock. The titre of the stocks was determined using the plaque assay (see performing

a viral plaque assay). For long-term storage, aliquots of baculovirus stocks were stored in cryotubes at -80^{o}C.

4.3.2.3 Viral Plaque Assay

The titre of the P3 baculovirus stock was calculated in plaque-forming units (pfu) per millilitre in the plaque assay. To perform the plaque assay, eight-log serial dilution (10^{-3} – 10^{-8}) of the virus stock were prepared in SF-900 II SFM medium and 1 mL aliquots of appropriate virus dilution were inoculated onto susceptible Sf9 cell monolayers (1 x 10^{6} cells) in a 6-well plate and gently rocked to evenly distribute the virus. After an incubation period of 1 hour at room temperature, the virus stock and medium was removed and replaced with neutral red agarose overlay (1 mg/ml neutral red solution in Sf-900 (1.3x) plaquing medium (Invitrogen) combined with 4% agarose (BD BaculoGold^{TM}) and allowed to set. The 6-well plate was then incubated in 27^{o}C humidified incubator for 7 – 10 days until plaques (a circular area of infected cells) were visible. To facilitate counting 0.5 mL of neutral red solution (1 mg/ml neutral red solution in cell-culture grade, distilled water) was added to each well and incubated for 1 – 2 hours at room temperature. After removing excess stain, plaques appeared as near clear spots in the gel contrasted against red background.

The titre was calculated as follows:

$$\text{Titre (pfu/ml)} = \text{no. of plaques} \times \text{dilution factor} \times \frac{1}{\text{ml of inoculum/well}}$$

P3 baculovirus stock titre was 2 x 10^7 pfu/ml.

4.3.2.4 Expression of recombinant GAP-43 protein in insect cells

The *Trichoplusia ni* High Five^{TM} cell line (20 x 10^6 cells/large flask) maintained in Express 5 SFM media (Gibco) supplemented with 2 mM of L-glutamine, and 100 U/ml of streptomycin and 100 µg/ml of streptomycin was transfected with the P3 recombinant 250 µl of baculovirus stock. The cells were incubated in a 27^{o}C humidified incubator and the transfected cell supernatants harvested at 72 hours post-infection. The level of protein expression (multiplicity of infection (MOI) and time course of infection) was optimised and protein expression was examined in western blots. Procedure was scaled up from one culture flask to six in order to increase the final GAP-43 protein yield.

Recombinant protein supernatants were centrifuged at 500 x *g*, filtered to remove cell debris and loaded into dialysis tube with a 10k molecular weight cut-off before dialysing in 1x PBS, pH 7.4 (Sigma). Samples were then stored at -80^{o}C awaiting purification.

4.3.2.5 Isolation of recombinant GAP-43 protein

Recombinant GAP-43 (His) protein was purified using a prepacked Ni^{2+}-Sepharose HiTrap Chelating HP column (1 ml, GE Healthcare, #71-5027-68 AH) according to manufacturer guidelines with slight modifications to achieve

higher purity. Distilled water and analytical grade chemicals were used. Solutions were filtered through 0.22 µm filters (Sartorius).

Briefly, the purification procedure (performed at +4^{o}C) consisted of the following steps. Firstly, the HiTrap column was washed with 5 ml of distilled water, followed by equilibration with 10 ml of 1x native binding buffer (see Appendix for chapter 4). The GAP-43 containing samples were then pooled and applied to the column at a flow rate of 1-4 ml/min manually using a 10 ml syringe. Some of the flow-through fraction was saved for later analysis. The column was then washed with 10 ml of native wash buffer with 20 mM imidazole (see Appendix for Chapter 4) to minimise the binding of host cell proteins and some of the wash fraction was collected for analysis. Finally, elution of GAP-43 was carried out using 5 ml of native elution buffer with 250 mM imidazole (see Appendix for Chapter 4) and the eluted fractions ware collected in small fractions of 0.5 ml to avoid dilution of the protein. These were then dialysed against 5 L of 1x PBS, pH 7.4 to remove trace amounts of imidazole. The purity of the final recombinant GAP-43 fusion protein thus obtained was assessed by western blotting and examined further by mass spectrometry (Dr Wendy Heywood, Biochemistry group, Institute of Child Health).

Purification procedure under denaturing conditions was also compared with the addition of urea to the binding, wash and elution buffers (see Appendix for Chapter 4). Protein concentrations were determined by using Bio-Rad (Bradford) protein assay. Briefly, 25 µl of Reagent A was loaded onto wells in a Nunc Maxisorp microtitre plate, followed by standards (0.063 mg/ml, 0.125 mg/ml, 0.25 mg/ml, 0.5 mg/ml, 1 mg/ml and 2 mg/l) and sample at 10 µl in each

well. Reagent B was loaded at 200 µl per well. The plate was then left to stand at room temperature for 10 minutes with gentle agitation and read at 750 nm using FLUOstar Omega (BMG Labtech). The standards were plotted and the total protein value was calculated from the standards.

4.3.2.6 Western blot analysis

Specificity of purified recombinant GAP-43 protein was analysed by western blot analysis. 6.5 µl protein sample was solubilised in 2.5 µl NuPAGE LDS buffer (4x) and 1µl NuPAGE sample reducing agent (10x), boiled for 15 min and separated on NuPage 4-12% Bis-Tris,10 well, 1.0 mm precast gel (Invitrogen) alongside a 10 to 191 kDa molecular weight marker. Immunoreactivity labelling was carried out with anti-GAP-43 primary antibody 1/1000 dilution (NM2, #MN1090, Thermo Scientific), detected using anti-mouse HRP-conjugated secondary antibody 1/2000 dilution (#P0260, Dako) and visualised with enhanced chemiluminescence (Thermo Scientific). A more detailed western blot methodology can be found in Chapter 2.

4.3.3 Proteomic analysis of recombinant GAP-43 protein

4.3.3.1 In-gel tryptic digestion of recombinant GAP-43 protein from 1D polyacrylamide gel

Coomassie blue stained bands at approximately 51 and 97 kDa of the GAP-43 fusion protein run on a 1D polyacrylamide gel were cut out for identification by mass-spectrometry. The excised gel pieces were placed into sialinised

eppendorfs that have been previously washed with 200 µl of methanol to remove any contaminants. The following portion of the work was performed by Dr Wendy Heywood.

The coomassie stained gel bands were placed into de-staining solution (300 µl of 50% methanol containing 0.1% acetic acid) incubated at 37^{o}C to remove as much of the coomassie as possible. The gel pieces were then washed with 200 µl of 50 mM ammonium bicarbonate buffer (pH 7.8) to remove any residual buffers. 500 µl of LC-MS grade acetonitrile was added to the gel pieces and rotated for 30 min to dehydrate them, and transferred into a centrifugal evaporator until completely dry (approximately 30 min). Any disulphide bridges that have reformed were re-broken using 10 mM DTE (Cleland's reagent) in 50 mM ammonium bicarbonate buffer, pH 7.8, incubated at 37^{o}C for 1 hr. Excess DTE solution was discarded and the gel pieces were again washed in ammonium bicarbonate buffer. Carboamidomethylation of the proteins was performed by adding 300 µl of 100 mM ammonium bicarbonate containing 55 mM iodoacetamide allowing the reaction to proceed in the dark for 45 min at room temperature. The supernatants were discarded and the gels were washed in ammonium bicarbonate buffer three times. Prior to in-gel digestion, gel pieces were dehydrated using methods outlined above. 60 µl of of 12.5 ng/µl of sequencing grade trypsin solution in 50 mM ammonium bicarbonate buffer, pH 7.8 were added to cover the gel pieces and incubated for 12 h or overnight at 37^{o}C in a waterbath. After digestion, the peptides from the gels were extracted 3 x 20 min each with: 1) 200 µl of 1% formic acid to collect the more hydrophilic peptides, 2) in a new, silanised eppendorf 300 µl of 50% ACN/1% formic acid to collect most of the tryptic peptides, and 3) a further 300 µl of 50% ACN/1%

formic acid. To the collected supernatants 200 µl of 1% formic acid was added, vortexed and freeze-dried.

4.3.3.2 LC-MS/MS (ESI-QTOF MS) analysis

The peptides in each digest were analysed using a nanoAcquity HPLC and Q-TOF Premier mass spectrometer (Waters Corporation, Manchester, UK). In brief, peptides were trapped and desalted using a Symmetry C18 5 µm, 5mm x 300 µm precolumn in 0.1% formic acid at a flow rate of 4 µl/min for a total of 4 min before elution and separation on a 15 cm x 75 µm reverse phase analytical column using a linear gradient of 3-40% acetonitrile [0.1% formic acid] over a period of 90 min at 300 nl/min. Peptides were analysed in a positive mode using Q-TOF Premier mass spectrometer and was operated in v-mode with a typical resolving power of 10,000 FWHM. Prior to analysis, [glu1]-fibrinopeptide B fragments, a mass calibrant was used to calibrate the TOF analyser using collision energy of 25 V and over the mass range 50-2000 *m/z*. Mass spectra were acquired in a data independent and alternating, low and high collision energy mode. Each low/high acquisition was 1.5 s with 0.1 s interscan delay. The collision energy used was performed for low energy data collections at 4 V and varied at 15-40 V ramp for high energy collisions.

The raw Q-TOF MS data was processed using the ProteinLynx Global Server ver 2.4. Database searching was with UniProt/Swiss-Prot databases to which the recombinant GAP-43 sequence was added manually. Protein identification form the low/high collision spectra for each sample was processed using a hierarchical approach where more than three fragment ions per peptide, seven

fragment ions per protein and more than two peptides per protein had to be matched.

4.3.4 Quantitation of GAP-43

4.3.4.1 Patients

Cell-free CSF samples and paired serum from 172 patients (age range 17 to 81 years; 69 males, Table 4-1) from the CSF laboratory archives approved by the local ethics committee was utilised for the detection of GAP-43. The sample age range was from 2009 – 2010 and stored at -20^{o}C (analysis was performed in 2010). Assays were performed blind to clinical data and their diagnoses are detailed below. Control CSF consisted of headache cases without features of raised CSF pressure and back pain. Full diagnostic work-up in this group failed to detect any neurological cause for their symptoms.

Further analysis of CSF GAP-43 was performed in 32 patients with secondary progressive MS (SPMS) participating in the Lamotrigine clinical trial described earlier (see Chapter 2). Their mean age was 52 and had steady progression of the disorder since its onset as evidenced by disability scores (EDSS) ranging from 4 to 8.

Diagnosis	N	Gender (M:F)	Age (years)
Dementia	26	9:17	60 (19-80)
BIH	22	21:1	30 (17-54)
Movement disorders	16	7:9	57 (29-71)
MS	38	21:17	44 (17-76)
Neuropathy	24	5:19	50 (17-81)
CNS infections	23	11:12	44 (29-74)
MND	10	6:4	54 (35-68)
Neurological controls	13	4:9	53 (49-60)

Table 4-1 Clinical characteristics of patients. Age values are expressed as means (ranges). *N* = number of individuals; *M* = male; *F* = female; BIH = Benign Intracranial Hypertension; MS = Multiple Sclerosis; MND = Motorneurone Disease.

4.3.4.2 Antibodies and standard curve

Monoclonal anti-GAP-43 primary antibodies, clones *NM2* (#MN1090) and *31* (#612262) were from Thermo Scientific and BD Transduction Laboratories, respectively. Secondary polyclonal antibody was a rabbit anti-GAP-43 antibody from GeneTex (#GTX 30199), whilst the tertiary antibody was swine anti-rabbit-HRP (#P0217) from Dako.

Newly purified recombinant GAP-43 protein was double diluted in 2% semi-skimmed milk (Marvel)/1 x PBS (Sigma), pH 7.4, from a top standard measuring 1.6 mean OD in duplicates, corresponding to 145 ng/ml of GAP-43 (refer to 4.3.2.5 for determination of recombinant protein concentration).

4.3.4.3 Enzyme-linked immunosorbent assay for GAP-43

Analyses of GAP-43 levels in CSF samples were carried out in duplicate wells by ELISA. Microwells of polystyrene Nunc-MaxiSorp^{TM} were coated overnight at +4^{o}C with either *NM2* antibody at 2 µg/ml or *31* antibody at 1.25 µg/ml in PBS (NaCl 0.138 M; KCl 0.0027 M), pH 7.4 (Sigma). Plates were washed with 200 µl of 1M PBS and incubated with 2% semi-skimmed milk (Marvel)/PBS for 1 hour at room temperature to block non-specific binding. The wells were emptied and again rinsed with 200 µl of PBS. Test CSF, recombinant standard and controls at 50 µl in 50 µl of 2% semi-skimmed milk/PBS were incubated for 1 hour at room temperature on a plate shaker. After being rinsed with PBS containing 0.05% Tween 20 (Sigma) five times, the plate was incubated with polyclonal rabbit anti-GAP-43 (2 µg/ml in 2% semi-skimmed milk/PBS) for 2 hours with shaking at room temperature. After washing as above, swine anti-rabbit-HRP was diluted 1/2000 in 2% semi-skimmed milk/PBS was added to the plate and incubated for 2 hours at room temperature with shaking. The wash steps were repeated, followed by a rinse with PBS only. 100 µl of 3, 3', 5, 5'-Tetramethylbenzidine (Sigma) chromogenic substrate was added to the wells and the reaction was allowed to proceed for 10 min in the dark at room temperature. The reaction was stopped using 50 µl 1 M hydrochloric acid and absorbance measured at 492 nm with wavelength correction at 540 nm in FLUOStar Omega plate reader (BMG Labtech). Sample values were expressed as ng/ml calculated from the standard curve of GAP-43 antigen.

4.3.4.4 Calculations of blood-brain barrier (BBB) function and IgG synthesis

Quantitative determination of serum and CSF albumin, and serum and CSF IgG was performed by nephelometry, using the BN *ProSpec* analyser (Siemens). The CSF/serum albumin (ALB) ratio was calculated as [ALB_{CSF} (mg/l)/ALB_{SERUM} (mg/l) x 100%] and utilised as an indicator of BBB function. IgG index was calculated as [(IgG_{CSF} (mg/l)/IgG_{SERUM} (mg/l)) x (ALB_{SERUM} (mg/l)/ALB_{CSF} (mg/l))] and utilised as an indicator of intrathecal IgG synthesis.

4.3.4.5 Statistical analysis

All analysis was performed using SPSS version 16. Comparisons between the different diagnostic categories were performed using ANOVA after establishing normality using the one-sample Kolmogrov-Smirnov test. The level of statistical significance was set at 0.05. Multiple comparisons were adjusted using Bonferroni correction. The effects of age and gender on GAP-43 concentrations were tested using regression analysis with age as a covariate and gender as a factor. Spearman-rank correlation was performed between CSF GAP-43, albumin quotient and IgG index to assess whether GAP-43 values rose with blood-brain barrier dysfunction or intrathecal IgG synthesis. Relative association of CSF GAP-43 concentrations to clinical measures of disease progression in patients with SPMS was tested by linear regression with CSF GAP-43 as the dependent variable. Log transformation was preformed because of the skewed distribution.

4.3.5 Western blot analysis of endogenous antibodies against GAP-43 in serum/CSF

A random selection of serum/CSF samples from MS subjects were tested for reactivity against recombinant GAP-43 by western immunoblotting looking for endogenous antibodies to GAP-43. A similar method to that described in Chapter 2.5.5 was used for this purpose; 20 µg of denatured purified recombinant GAP-43 protein was run on NuPage 4-12% Bis-Tris 2D well precast gel (Invitrogen), and polyclonal rabbit anti-GAP-43 (GeneTex, #GTX 30199) at a dilution of 1/500 was used to probe the positive control and detected using 1 in 1000 dilution of anti-rabbit IgG/HRP (Dako, #P0217), whilst anti-human IgG/HRP (Dako, #P0214) at a dilution of 1/1000 was used for the MS samples.

4.4 Results

4.4.1 Recombinant GAP-43 protein

4.4.1.1 Secretion of GAP-43 protein

Supernatants from the baculovirus infections were resolved by SDS-PAGE and immunodetected with anti-V5 antibodies. Figure 4-7, lanes 1 – 3, shows the protein profile of recombinant GAP-43 at differing sample volumes purified under native conditions, whilst lanes 4 – 6 shows the protein staining pattern purified under denaturing conditions (using urea). Both procedures show the same characteristics for GAP-43; a major band at M_r 51 kDa and a minor band

at M_r 97 kDa were identified, indicating that the two methods of purification did not differ. Subsequent in-gel trypsin digestion of Coomasie stained protein bands followed by LC-MS/MS identified them as GAP-43 with 60 – 72% peptide coverage against the modified GAP-43 sequence (Figure 4-8). These may represent post-translational modifications that occur during production and secretion of the fusion protein or represent protein dimerisation.

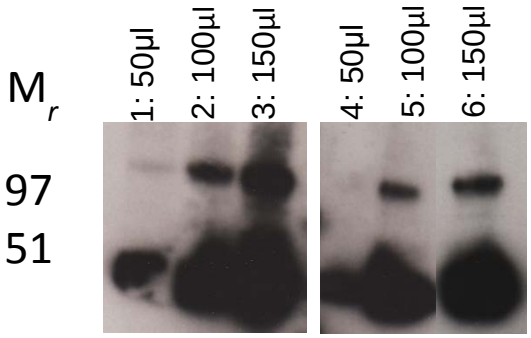

Figure 4-7 Western blot of GAP-43 fusion protein purified under native (lanes 1-3) and denaturing (lanes 4-6) purification conditions. The blot was probed using anti-V5 antibody. Different volumes of the protein were run (lanes 1+4=50 µl, 2+5=100 µl, 3+6 =150 µl) demonstrating that both native and urea-purified GAP-43 do not differ significantly. SDS-PAGE was run in denaturing conditions.

A

M_r 51 kDa:

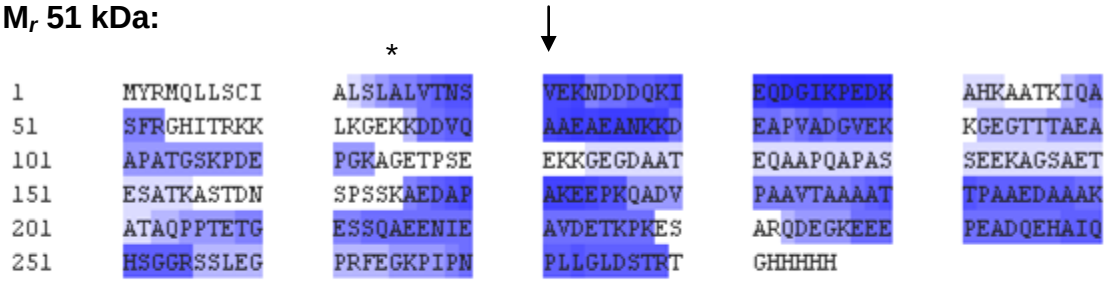

Entry	Description	PLGS Score	Peptides	Coverage (%)
REC_GAP43	Neuromodulin GAP 43	9587	52	72

B

M_r 97 kDa:

Entry	Description	PLGS Score	Peptides	Coverage (%)
REC_GAP43	Neuromodulin GAP 43	6291	38	60

Figure 4-8 Peptide coverage maps of the (A) 51 kDa and (B) 97 kDa recombinant GAP-43 protein bands. Regions of the protein sequence that matched to a peptide are highlighted in blue. The arrow marks the start of the GAP-43 protein, but peptide matches are evident also for the N-terminal signalling protein (*) demonstrating variation in cloning in the Baculovirus system. Percentage sequence coverage is included for both bands as well as their PLGS scores. The PLGS score is a statistical measure of accuracy of assignation and is calculated by Protein

Lynx Global Server (Waters) from all available mass spectrometry data, a higher score implies a greater confidence of protein identity.

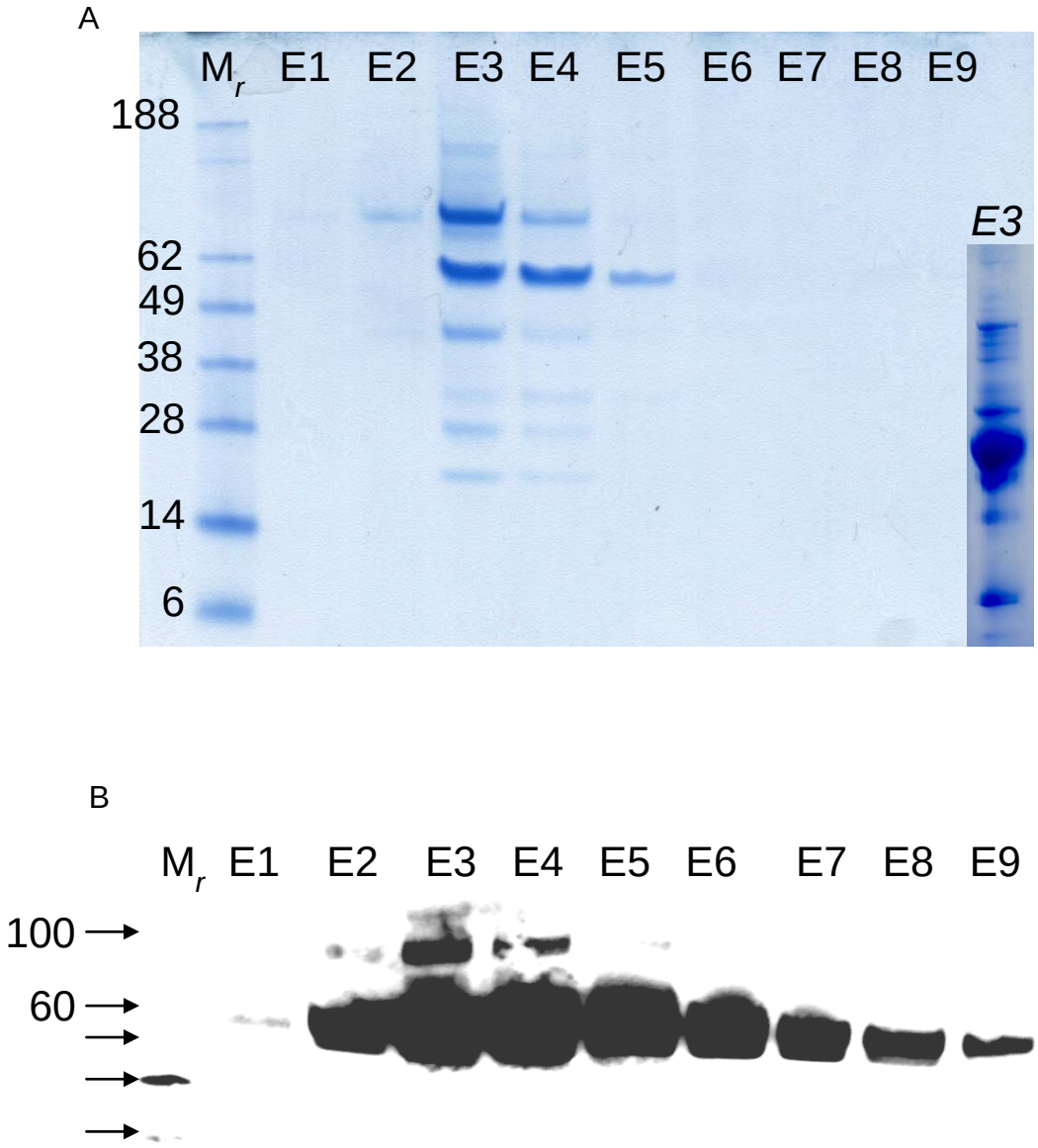

Figure 4-9 Coomassie blue stained gel (A) and western blot (B) probed using anti-GAP-43 NM2 antibody of recombinant GAP-43. HiTrap column sequential elutes are labelled E1-E9. The gel and the corresponding blot demonstrate a predominant band at <60 kDa and a lesser one at <100kDa. Adding imidazole to the wash improved the purity of GAP-43 obtained (*compare E3 pre-imidazole elute in the right hand corner of the gel with E3 post-imidazole in the main gel*).

4.4.1.2 Isolation of recombinant GAP-43 protein

Figure 4.9 shows the elution of the purified recombinant GAP-43 protein from a HiTrap 1 ml column. Adding imidazole to the wash yielded a highly purified product (see *E3* in the far right corner of the coomassie gel pre-imidazole). Elutes 3, 4 and 5 were selected for use in ELISA development, protein concentration of 0.45 mg/ml.

4.4.2 GAP-43 immunoassay performance characteristics

4.4.2.1 Monoclonal 31 versus NM2 GAP-43 ELISA

Agreement between CSF GAP-43 levels measured using *31* and *NM2* antibodies was calculated across the assay working range (n=30) using the Bland-Altman plot (where *x*-axis is the mean of the two measurements of GAP-43 and *y*-axis is the difference between the two values, Figure 4.10) [216]. The correlation between the two methods was r^2 = 0.88, 95% limits of agreement of +32.2 ng/ml (mean +2SD) and -18.8 ng/ml (mean -2SD) with only a few readings outside this range. The *31* assay over-estimated GAP-43 values compared to the *NM2* assay. Based on this and a signal-to-noise ratio of 1.6 OD using the *NM2* assay compared to *31* assay of 1.3. OD, it was decided to continue using the *NM2* assay for future work.

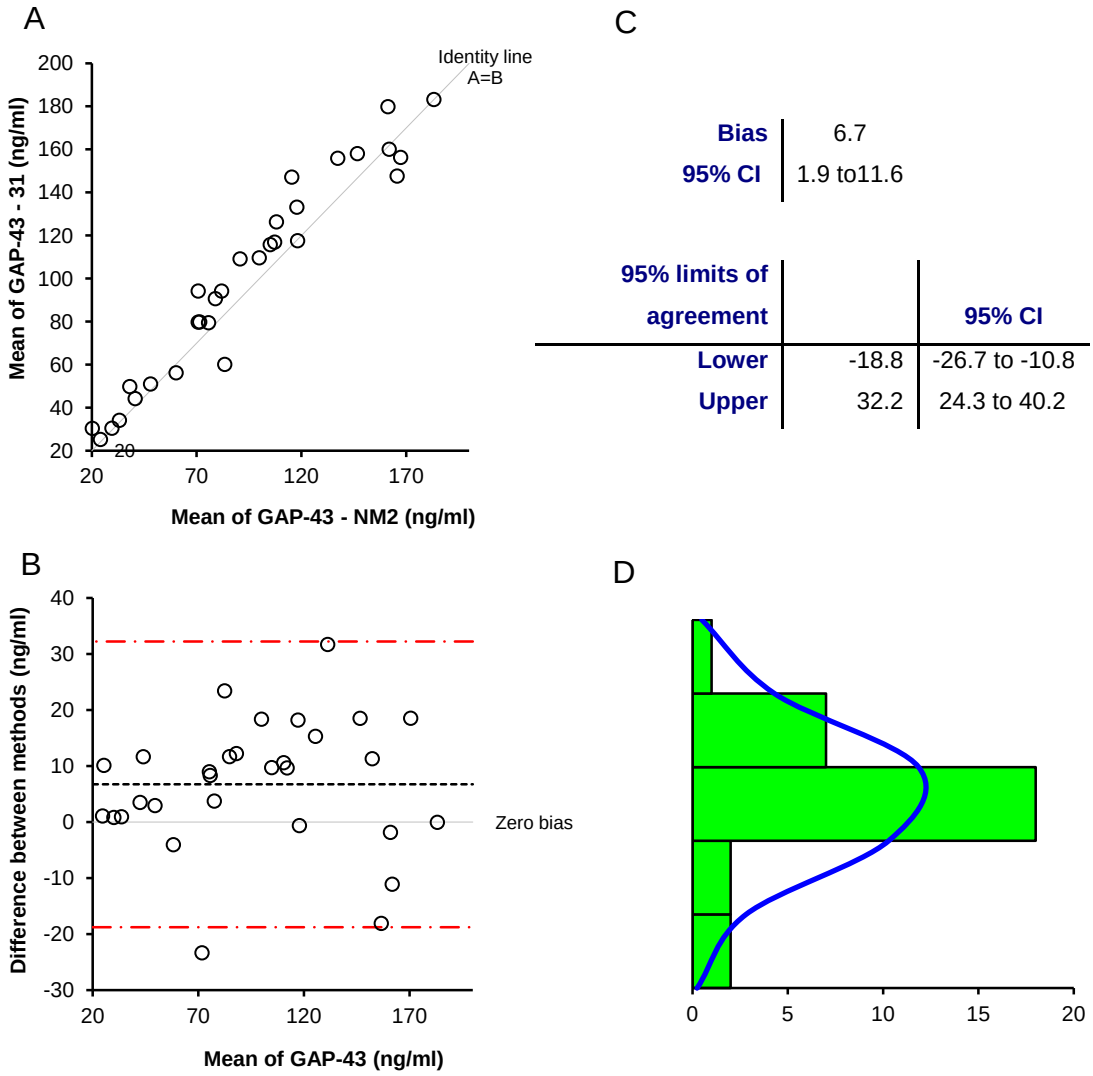

Figure 4-10 Correlation of mean GAP-43 concentrations measured using GAP-43-31 and GAP-43-NM2 (A) and Bland-Altman plot of the two methods (B). The Bland-Altman plot calculates the mean difference between the two methods of measurement (the 'bias'), and 95% limits of agreement (2 SD) to show how well the two methods of measurement agree. GAP-43-31 method reads slightly higher creating a bias of 6.7 ng/ml and limits of agreement of -18.2 (mean-2SD) and 32.2 (mean+2SD) ng/ml (C). The bias between the two assays is demonstrated graphically in the histogram but majority of the readings read with zero bias.

4.4.2.2 Assay sensitivity and precision

The limit of sensitivity of the NM2 GAP-43 ELISA was calculated by assaying the zero standard repeatedly twenty times and taking the concentration corresponding to 2SD above the mean. The sensitivity of the assay was 4.1 ng/ml. Within-run (intra-assay) precision was based on the mean and standard deviation of 5 replicates of the standard curve run in a single assay and expressed as the percentage coefficient of variation (CV%), whilst between run (inter-assay) precision was based on the mean and standard deviation of 5 replicates of the standard curve from run to run and day to day and expressed as the percentage CV (Table 4-2). The quality control data over twenty days plotted on to the Levey-Jennings plot demonstrates that the ELISA is working well (Figure 4.11).

GAP-43 concentration (ng/ml)	n	Intra-assay		Inter-assay	
		SD	CV	SD	CV
4.5	5	0.10	2.1%	0.09	2.1%
9.1	5	0.39	4.3%	0.31	3.4%
18.1	5	0.57	3.2%	0.36	2.0%
36.3	5	2.34	6.5%	1.58	4.4%
72.5	5	5.55	7.7%	3.25	4.5%
145	5	7.53	5.2%	5.56	3.8%

Table 4-2 Precision profile describing the GAP-43 assay performance across the assay range. The amount of error (standard deviation [SD], % Coefficient of variation [CV]) at specific concentration values is shown.

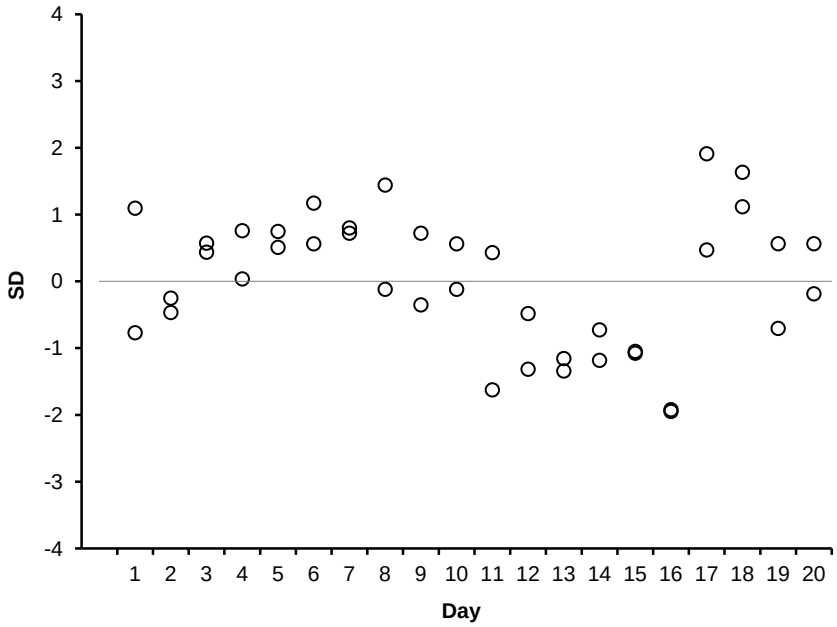

Figure 4-11 Levey-Jennings Plot with the quality control data of GAP-43 ELISA plotted over 20 days. Majority of the readings are within the upper and lower limits of two standard deviations from the mean.

4.4.2.3 Parallelism and recovery

The parallelism of the assay was determined by assaying four CSF of similar concentration as the top standard diluted to the zero standard, demonstrating that the dilutions lie parallel to the standard curve (Figure 4.12). Recovery studies were performed using four samples spiked with four different concentrations of analyte (1:1 dilution factor) and the percentage recovery calculated. The average recovery across four pairs of CSF samples was 104.5% (range 80.8 – 114%). Whilst mean recovery in sera were 103.7% (range 96.9 – 108.9%).

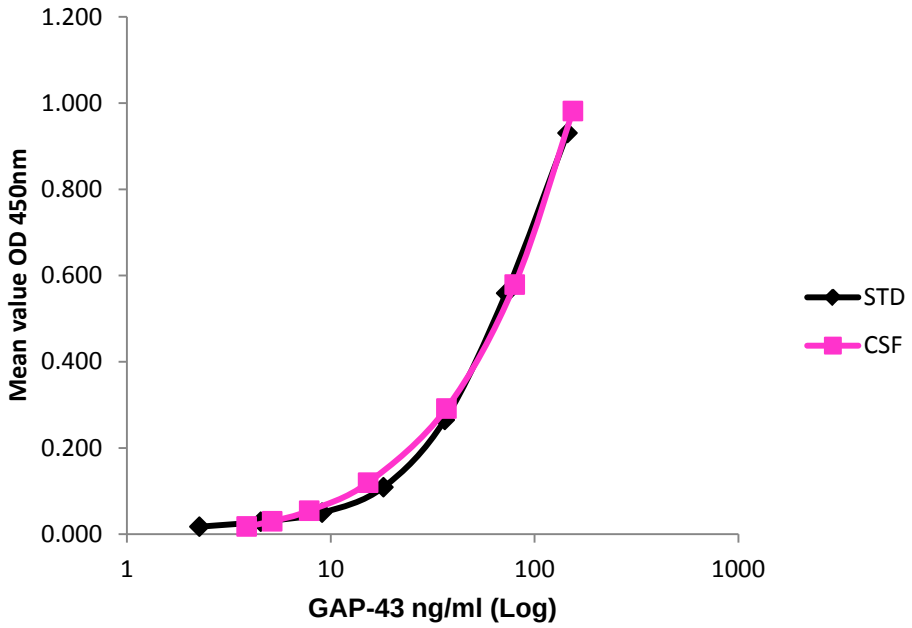

Figure 4-12 Comparison of recombinant GAP-43 standard and natural GAP-43 in CSF sample from a patient tested in dilutions. Parallelism between standard and natural GAP-43 was demonstrated in this comparison.

4.4.2.4 GAP-43 stability as determined by freeze-thaw cycles and temperature adjustments

Triplicate aliquots of CSF were frozen at -80^{o}C and then taken through five repeated freeze-thaw cycles, and also stored at room temperature, +4^{o}C, and -20^{o}C for a seven-day period. Analysis shows that CSF GAP-43 values were not strongly influenced by these adjustments (Figure 4-13).

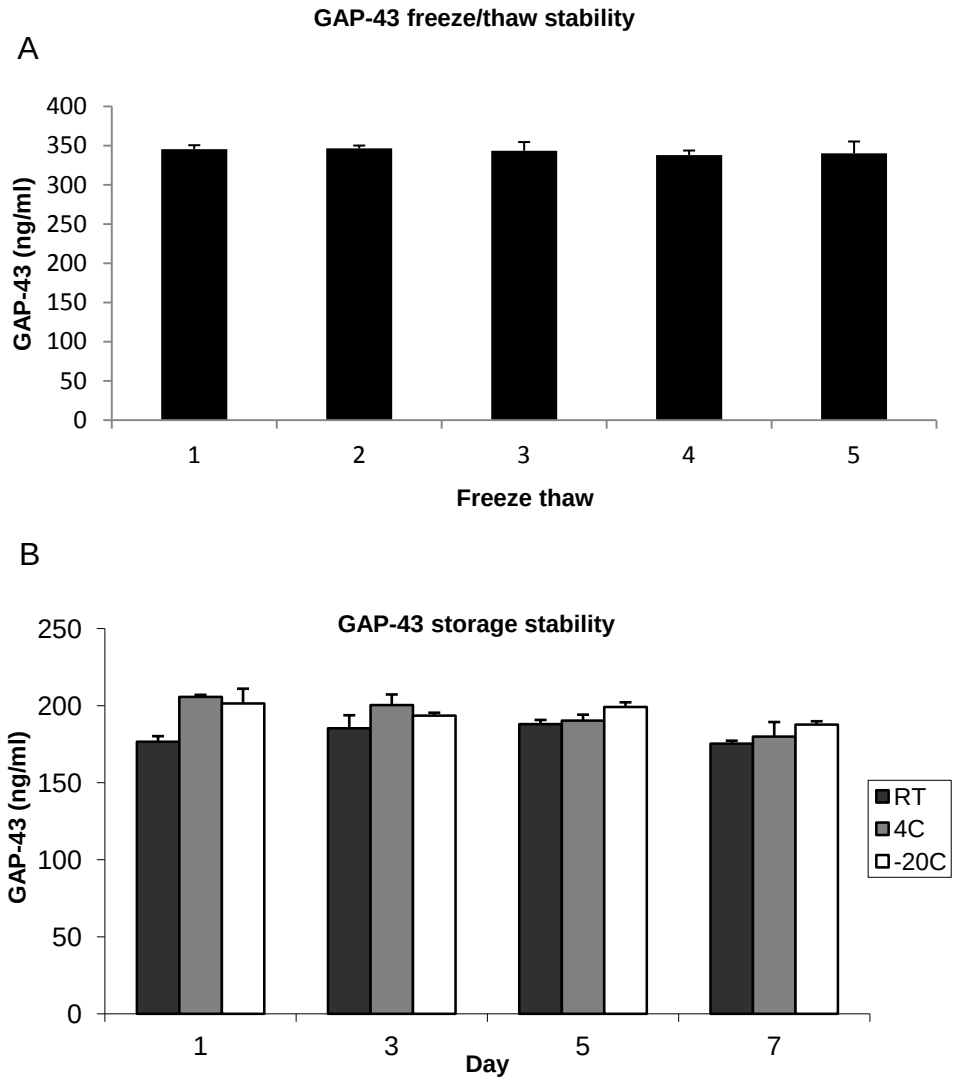

Figure 4-13 GAP-43 stability (freeze/thaw cycles, A) and storage (B). This demonstrates that the stability of GAP-43 is not influenced by five freeze/thaw cycles or storage at different temperatures over seven days.

4.4.3 GAP-43 in neurological disorders determined by the NM2 GAP-43 assay

The mean GAP-43 values ± SD (ng/ml) were 303 ± 388 (dementia), 287 ± 295 (benign intracranial hypertension), 136 ± 83 (movement disorders), 152 ± 117

(MS), 337 ± 283 (neuropathy), 331 ± 289 (CNS infections), 174 ± 128 (MND), and 522 ± 203 (neurological controls – headache subjects) (Figure 4-14). Mean CSF GAP-43 levels were significantly lower in movement disorders (p=0.001), MS (p<0.001), MND (p=0.03) than in neurological controls. The high outlying values noted in dementia, BIH and neuropathy were not uniquely different from the rest of their group with regard to their diagnosis, except in the CNS disorders where the highest GAP-43 level by far was found in a case of *staphylococcus aureus* meningitis (CSF GAP-43 of 1013 ng/ml) and cases of TB meningitis (CSF GAP-43 levels 632 to 996 ng/ml).

There were no significant correlations between CSF GAP-43 levels, and albumin quotient (mean 0.83 mg/l (0.15 – 5.51 mg/l); r=-0.11, p=0.47) and IgG index (mean 0.59 mg/l (0.30 – 1.65 mg/l); r=-0.02, p=0.88). Per milliliter GAP-43 concentrations were approximately ten times more in the CSF than in paired serum samples (Figure 4-15). Moreover, GAP-43 concentrations in CSF were not significantly associated with GAP-43 in serum (r=0.17, p=0.18). Linear regression analysis revealed that CSF GAP-43 levels were not associated with either age (p=0.83) or gender (p=0.34).

Having established that CSF GAP-43 levels were low in patients with MS, a sub-group analysis was performed between the clinical MS subtypes. Mean GAP-43 ± SD were 168 ± 122 ng/ml (clinically isolated syndromes, CIS), 193 ± 154 ng/ml (relapsing-remitting MS, RRMS), 116 ±112 ng/ml (secondary progressive MS, SPMS), and 142 ± 80 ng/ml (primary progressive MS, PPMS), without significant differences on statistical analysis (p=1.00, 1-ANOVA). I also examined whether CSF GAP-43 levels could reflect the degree of disability. To

this purpose, GAP-43 was assayed in SPMS patients with EDSS scores ranging from 4 to 8 (mean EDSS ± SD of 6.0 ± 1.0), disease duration ± SD of 22.1 ± 9.8 years, and duration of progression ± SD of 11 ± 6.1 years. CSF GAP-43 concentrations were not significantly correlated with EDSS scores (r=-0.01, p=0.47), disease duration (r=-0.16, p=0.19) or duration of progression (r=-0.15, p=0.21).

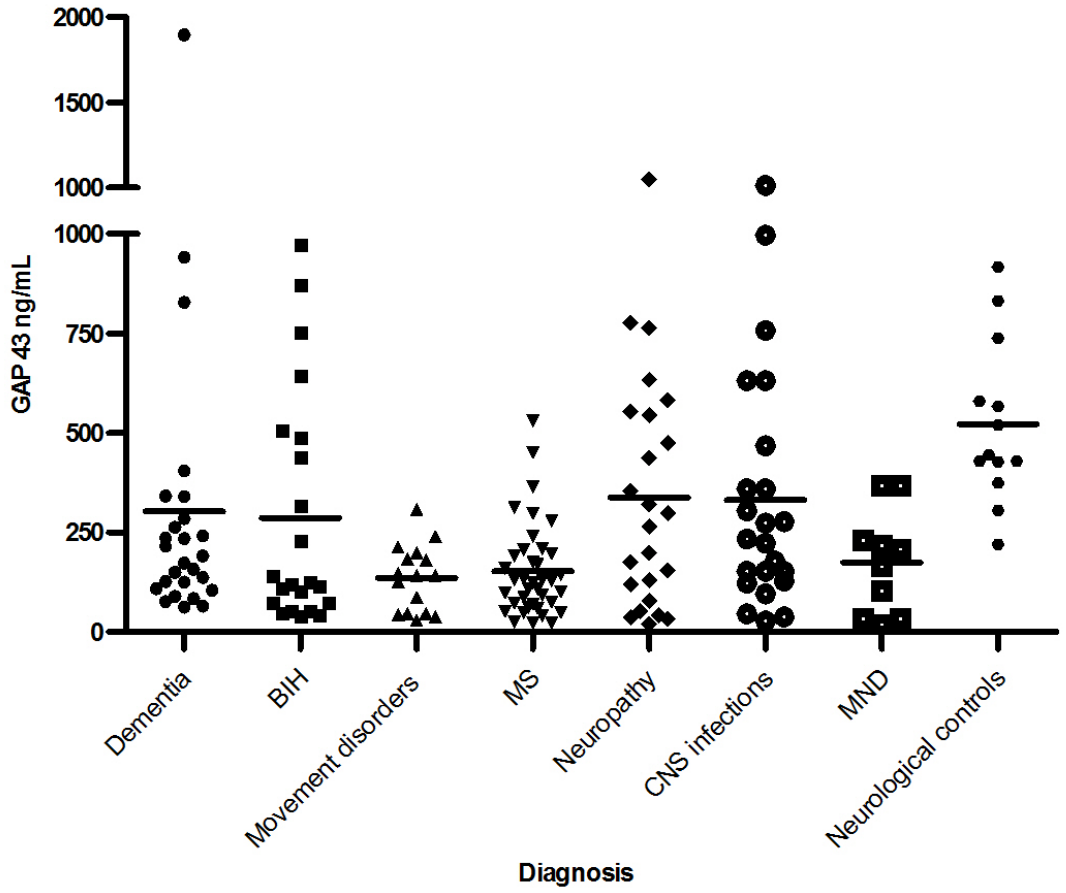

Figure 4-14 CSF GAP-43 in neurological controls versus neurological disorders The dementia cohort comprises 10 Alzheimer's disease, 8 unspecified memory problems, 5 minimal cognitive impairment, 1 frontotemporal dementia, 1 semantic dementia, 1 vascular dementia. The movement disorders cohort comprises of 7 Parkinson's disease, 5 progressive supranuclear palsy, 1 multisystem atrophy, 1 ballismus, 1 akinetic rigid syndrome, 1 involuntary movements. The multiple sclerosis (MS) cohort comprises 19 relapsing remitting MS, 7 clinically isolated syndrome, 7 primary progressive MS, 5 secondary progressive MS. The neuropathy cohort comprises of 7 peripheral neuropathy, 5 Guillain-Barre syndrome, 3 chronic inflammatory polyneuropathy, 2 motor neuropathy, 2 multifocal motor neuropathy, 1 mononeuritis multiplex, 1

ganglioneuropathy, 1 Charcot-Marie-Tooth disease, 1 small fibre neuropathy, 1 compressive neuropathy. CNS infections cohort comprises of 11 unspecified viral encephalitis, 5 tuberculous meningitis, 2 HIV, 1 *Staphylococcus aureus* meningitis, 1 zoster encephalitis, 1 HTLV-I, 1 meningococcal meningitis, 1 neuroretinitis. GAP-43 levels were lower in movement disorders (*P*=0.001), MS (*P*<0.001), motorneurone disease (MND) (*P*=0.03) than in neurological controls (headache subjects).

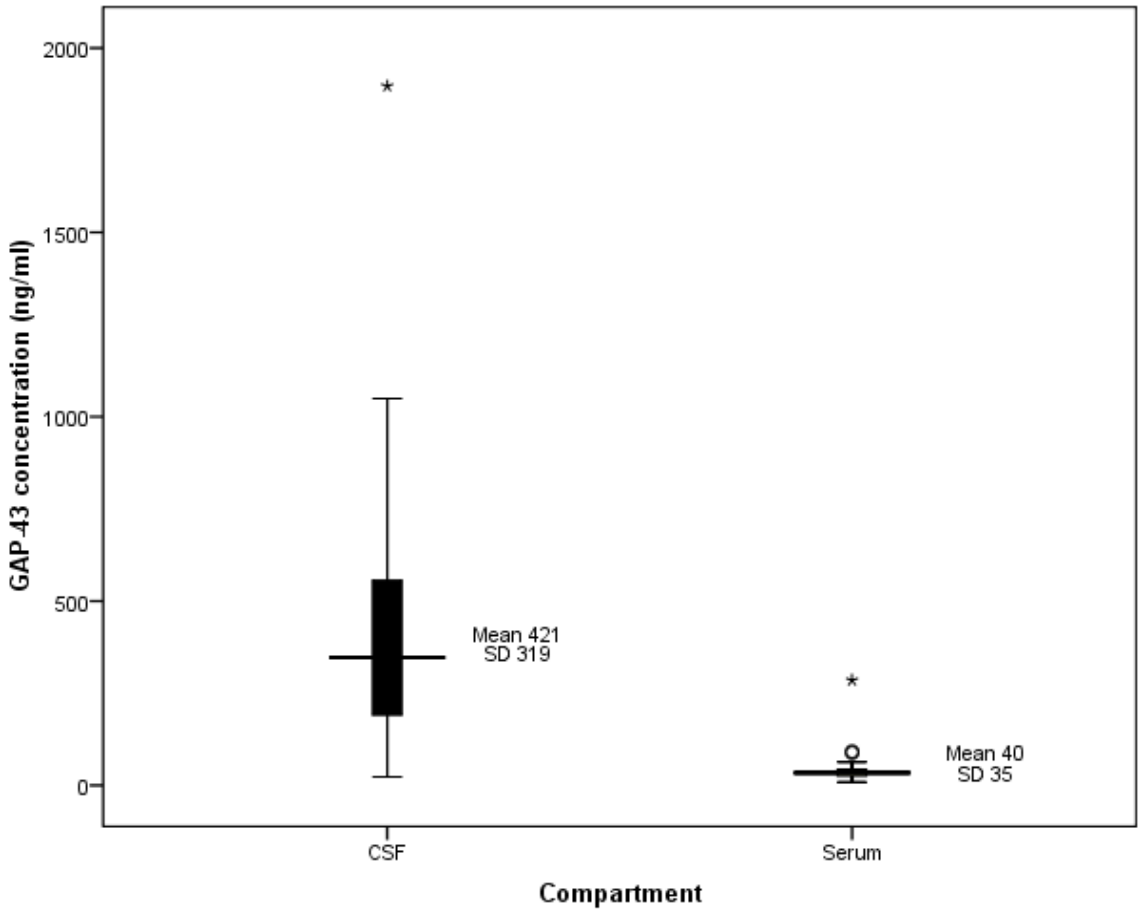

Figure 4-15 Comparison of GAP-43 concentrations in paired CSF and serum samples. GAP-43 concentrations were higher in CSF than in serum.

4.4.4 GAP-43 antigen-specific antibodies in serum/CSF

Antibodies to GAP-43 were uncommon in the CSF, with only one weakly positive sample out of the 50 CSF samples tested (Figure 4-16). There were no GAP-43 antigen-specific antibodies identified in the serum samples tested.

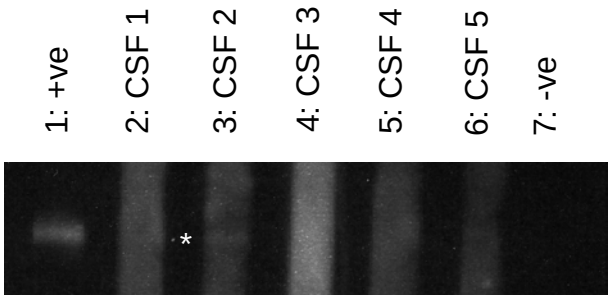

Figure 4-16 Western blots of GAP-43 antigen-specific antisera in MS CSF and controls. Weakly positive band was seen in lane 3 only (marked by *). Lane 1 and 7 includes the positive and negative controls, respectively.

4.5 Discussion

GAP-43, arguably one of the best characterised markers of growing, developing and regenerating neurones (see reviews by Benowitz *et al*. [35], Oestreicher *et al*. [217] and Strittmatter *et al*. [218]), is poorly understood when it comes to its neurogenic properties in the spinal fluid. As there are very few publications in the literature dedicated to this matter, it is very difficult, at present, to draw clear conclusions. Nonetheless, due to the inaccessibility of the human brain, the study of CSF proteins derived from the CNS, remains the next best alternative. In this chapter, I described the development of recombinant GAP-43 protein in

preparatory amounts to be able to be used in an ELISA system for directly quantifying CSF GAP-43 concentrations. Previous descriptions of GAP-43 ELISA reported on relative amounts of GAP-43 concentrations using partially purified GAP-43 [199; 212; 219; 220] as the standard, although more recently an assay using recombinant GAP-43 has been reported on, though there is no description of its production beyond that of personal communication [110]. To the best of my knowledge, there is no readily available commercial source for recombinant GAP-43 protein at the time of writing.

GAP-43's first ten amino acids which include cysteines 3 and 4 that are crucial for its membrane binding properties and once processed binds tightly to the inner growth cone membrane [35]. Therefore, for GAP-43 to be reliably secreted from an expression system this span of amino acids at the N-terminus of the protein would have to be removed, which we did. Altering the amino acid sequence affects the primary structure, which may lead to major conformational changes affecting the tertiary structure of a protein, thereby making their recognition with monoclonal antibodies by immunoassay or simple immunoblot methods difficult. A 20 amino acid signal peptide sequence from the IL-2 gene was introduced upstream of the GAP-43 sequence into the vector to ensure that the protein was secreted from the infected cells with greater efficiency. We assume the recombinant GAP-43 is processed and released from the insect cells along a similar secretory pathway to the one described in vertebrates [221]. However, from the peptide sequence coverage (Figure 4-8) it is evident that part of the IL-2 signalling peptide has been coded into the finished recombinant protein, suggesting that there are subtle differences between insect cells and mammalian cells after all.

The recombinant GAP-43 proteins thus produced was immunodetected with GAP-43 antiserum and subjected to immunoblot analysis, revealing a major labelled protein at approximately M_r 50 kDa and a secondary M_r 97 kDa protein was also detected. GAP-43 is considered to migrate anomalously in SDS-polyacrylamide gels with an apparent M_r of 43 – 53 kDa which might be related to microheterogeneity caused by posttranslational modifications [211; 222]. In fact, the second protein is probably too large to represent a posttranslational modification or even a pre-GAP-43 polypeptide, and most likely represents a dimeric molecule. Direct determination of the peptide sequences from proteolytic fragments using mass spectrometry, corresponded to 60 – 70% of the GAP-43 amino acids and confirmed their identity as GAP-43. Recently, Zaharov *et al*. [223] demonstrated that it was possible for GAP-43 to oligomerise in the presence of the anionic detergent SDS. Normally SDS is considered to be a strong denaturant unfolding secondary and non-disulfide-linked tertiary protein structures, but at concentrations below or near critical micelle concentration, which is about 0.005 – 0.01% SDS, SDS induces maximum cross-linking of proteins into oligomers. The final SDS concentration in the NuPAGE MES running buffer used for electrophoresis in my experiments was between 0.005% and 0.025%, which is within this range. SDS binding to the positively charged N-terminal domain (residues 1-40) and effector domain (residues 39-55) of GAP-43 favours this interaction.

The results of CSF GAP-43 determinations obtained from the ELISA demonstrated significantly lower mean concentrations of GAP-43 in the movement disorders, MS and MND categories compared to controls. Previous studies of CSF GAP-43 have noted similar reductions in concentrations in MS

patients and PD patients [110; 111], it was not possible to make direct comparisons as the assays worked in very different ranges (picograms as opposed to nanograms per millilitre). CSF GAP-43 has not been previously measured in MND patients, however its neuronal expression had been found to be increased in amyotrophic lateral sclerosis tissues [224]. The biological basis for the drop in GAP-43 levels in these groups can only be speculated upon; however, it is plausible since GAP-43 is involved in neuronal outgrowth and synaptogenesis, increased utilisation of the protein during degeneration might explain the decreased levels observed in the CSF. Alternatively, the drop in levels may be the result of increased protein turnover with the breakdown and removal of damaged neurones, or reflect a reduction in the number of neurones in the CNS [110; 111]. These explanations are not universally encompassing, since they cannot explain why three patients from the AD category had very high levels in CSF GAP-43 compared to the rest. Coleman *et al*. [202] alludes to this heterogeneity in AD cases, stating that GAP-43 expression in AD could be differentiated on the basis of neurofibrillary tangle density with reduced messenger levels in high tangle density and vice versa. In immunoassays, the presence of naturally occurring antibodies to the analyte within samples through interference, may lead to falsely low results especially in the case of an autoimmune-mediated disorder such as MS, however we found this not to be case after analysing a series of MS samples for anti-GAP-43 antibodies by western blotting.

The BIH, neuropathy and CNS infections (including the cases of TB meningitis) categories were not found to be significantly different from that of the control group, the spread of data points indicates a heterogeneous study group,

emphasising that clinical characteristics alone are not always sufficient for interpretation and more information is needed on pathological correlates.

In MS, further subgroup analyses revealed no significant differences in CSF GAP-43 levels when comparing CIS to RRMS to SPMS to PPMS. Moreover, GAP-43 in SPMS patients did not correlate with the degree of disability as assessed by the EDSS score, or the duration of disease or disease progression. The fact that majority of the subjects were scored at an EDSS of 6.0 may be an obvious explanation for the lack of correlation, but does not explain the lack of correlation observed with the other two measures of overall disease activity. A relatively small number of subjects were included in this initial study, I would like to have included a larger cohort with an even spread of EDSS measurements, and this will form the basis of a future study. Teunissen *et al*. [111] in their study, observed only a tendency towards a negative correlation between GAP-43 levels and EDSS (r=0.30, P<0.1), but again no correlation with disease duration.

Only one study has been performed on serum levels of GAP-43 and found to be below the sensitivity level of the assay [111]. I was able to detect GAP-43 in serum samples using my assay with negligible matrix interference, although the recorded levels were ten times less than the corresponding CSF level. Levels did not correlate with the albumin quotient, an index of blood-brain barrier function or IgG index, a measure of intrathecal IgG synthesis, supporting the notion that CSF GAP-43 levels are independent of both blood-brain barrier impairment and immune stimulation. Moreover, results from the paired CSF-serum samples indicate that variation of GAP-43 concentrations in CSF was not

correlated with serum GAP-43 concentrations, suggesting that they may originate from different sources. But, what is clear from these results is that GAP-43 is primarily derived from the CNS, and thus is essential to sample the CSF. I also noted no differences in CSF GAP-43 levels between age and gender groups, and adjustments based on age and gender are not anticipated.

In summary, I have presented a novel method for the production of recombinant GAP-43 protein using the baculovirus expression system. There was some microheterogeneity upon SDS-electrophoresis, but the structure of GAP-43 including the epitopes for GAP-43 antibodies is preserved, enabling its use as an antigen within an ELISA system. A new method for the quantitation of GAP-43 concentrations by ELISA, including validation steps are outlined in this chapter. The ELISA has sufficient sensitivity to be able to detect GAP-43 in both the CSF and serum, although paired CSF/serum analysis point to GAP-43 being exclusively CNS derived and do not vary as a function of serum GAP-43 concentrations. Lastly, CSF GAP-43 analyses from this study supports earlier findings for a role of GAP-43 in neuronal plasticity and neurodegeneration.

5 Uniform reporting of biomarker studies in neurological disorders

5.1 Introduction

Hopes to bring the vast array of post-genomic era biomarkers to the bedside have so far been disappointing. Experience in other specialities outside of neuroscience have shown that candidate markers which were initially promising have not stood the test of time [225; 226]. The lack of rigorous study design, sub-group analyses without adequately powered sample sizes, differences in methodology and analytical incompleteness have produced different and biased conclusions from scientific groups despite the rigour of the peer review process [227; 228; 229; 230]. Premature acceptance of poorly validated markers have resulted in numerous publications [231; 232; 233]; which still require further confirmation, engendering translational attrition of biomarkers to clinical practice [234; 235].

Advances in the fields of neuroscience, developmental neurobiology and discovery tools have revolutionised our understanding of the disease pathogenesis and pathophysiology affecting the nervous system. Specific examples include, beta amyloid and Tau protein in Alzheimer's disease, inflammatory mediators in multiple sclerosis, inhibitory growth factors in spinal cord repair, and gene mutations in inherited neurological disorders to name but a few. Majority of these are process-specific biomarkers that provide a mechanistic understanding of the pathophysiology of the disease in question. More recently, there has been a growing interest in developing biomarkers for diagnosis, risk-stratification, prognostication, or assessing treatment response. As a result many biomarkers are available in the literature that appear feasible in theory but unrealised in practice. The problem arises when investigators try to reproduce the work, by which stage it becomes clear that the published work is

either unclear or inadequate in its methodology, there is dubious use of statistics or the particular statistical approach does not provide clinically relevant information, or simply that the biomarker is of no clinical value after performing a larger screen. To date, only Aβ and Tau in Alzheimer's disease and several autoantibodies have reached a stage of universal acceptance, albeit after extensive and prolonged research [236; 237]. To my knowledge no other biological markers have come close to surrogate end-point status in neuroscience. A framework is therefore needed to ensure that emerging biomarkers in neuroscience are developed from well-designed studies with clearly-defined methodology, analysis and commentaries, and are presented in a standardised manner.

The European Biomarkers in Multiple Sclerosis (BioMS-*eu*) consortium (http://www.bioms.eu/) is a collaborative network working towards improving the quality of biomarker research in MS, incorporating experts in the field of neuroscience with experience in the critical process of biomarker validation. The consortium has previously developed criteria for the standardisation of cerebrospinal fluid collection and biobanking [238]. There are already several sets of published guidelines which deal specifically with different aspects of biomedical science, for instance REMARK (tumour marker prognostic studies) [239], STARD (diagnostic accuracy) [240] and CONSORT (randomised control trials) [241]; but there are no official guidance for the reporting of early, exploratory biological research including work on potential surrogate end-points, treatment-response biomarkers and diagnostic markers which focus on method development and validation.

5.2 Aims

To develop guidelines that standardise the process of reporting biomarker studies in neuroscience; to make biomarker studies more uniform and transparent, in line with existing standards for reporting research in other areas. The formalised set of guidelines should provide a clear framework for the reporting of biomarker studies work from early, exploratory biological research including work on potential surrogate end-points, treatment-response biomarkers and diagnostic markers. Specifically the guidelines developed should address the major problem areas, such as:

- Methodology
- Method validation/robustness
- Data extraction and statistics
- Clinical translational value

The guidelines were a coordinated effort between myself the BioMS-*eu* consortium and were developed as part of a compatible series; the first being “A consensus protocol for the standardisation of cerebrospinal fluid collection and biobanking” [238].

5.3 Methods

We used the definition of biomarker established by the NIH Biomarkers Definition Working Group (BDWG):

“Biological Marker (Biomarker) – a characteristic that is objectively measured and evaluated as an indicator of normal biologic processes, pathogenic processes, or pharmacologic responses to a therapeutic intervention”

“Clinical endpoint – a characteristic that reflects how a patient feels, functions and survives”

“Surrogate endpoint – a biomarker that is intended to substitute for a clinical endpoint” [90].

We also considered elementary standards for reporting biomarker work arising from key conferences (The Biomarker World Congress, Annual Biomarkers Congress) and Food and Drug Administration (FDA) regulatory recommendations (http://www.fda.gov). A checklist of items were created and circulated via email to all members of the BioMS-*eu* committee. The merits of including specific recommendations were discussed at the annual BioMS-*eu* meetings 2007 - 2010 between committee members (a list of the members is provided in the appendix) before finalisation. The importance, relevance and practicality of each of the items were deliberated over. The final format and wording of guidelines were decided after discussions between the scientific and steering committee members by email.

The guidelines reflect the consensus of the BioMS-*eu* at the time of writing and should be viewed as only recommendations. They will be subject to change in the future based on new emerging evidence.

5.4 Results

We started with a checklist of 61 items based on recommendations from previous published guidelines, biomarker publications and input from the scientific and steering committee of the BioMS-*eu*. This was later reduced to a final optimal format consisting of 10 main items, which are presented here (Table 5-1).

Items were excluded on the basis of lack of generalisability to different types of biomarker research, items that were desirable but not essential, and those that were considered outside the remit of the guidance. The checklist is divided into introduction, materials and methods, results and discussion, reflecting the subheadings used in a scientific publication. A detailed commentary on individual items is given below.

For studies in which the primary focus was the clinical trial, discovery biomarkers using proteomics or microarrays, or prognostic studies the use of existing published guidelines specifically for these purposes was recommended (a full list is provided in the appendix to Chapter 5).

5.4.1 Commentary on the checklist items

1-2. The introduction should be sufficient to describe scientific background and rationale i.e. the hypothesis, the biomarker(s) or its identification if relevant, mechanism of action and its intended use.

Note: pertinent information on surrogate status may not be available at an early stage, in which case references from other publications may be provided in support.

3. This section should contain the study protocol. Detailed information on study or sample population (such as size and diversity) is encouraged. Techniques for calculating sample size should be mentioned here if used. Where samples from specific studies are used for analysis, reference the applicable study protocols.

4. The study should conform to any applicable ethics review regulations.

5. Refers to the primary outcome (i.e the study's objective and the relevant biomarker(s)) and if applicable secondary outcome measures used in the study (e.g. imaging, neurophysiology, clinical scores (disability scales, patient-reported outcome measures)).

6. This section should contain a detailed description of the assay methods and pre-analytical and analytical parameters, and unless well recognised (e.g. ELISA) avoid using acronyms wherever possible. Please refer to the collection protocol for information on sample handling. Additional information on performance characteristics (testing environment, conformity to a recognised standard) would inform on whether the assay is appropriate for the intended use.

7. This section should contain a description of the data analysis method(s) used, including methods for dealing with missing values and outliers where

applicable. When using more complex statistical models (e.g. mixed-effects in the study of repeated measures) provide a description of the model and including any assumptions made on the model components.

8. We recommend that summary descriptions of the study or sample populations should be assembled in tabular format in order for any variances between the groups to be seen more readily. The table should include any variables that you think may influence the study outcomes (e.g. disease activity, disability score, smoking status etc.). Similarly, key experimental findings should be summarised in tables or graphs, together with a brief description of the results.

9-10. This is the discussion section of the work. It should contain a summary description of the biomarker(s) characteristics, whether the study aims and objectives were met, if relevant, relationship to existing biomarkers, and intended use(s). It should also address limitations or variability due to pathophysiological, environmental or demographic factors. And finally, address areas for future work (e.g. a larger population based study, add-on study to clinical trials etc.).

Figure 5-1 Summary guidance framework for the reporting of biomarker research. The framework follows a similar style to that of an original article and includes an introduction, materials and methods, results and discussion section for standardized reporting.

INTRODUCTION

1. General introduction
    a. Details on scientific background and rationale.
2. Specific introduction
    a. Identification of the biomarker and its expected role.
    b. The role or intended use of the biomarker (s).

MATERIALS AND METHODS

3. Include information on study or sample population
    a. Species, gender, age, disease/non-disease, disease stage, treatments, as well as use of specific cohorts (randomised control trial or cross-sectional and time-course). If relevant, include also reasons for sample exclusion.
    b. Type of sample – cerebrospinal fluid, plasma, serum etc
    c. Evidence of how sample size was calculated is desirable.
4. State the ethical procedures adopted.
5. Include a detailed account of outcome measures used, experimental as well as clinical end-points.
6. Assay methods
    a. Include information on sample/reagent preparation and handling
        i. Pre-analytical parameters – use of serum separators, special precautions, storage (refer to collection protocols).
        ii. Analytical parameters (sample preparation; source of reference material or calibrants and antibodies; analytical specificity – linearity, and recovery; sensitivity – upper and lower limit of quantitation (LOQ), quality control measures – inter- and intra-assay coefficient of variation (CV), precision; potential interference – haemolysis, lipaemia, drugs etc)
    b. Provide adequate descriptions of any analytical techniques you have used including kits and type of platform. If you are using an existing method, you may cite the method as described previously. If you modify a method, you may cite the method, but must also describe the changes and reasons for them.
    c. Performance characteristics
        i. Performance in the testing environment where it will ultimately be used i.e. laboratory or bedside.
        ii. Cross-validation with other technologies or technique.
7. Statistical analyses
    a. General
        i. Describe the statistical methods used, parametric *vs.* non-parametric analyses. Directly reference statistical packages and versions used.
        ii. P-values, median or mean, standard deviation or range should be used as standard.
        iii. Correct for multiple comparisons if required.
    b. Specific
        i. Describe properties of statistical models if used.
        ii. Use ROC curves to convey the performance characteristics of diagnostic markers if relevant.
        iii. Where applicable, provide information on the treatment of missing values and outliers.

RESULTS

8. Data analysis and presentation
    a. Show the summarized demographics of the study or sample population
    b. Present experimental data in tables or graphs as required together with a description of the results to aid interpretation.

.

c. Biomarker specific characteristics
    i. Show data on the relationship between the biomarker(s) and existing prognostic measures.
    ii. Diagnostic biomarkers – sensitivity, specificity, PPV/NPV, receiver operating characteristic curve (ROC curve) and odds ratio, as appropriate.

DISCUSSION

9. A discussion of the results based on the original aims & objectives including any inferred clinical value. Discuss results in the context of comparable or similar previous studies.
10. Address limitations, sources of potential bias and suggest areas for future work.

5.5 Discussion

There is an overriding need in biomedical research to find clinically useful biomarkers to inform regulatory and therapeutic decisions without the need for expensive and time consuming experimental work. However, many biomarkers have failed in their application and their high attrition has left many doubtful and cynical, with thoughts of biomarkers being desirable but not essential becoming more prevalent [234; 235; 242; 243]. There is a growing need for standardised guidelines relating to every step of biomarker research representative of good experimental design with stringent criteria for data analysis and representation.

The guidelines outlined here represent minimal criteria required for the reporting of biomarker studies, and represents a unifying approach to biomarkers in neurological disorders that are in line with guidelines already published for other experimental studies. The European BioMS Society hopes the provision of these guidelines will ultimately lead to the content of publications being high, thereby reinforcing and increasing confidence in biomarker research.

Guidance's can now be found on many aspects of research (STARD, CONSORT, REMARK, PRISMA) and many journals require these as minimum reporting standards to be adhered to, making it easier for reviewers and editors to assess quality of work, but also for authors to view the standards and their justifications and provide a structure to their manuscript. Although there are existing guidance's, none are specific for biomarker reporting *per se* which is currently left to the direction of the journal/reviewer and much more clarity is needed here. The reporting guidelines should be able to provide a framework wherein clear and transparent reporting of study aims, methods, outcome(s) and interpretation of the results can take place, reflecting particularly on possible problem areas. Proposed standards should be weighted in toward scientific validity with requirements that impose data integrity constraints to permit reproduction of scientific work. Its production should follow a style that is universally accessible to all journals across many disciplines; a manuscript style is therefore favoured. It is important however that they do not evolve into critical appraisal tools for evaluating study quality and remain as their title indicates reporting guidelines which are there to assist authors in writing good biomarker articles [244]. Similarly, reporting guidelines should not stifle creativity in research but simply encourage clear explanations of individual decisions made in the study to provide clarity and completeness of reporting.

With all of the above recommendations in mind the BioMS-*eu* committee have developed a minimum framework for reporting biomarker research not to be re-produced at verbatim but to act as guides when preparing manuscripts. The development of comprehensive guidelines in practice is a continuous process and will be subject to change in the future based on new emerging evidence.

Ultimately, their value in reporting biomarker research will depend on how widely they are adopted by the scientific committee.

In the course of this thesis I have aimed to provide a clear representation of the analytical methods and results using this framework that can be used to judge the quality, reliability and reproducibility of the findings.

6 Concluding remarks and future directions

The observations made in this thesis point to one important over-riding conclusion about adult CNS plasticity and its capacity for repair for the first time that the author is aware of, that is guidance cues fundamental to axonal elongation and targeting is damaged during disease and fail to recover both in cell culture and *in-vivo*. Henceforth, abbreviating the potential for long-term recovery. Individuals most affected were those with primary neurodegenerative conditions, such as Alzheimer's disease or disorders with an underlying neurodegenerative predisposition, such as multiple sclerosis and motorneurone disease. This has obvious clinical implications for the treatment of CNS axonal injury. This supplements previous work in this area about recovery from neuronal injury in the adult CNS. Certainly, work by Rolf *et al.* [176] supports this, demonstrating that the long axonal projections of the corticospinal tract (CST) are impaired in the absence of neural cell adhesion molecule and may not be capable of long-term survival, leading to disease progression.

A key event in axonal recovery after injury is the elaboration of a growth cone – the motile tip that navigates the axon across the tissue substratum; which is preceded by induction of growth cone components, including GAP-43 and NCAM, that persist in the adult brain in regions of neuronal plasticity, making them the logical choice for measuring regenerative potential in the mature CNS [59; 245; 246; 247]. Higher vertebrates have to a greater degree lost their ability to regenerate CNS axons over the long-term during the course of evolution, unlike their anamniotic vertebrate (fish and amphibians) counterparts. Within the rat neuronal culture system there is a gradual repression in NCAM over time, with a failure to re-express more following injury. In experimental autoimmune encephalomyelitis (EAE), NCAM is lost precipitously irrespective of disease

type, whether it is relapsing-remitting (SJL mice) or a more chronic course without complete remissions (C57BL/6 mice). From this it may be inferred that repair in the CNS is hampered by two negative conditions: 1) the lack of reserve in the ageing nervous system; 2) the absence of growth cone trophic substances able to sustain longitudinal extension of interrupted nerve fibers. Epidemiological evidence from multiple sclerosis patients alludes to this possibility; with the finding that disability onset is age-dependent with younger onset reaching disability milestones earlier, not significantly affected by disease type, be it relapsing-remitting or progressive [188; 248].

The existence of soluble forms of NCAM in blood, CSF and cell culture supernatants has long been known [75; 131; 142]. Although, GAP-43 was originally isolated synaptic plasma membranes, it is also present in substantial quantities in the CSF, but not in blood. Whether they are actively secreted into extracellular space or released by detachment is difficult to ascertain. Although their constant level in subjects without significant neurological disease implies the existence of active secretion mechanism with the establishment of a dynamic equilibrium in the CSF. Previously soluble NCAM has been found to be present in culture medium before the appearance of membrane-associated NCAM on the cell surface, indicating that soluble NCAM contains a secreted component [75; 142]. The exact role of both soluble NCAM and GAP-43 remains to be fully elucidated. Nonetheless, it may be plausible that they act as local trophic factors in the process of restorative neurogenesis, akin to neuroendocrine hormones involved in autocrine and paracrine signaling.

A critical threshold value for NCAM expression that is required for increased neurite outgrowth has been demonstrated in neurons cultured on monolayers of cells expressing transfected NCAM. Above this threshold, even small increases in NCAM induced a significant increase in neurite outgrowth [249]. An intriguing speculation would be whether parallels can be drawn from this work to soluble CSF NCAM levels where similar threshold values may in theory be in operation. It is then plausible that the low levels demonstrated in the neurodegenerative disorders are not conducive to neurite outgrowth, resulting in a reduced potential for recovery after injury. Some support for this concept is evidenced by the polarization in NCAM values between relapsing-remitting MS and secondary progressive MS. Although, GAP-43 measurements showed no such trend, it would be worthwhile reinvestigating the existence of a threshold value for neuronal responsiveness to GAP-43 in a larger sample size. Although Teunissen *et al*. have demonstrated that GAP-43 expression was found to be reduced in majority of white matter plaques in MS, this was independent of the lesion stage [111].

These experiments have opened several avenues for investigating the impact of disease on neurons at a molecular level. If these findings are supported by future investigations, this has significant implications for being able to measure repair in the adult CNS and the notion of discovering possible targets for clinical intervention in the process is intuitively appealing. With this in mind areas for future work are considered below:

1) Functional evidence to support a role for NCAM in repair and disability using $NCAM^{-/-}$ knock out mice. During development the overall brain architecture of

the knock outs is surprisingly normal with a mild phenotype that is puzzling considering the prominent role assigned to NCAM in regulating axonal growth. With Experimental autoimmune encephalomyelitis (EAE) we have found a severe drop in the NCAM content of spinal cords, and previous investigators have demonstrated hypoplasia of the corticospinal tract in adult NCAM-deficient mice – what then would be the result of inducing EAE in $NCAM^{-/-}$ mice? This work will aim to dissect the molecular effects of inflammation/demyelination on axonal plasticity in the face of NCAM deficiency, and assess the effect on corticospinal tract function using real-time mobility measures (rota-rod) and disability scoring systems (EAE scoring system).

2) NCAM immunoreactivity in acutely demyelinated plaques has been demonstrated to be greatly reduced, further work studying NCAM in various stages of the demyelinated MS plaque will favor a hypothesis of reduced plasticity in chronic MS.

3) CSF NCAM and to some extent GAP-43 (although further clarification from *in-vitro* and *in-vivo* models is needed) have the potential to be used as prognostic biomarkers to assess the risk of disease progression in the context of neuroprotective clinical trials and can be used in patient stratification either at the beginning or end of the trial, thereby simplifying subsequent interpretation of the clinical findings and providing benchmarks for future trials.

This would require adding a biological arm to longitudinal Phase II clinical trials with repeated lumbar puncture analysis. Our inability to measure these biomarkers in the blood reliably makes this the only viable option, *cf.* Tau and

Aβ measures in Alzheimer's disease. Moreover, analysis performed during or right after treatment may provide mechanistic explanations for a drug's action and its role in plasticity.

4) Lastly, the precise role of soluble NCAM and GAP-43 in plasticity of the adult CNS is not well understood. It would be important with future experiments to address a) the mechanisms whereby these factors regulate cell adhesion and synaptic function, respectively, b) whether there is a critical threshold for neuronal responsiveness to soluble NCAM and GAP-43 and c) whether boosting their levels lead to improved repair/recovery following injury in the adult nervous system.

7 Appendix

7.1 Chapter 2

7.1.1 Polyacrylamide gel electrophoresis (PAGE) and ELISA: Buffers and solutions

Product no.	Uses	Constituents, product
NuPAGE MES SDS buffer	Running buffer in PAGE	500mL (20x), pH of 1x solution is 7.3 50mM MES, 50mM Tris Base, 0.1% SDS, 1mM EDTA #NP0002, Invitrogen
NuPAGE LDS sample	Sample solubilisation	10mL (4x) #NP0007, Invitrogen
DL-Dithiothreitol (DTT), Cleland's reagent	Reducing protein disulfide bonds prior to PAGE	1g #D0632, Sigma
NuPAGE Transfer buffer	Immunoblotting	500mL (20x), pH of 1x solution is 7.2 25mM Bicine, 25mM Bis-Tris, 1mM EDTA, 0.05mM Chlorobutanol
Methanol, CH_3OH	Immunoblotting	2.5L GPR Rectapur #20846.326, VWR
Enhanced chemiluminescent	Chemiluminescence	500mL SuperSignal® West Pico

developing solution		Chemiluminescent substrate #34078, Thermo Scientific
PBS solution	Binding, diluent and wash solutions in ELISA	Dry powder dissolved in 1L deionised water will yield 1M PBS, pH 7.4 #P5368, Sigma
Supersensitive TMB substrate	Detection of antibody reactivity in ELISA	#T4444, Sigma

7.1.2 Proteomics buffers

Product no.	**Uses**	**Constituents, product**
BSA solution	Blocking buffer	0.1% BSA/1M PBS, pH 7.4 #A3294, Sigma
Triton X-100 wash solution	Washing buffer	1M PBS with 0.1% Triton X-100 #T9284, Sigma
5mM ammonium acetate	Removal of salts	0.3854g in 1L, pH 7.0 (pH using solution of ammonia or acetic acid, never HCL or NaOH) #A7330, Sigma
Sinapinic acid matrix	Matrix for MS	SPA in 50% ACN and 0.1% TFA

		#49508, Fluka
ACN and formic acid Solutions	Removal of proteins from chips	70% ACN/0.2% TFA followed by 50% formic acid/25% ACN/15% isopropanol/10%H_2O

7.2 Chapter 3

7.2.1 D1 Solution [250]

All purchased from Sigma (UK) unless specified:

138 mM NaCl

5.4 mM KCl

0.17 mM Na_2HPO_4

0.22 mM KH_2PO_4

5.55 mM D-glucose

58.43 mM sucrose

5 mg/L phenol red solution (Gibco BRL Life Technologies Ltd, UK)

7.2.2 Aggregate media

Serum free high glucose Dulbecco's modified Eagle's medium without sodium pyruvate (DMEM; Gibco BRL), supplemented with:

0.8 μM bovine insulin

Trace hormones, vitamins and elements [186]

100 U/mL penicillin (Gibco BRL)

100 μg/mL streptomycin (Gibco BRL)

7.3 Chapter 4

7.3.1 Purification recipes: native and denaturing conditions

7.3.1.1 Buffer Stock Solutions (10x)

Prepare sodium phosphate stock solutions as follows:

Stock Solution A (10x)

200 mM sodium phosphate, monobasic (NaH_2PO_4); #S0751 Sigma

5 M NaCl; #S5886 Sigma

Dissolve 27.6 g sodium phosphate, monobasic and 292.9 g NaCl in 900 mL of deionized water. Mix well and adjust volume to 1L with deionized water. Store solution at room temperature.

Stock Solution B (10x)

200 mM sodium phosphate, dibasic (Na_2HPO_4); #71284 Sigma

5 M NaCl

Dissolve 28.4 g sodium phosphate, dibasic and 292.9 g NaCl in 900 mL of deionized water. Mix well and adjust volume to 1L with deionized water. Store solution at room temperature.

7.3.1.2 5x Native Purification Buffer, pH 8.0

250 mM NaH_2PO_4

2.5 M NaCl

Prepare 200 mL solution as follows:

1. To 180 mL deionized water, add

NaH_2PO_4	7 g
NaCl	29.2 g

2. Adjust pH with NaOH to pH 8.0
3. Bring the final volume to 200 mL with water
4. Store buffer at room temperature.

7.3.1.3 3 M imidazole, pH 6.0

3 M imidazole; #I202 Sigma

500 mM NaCl

20 mM Sodium phosphate buffer, pH 6.0

Prepare 100 mL solution as follows:

1. To 90 mL deionized water, add

Imidazole	20.6 g
Stock Solution A (10x)	8.77 mL
Stock Solution B (10x)	1.23 mL

2. Adjust pH to 6.0 with HCL or NaOH as necessary
3. Bring the final volume to 100 mL with deionized water. If the solution forms a precipitate, heat the solution until the precipitate dissolves.
4. Store buffer at room temperature.

7.3.1.4 Native conditions

<u>1x Native Purification Buffer</u>

To prepare 100 mL 1x Native Purification Buffer:

80 mL sterile distilled water

20 mL 5x Native Purification Buffer

Adjust pH to 8.0 with NaOH or HCL.

Native Binding Buffer

Use 1x Native Purification Buffer as Native Binding Buffer.

Native Wash Buffer

To prepare 50 mL Native Wash Buffer with 20mM imidazole:

50 mL 1x Native Purification Buffer

335 µL of 3M Imidazole, pH 6.0

Adjust pH to 8.0 with NaOH or HCL

Native Elution Buffer

To prepare 15 mL Native Elution Buffer with 250 mM imidazole:

13.75 mL 1x Native Purification Buffer

1.25 mL 3M imidazole, pH 6.0

Adjust pH to 8.0 with NaOH or HCL.

7.3.1.5 Denaturing conditions

Denaturing Binding Buffer

8 M urea

50 mM NaCl

20 mM sodium phosphate, pH 7.8

Prepare 100 mL solution as follows:

1. To 90 mL deionized water, add

Stock Solution A (10x)	0.58 mL
Stock Solution B (10x)	9.42 mL
Urea	48.1 g

2. Stir the solution with gentle heating (50-60^{o}C) until completely dissolved. When cooled at room temperature, adjust pH to 7.8 using NaOH or HCL.
3. Bring volume to 100 mL.
4. Store buffer at room temperature.

<u>Denaturing Wash buffer</u>

8 M urea

500 mM NaCl

20 mM Sodium phosphate, pH 6.0

Prepare 100 mL solution as follows:

1. To 90 mL deionized water, add

Stock Solution A (10x)	7.38 mL
Stock Solution B (10x)	2.62 mL
Urea	48.1 g

2. Stir the solution with gentle heating (50-60^{o}C) until completely dissolved. Adjust pH to 6.0 using NaOH or HCL.
3. Bring the volume to 100 mL.
4. Store buffer at room temperature.

<u>Denaturing Elution Buffer</u>

8 M urea

500 mM NaCl

20 mM Sodium phosphate, pH 4.0

Prepare 100 mL as follows:

1. To 90 mL deionized water, add

Stock Solution A (10x)	10 mL
Urea	48.1 g

2. Stir the solution with gentle heating (50-60^{o}C) until completely dissolved. Adjust pH to 4.0 using NaOH or HCL.
3. Bring the volume to 100 mL.
4. Store buffer at room temperature.

NB: Filter steralise all buffers using a 0.45 µm filter (autoclaving the solution will alter the pH of the buffer).

7.4 Chapter 5

Members of the BioMS-*eu* committee:

<u>Steering Committee</u>

- General manager: C. Teunissen (Amsterdam)
- Vice manager: G. Giovannoni (London)
- F. Deisenhammer (Innsbruck)
- H. Tumani (Ulm)

<u>Scientific committee</u>

- B. Hemmer (Munich)
- G. Giovannoni (London)

Other members

- A. Altintas (Istanbul)
- A. Bartos (Prague)
- L. Brundin (Stockholm)
- M. Comabella (Barcelona)
- E. Fainardi (Ferrara)
- D. Franciotta (Pavia)
- J. Frederiksen (Copenhagen)
- R. Furlan (Milano)
- D. Galimberti (Milan)
- S. Gnanapavan (London)
- E. Havrdova (Prague)
- J. Hillert (Stockholm)
- R. Hintzen (Rotterdam)
- M. Khademi (Stockholm)
- R. Lindberg (Basel)
- R. Martin (Barcelona)
- X. Montalban (Barcelona)
- K. Rejdak (Warsaw)
- J. Richert (USA)
- C. Sindic (Bruxelles)
- A. Siva (Istanbul)
- L. Vecsei (Szeged)
- F. Berven (Bergen)

Reporting guideline	Description	URL/Reference
CONSORT: Consolidated Standards of Reporting Trials	Reporting of randomised control trials	http://www.consort-statement.org/
EQUATOR: Enhancing the QUAlity and Transparency Of health Research	For good reporting of health research studies	http://www.equator-network.org/
MIAPE: The Minimum Information About a Proteomics Experiment	Reporting guidelines for proteomics	http://www.psidev.info/index.php?q=node/91
MIBBI: Minimum Information of Biological and Biomedical Investigations	For reporting aspects of biological and biomedical science	http://www.mibbi.org/index.php/Main_Page
MOOSE: Meta-analysis of Observational Studies in Epidemiology	Proposal for reporting meta-analyses of observational studies in epidemiology	Stroup,D.F. *et al.* JAMA. 2000 Apr 19; 283 (15): 2008-12. Review. PubMed PMID: 10789670
PRISMA: Preferred Reporting Items for Systematic Reviews and Meta-Analyses	Minimum set of items for reporting in systematic reviews and meta-analyses	http://www.prisma-statement.org/
QUOROM: QUality Of Reporting Meta-analyses	Reporting meta-analyses of randomised control trials	http://www.consort-statement.org/
REMARK:	Guidelines for	McShane,L.M. *et al*. Breast Cancer Res.

REporting recommendations for tumor MARKer prognostic studies	reporting tumour marker studies	Treat. 2006 Nov; 100 (2):229-35. PubMed PMID: 16932852
STARD: STAndards for the reporting of Diagnostic accuracy	Reporting studies of diagnostic accuracy	http://www.stard-statement.org/
STREGA: STrengthening the REporting of OBservational Studies in Epidemiology	Guidelines to promote clear reporting of genetic association studies	http://www.cdc.gov/genomics/hugenet/workshops/strega.htm
STROBE: STrengthening the Reporting of OBservational studies in Epidemiology	Reporting of observational studies	http://www.strobe-statement.org/Support.html

7.5 Publications

1. **Gnanapavan, S.**, Grant, D., Illes-Toth, E., Lakdawala, N., Keir, G. & Giovannoni, G. Neural cell adhesion molecule--description of a CSF ELISA method and evidence of reduced levels in selected neurological disorders (2010). J Neuroimmunol **225**, 118-22.

2. **Gnanapavan, S.** & Giovannoni, G. Neural cell adhesion molecules in brain plasticity and disease (2013). Multiple Sclerosis and Related Disorders **2**, 13-20.

3. **Gnanapavan, S.**, Ho, P., Heywood, W., Jackson, S., Grant, D., Rantell, K., Keir, G., Mills, K., Steinman, L. & Giovannoni, G. Progression in multiple sclerosis is associated with low endogenous NCAM (2013). J Neurochem **125**, 766-73.

4. **Gnanapavan, S.**, Grant, D., Morant, S., Furby, J., Hayton, T., Teunissen, C., Leoni, V., Marta, M., Brenner, R., Palace, J., Miller, D., Kapoor, R. & Giovannoni, G. Biomarker report from the Phase II Lamotrigine Trial in Secondary Progressive MS – neurofilaments as a surrogate of disease progression (2013). PLoS One, *in press.*

7.6 Presentations

2006

NMSS National Conference '1st Translational Research Partnerships Investigator Meeting' A Promise 2010 Initiative, FL, United States, "Modelling Multiple Sclerosis using biological markers and 3D neuronal cell cultures".

2008

Inims-symposium 2008, Hamburg, Germany, "Markers of degeneration/regeneration, demyelination/axonal damage".

2009

Don Gnocchi Foundation, Milan, Italy, “Evaluation of axonal pathology”.

2010

7th BioMS-*eu* meeting, Amsterdam, “Neural cell adhesion molecule (NCAM)”.

Health Education Services, London, “Biomarkers: Their application in clinical trials course”.

ECTRIMS, Teaching course 5, Gothenburg, Sweden, “NCAM and related markers in th CSF of patients with MS”.

2012

9th BioMS-*eu* meeting, Lyon, France, “Neural cell adhesion molecule in plasticity”.

7.7 References

1. Nath, S., Agholme, L., Kurudenkandy, F. R., Granseth, B., Marcusson, J. & Hallbeck, M. (2012). Spreading of neurodegenerative pathology via neuron-to-neuron transmission of beta-amyloid. *J Neurosci* **32**, 8767-77.
2. Koo, E. H., Lansbury, P. T., Jr. & Kelly, J. W. (1999). Amyloid diseases: abnormal protein aggregation in neurodegeneration. *Proc Natl Acad Sci U S A* **96**, 9989-90.
3. Stefanis, L. (2012). alpha-Synuclein in Parkinson's disease. *Cold Spring Harb Perspect Med* **2**, a009399.

4. Xilouri, M., Brekk, O. R. & Stefanis, L. (2012). Alpha-synuclein and protein degradation systems: a reciprocal relationship. *Mol Neurobiol* **47**, 537-51.
5. Trapp, B. D., Peterson, J., Ransohoff, R. M., Rudick, R., Mork, S. & Bo, L. (1998). Axonal transection in the lesions of multiple sclerosis. *N Engl J Med* **338**, 278-85.
6. Tator, C. H. (1995). Update on the pathophysiology and pathology of acute spinal cord injury. *Brain Pathol* **5**, 407-13.
7. Raineteau, O. & Schwab, M. E. (2001). Plasticity of motor systems after incomplete spinal cord injury. *Nat Rev Neurosci* **2**, 263-73.
8. Martino, G. (2004). How the brain repairs itself: new therapeutic strategies in inflammatory and degenerative CNS disorders. *Lancet Neurol* **3**, 372-8.
9. Filippi, M., Paty, D. W., Kappos, L., Barkhof, F., Compston, D. A., Thompson, A. J., Zhao, G. J., Wiles, C. M., McDonald, W. I. & Miller, D. H. (1995). Correlations between changes in disability and T2-weighted brain MRI activity in multiple sclerosis: a follow-up study. *Neurology* **45**, 255-60.
10. Price, J. L., Ko, A. I., Wade, M. J., Tsou, S. K., McKeel, D. W. & Morris, J. C. (2001). Neuron number in the entorhinal cortex and CA1 in preclinical Alzheimer disease. *Arch Neurol* **58**, 1395-402.
11. Mirmiran, M., van Someren, E. J. & Swaab, D. F. (1996). Is brain plasticity preserved during aging and in Alzheimer's disease? *Behav Brain Res* **78**, 43-8.
12. Palop, J. J., Chin, J. & Mucke, L. (2006). A network dysfunction perspective on neurodegenerative diseases. *Nature* **443**, 768-73.
13. Mesulam, M. M. (1999). Neuroplasticity failure in Alzheimer's disease: bridging the gap between plaques and tangles. *Neuron* **24**, 521-9.
14. Mesulam, M. M. (2000). A plasticity-based theory of the pathogenesis of Alzheimer's disease. *Ann N Y Acad Sci* **924**, 42-52.
15. Shankar, G. M. & Walsh, D. M. (2009). Alzheimer's disease: synaptic dysfunction and Abeta. *Mol Neurodegener* **4**, 48.
16. Correale, J. & Villa, A. (2004). The neuroprotective role of inflammation in nervous system injuries. *J Neurol* **251**, 1304-16.
17. Neumann, H., Kotter, M. R. & Franklin, R. J. (2009). Debris clearance by microglia: an essential link between degeneration and regeneration. *Brain* **132**, 288-95.
18. Sim, F. J., Zhao, C., Penderis, J. & Franklin, R. J. (2002). The age-related decrease in CNS remyelination efficiency is attributable to an impairment of both oligodendrocyte progenitor recruitment and differentiation. *J Neurosci* **22**, 2451-9.
19. Kim, J. E., Li, S., GrandPre, T., Qiu, D. & Strittmatter, S. M. (2003). Axon regeneration in young adult mice lacking Nogo-A/B. *Neuron* **38**, 187-99.
20. Shewan, D., Dwivedy, A., Anderson, R. & Holt, C. E. (2002). Age-related changes underlie switch in netrin-1 responsiveness as growth cones advance along visual pathway. *Nat Neurosci* **5**, 955-62.
21. Lanahan, A., Lyford, G., Stevenson, G. S., Worley, P. F. & Barnes, C. A. (1997). Selective alteration of long-term potentiation-induced transcriptional response in hippocampus of aged, memory-impaired rats. *J Neurosci* **17**, 2876-85.
22. Scheff, S. W., Benardo, L. S. & Cotman, C. W. (1980). Decline in reactive fiber growth in the dentate gyrus of aged rats compared to

young adult rats following entorhinal cortex removal. *Brain Res* **199**, 21-38.
23. Jin, K., Wang, X., Xie, L., Mao, X. O., Zhu, W., Wang, Y., Shen, J., Mao, Y., Banwait, S. & Greenberg, D. A. (2006). Evidence for stroke-induced neurogenesis in the human brain. *Proc Natl Acad Sci U S A* **103**, 13198-202.
24. Arvidsson, A., Collin, T., Kirik, D., Kokaia, Z. & Lindvall, O. (2002). Neuronal replacement from endogenous precursors in the adult brain after stroke. *Nat Med* **8**, 963-70.
25. Parent, J. M., Vexler, Z. S., Gong, C., Derugin, N. & Ferriero, D. M. (2002). Rat forebrain neurogenesis and striatal neuron replacement after focal stroke. *Ann Neurol* **52**, 802-13.
26. Javier DeFelipe, E. G. J., Ed. (1991). Cajal's Degeneration & Regeneration of the Nervous System: Oxford University Press.
27. Illis, L. S. (2012). Central nervous system regeneration does not occur. *Spinal Cord* **50**, 259-63.
28. Bandtlow, C. E. (2003). Regeneration in the central nervous system. *Exp Gerontol* **38**, 79-86.
29. Yiu, G. & He, Z. (2006). Glial inhibition of CNS axon regeneration. *Nat Rev Neurosci* **7**, 617-27.
30. Murray, M., Tobias, C.A. (2003). Regeneration and sprouting in the injured spinal cord: a decade of growth. *Top Spinal Cord Inj Rehabil* **8**, 37-51.
31. Goodman, C. S. (1996). Mechanisms and molecules that control growth cone guidance. *Annu Rev Neurosci* **19**, 341-77.
32. Koeberle, P. D. & Bahr, M. (2004). Growth and guidance cues for regenerating axons: where have they gone? *J Neurobiol* **59**, 162-80.
33. Walsh, F. S. & Doherty, P. (1997). Neural cell adhesion molecules of the immunoglobulin superfamily: role in axon growth and guidance. *Annu Rev Cell Dev Biol* **13**, 425-56.
34. Harel, N. Y. & Strittmatter, S. M. (2006). Can regenerating axons recapitulate developmental guidance during recovery from spinal cord injury? *Nat Rev Neurosci* **7**, 603-16.
35. Benowitz, L. I. & Routtenberg, A. (1997). GAP-43: an intrinsic determinant of neuronal development and plasticity. *Trends Neurosci* **20**, 84-91.
36. Benowitz, L. I. & Schmidt, J. T. (1987). Activity-dependent sharpening of the regenerating retinotectal projection in goldfish: relationship to the expression of growth-associated proteins. *Brain Res* **417**, 118-26.
37. Skene, J. H. (1989). Axonal growth-associated proteins. *Annu Rev Neurosci* **12**, 127-56.
38. Grill, R., Murai, K., Blesch, A., Gage, F. H. & Tuszynski, M. H. (1997). Cellular delivery of neurotrophin-3 promotes corticospinal axonal growth and partial functional recovery after spinal cord injury. *J Neurosci* **17**, 5560-72.
39. Jones, L. L., Oudega, M., Bunge, M. B. & Tuszynski, M. H. (2001). Neurotrophic factors, cellular bridges and gene therapy for spinal cord injury. *J Physiol* **533**, 83-9.
40. Novikova, L., Novikov, L. & Kellerth, J. O. (1996). Brain-derived neurotrophic factor reduces necrotic zone and supports neuronal survival after spinal cord hemisection in adult rats. *Neurosci Lett* **220**, 203-6.

41. Oudega, M. & Hagg, T. (1996). Nerve growth factor promotes regeneration of sensory axons into adult rat spinal cord. *Exp Neurol* **140**, 218-29.
42. Sayer, F. T., Oudega, M. & Hagg, T. (2002). Neurotrophins reduce degeneration of injured ascending sensory and corticospinal motor axons in adult rat spinal cord. *Exp Neurol* **175**, 282-96.
43. Liu, B. P., Cafferty, W. B., Budel, S. O. & Strittmatter, S. M. (2006). Extracellular regulators of axonal growth in the adult central nervous system. *Philos Trans R Soc Lond B Biol Sci* **361**, 1593-610.
44. Yiu, G. & He, Z. (2003). Signaling mechanisms of the myelin inhibitors of axon regeneration. *Curr Opin Neurobiol* **13**, 545-51.
45. Azevedo, F. A., Carvalho, L. R., Grinberg, L. T., Farfel, J. M., Ferretti, R. E., Leite, R. E., Jacob Filho, W., Lent, R. & Herculano-Houzel, S. (2009). Equal numbers of neuronal and nonneuronal cells make the human brain an isometrically scaled-up primate brain. *J Comp Neurol* **513**, 532-41.
46. Sur, M. & Rubenstein, J. L. (2005). Patterning and plasticity of the cerebral cortex. *Science* **310**, 805-10.
47. Kiryushko, D., Berezin, V. & Bock, E. (2004). Regulators of neurite outgrowth: role of cell adhesion molecules. *Ann N Y Acad Sci* **1014**, 140-54.
48. Ronn, L. C., Hartz, B. P. & Bock, E. (1998). The neural cell adhesion molecule (NCAM) in development and plasticity of the nervous system. *Exp Gerontol* **33**, 853-64.
49. Tomasiewicz, H., Ono, K., Yee, D., Thompson, C., Goridis, C., Rutishauser, U. & Magnuson, T. (1993). Genetic deletion of a neural cell adhesion molecule variant (N-CAM-180) produces distinct defects in the central nervous system. *Neuron* **11**, 1163-74.
50. Rutishauser, U., Acheson, A., Hall, A. K., Mann, D. M. & Sunshine, J. (1988). The neural cell adhesion molecule (NCAM) as a regulator of cell-cell interactions. *Science* **240**, 53-7.
51. Cremer, H., Chazal, G., Goridis, C. & Represa, A. (1997). NCAM is essential for axonal growth and fasciculation in the hippocampus. *Mol Cell Neurosci* **8**, 323-35.
52. Cox, E. T., Brennaman, L. H., Gable, K. L., Hamer, R. M., Glantz, L. A., Lamantia, A. S., Lieberman, J. A., Gilmore, J. H., Maness, P. F. & Jarskog, L. F. (2009). Developmental regulation of neural cell adhesion molecule in human prefrontal cortex. *Neuroscience* **162**, 96-105.
53. Chuong, C. M. & Edelman, G. M. (1984). Alterations in neural cell adhesion molecules during development of different regions of the nervous system. *J Neurosci* **4**, 2354-68.
54. Daston, M. M., Bastmeyer, M., Rutishauser, U. & O'Leary, D. D. (1996). Spatially restricted increase in polysialic acid enhances corticospinal axon branching related to target recognition and innervation. *J Neurosci* **16**, 5488-97.
55. Fraser, S. E., Murray, B. A., Chuong, C. M. & Edelman, G. M. (1984). Alteration of the retinotectal map in Xenopus by antibodies to neural cell adhesion molecules. *Proc Natl Acad Sci U S A* **81**, 4222-6.
56. Williams, D. K., Gannon-Murakami, L., Rougon, G. & Udin, S. B. (1996). Polysialylated neural cell adhesion molecule and plasticity of ipsilateral connections in Xenopus tectum. *Neuroscience* **70**, 277-85.

57. Yin, X., Watanabe, M. & Rutishauser, U. (1995). Effect of polysialic acid on the behavior of retinal ganglion cell axons during growth into the optic tract and tectum. *Development* **121**, 3439-46.
58. Polo-Parada, L., Bose, C. M. & Landmesser, L. T. (2001). Alterations in transmission, vesicle dynamics, and transmitter release machinery at NCAM-deficient neuromuscular junctions. *Neuron* **32**, 815-28.
59. Skene, J. H., Jacobson, R. D., Snipes, G. J., McGuire, C. B., Norden, J. J. & Freeman, J. A. (1986). A protein induced during nerve growth (GAP-43) is a major component of growth-cone membranes. *Science* **233**, 783-6.
60. Oestreicher, A. B. & Gispen, W. H. (1986). Comparison of the immunocytochemical distribution of the phosphoprotein B-50 in the cerebellum and hippocampus of immature and adult rat brain. *Brain Res* **375**, 267-79.
61. Skene, J. H. & Willard, M. (1981). Changes in axonally transported proteins during axon regeneration in toad retinal ganglion cells. *J Cell Biol* **89**, 86-95.
62. Aigner, L., Arber, S., Kapfhammer, J. P., Laux, T., Schneider, C., Botteri, F., Brenner, H. R. & Caroni, P. (1995). Overexpression of the neural growth-associated protein GAP-43 induces nerve sprouting in the adult nervous system of transgenic mice. *Cell* **83**, 269-78.
63. Strittmatter, S. M., Fankhauser, C., Huang, P. L., Mashimo, H. & Fishman, M. C. (1995). Neuronal pathfinding is abnormal in mice lacking the neuronal growth cone protein GAP-43. *Cell* **80**, 445-52.
64. Coleman, P. D. & Flood, D. G. (1987). Neuron numbers and dendritic extent in normal aging and Alzheimer's disease. *Neurobiol Aging* **8**, 521-45.
65. Nagata, I. & Schachner, M. (1986). Conversion of embryonic to adult form of the neural cell adhesion molecule (N-CAM) does not correlate with pre- and postmigratory states of mouse cerebellar granule neurons. *Neurosci Lett* **63**, 153-8.
66. Linnemann, D., Gaardsvoll, H., Olsen, M. & Bock, E. (1993). Expression of NCAM mRNA and polypeptides in aging rat brain. *Int J Dev Neurosci* **11**, 71-81.
67. Pollerberg, E. G., Sadoul, R., Goridis, C. & Schachner, M. (1985). Selective expression of the 180-kD component of the neural cell adhesion molecule N-CAM during development. *J Cell Biol* **101**, 1921-9.
68. Persohn, E., Pollerberg, G. E. & Schachner, M. (1989). Immunoelectron-microscopic localization of the 180 kD component of the neural cell adhesion molecule N-CAM in postsynaptic membranes. *J Comp Neurol* **288**, 92-100.
69. Willcox, B. J. & Scott, J. N. (2004). Growth-associated proteins and regeneration-induced gene expression in the aging neuron. *Mech Ageing Dev* **125**, 513-6.
70. Schmidt, R. E., Spencer, S. A., Coleman, B. D. & Roth, K. A. (1991). Immunohistochemical localization of GAP-43 in rat and human sympathetic nervous system--effects of aging and diabetes. *Brain Res* **552**, 190-7.
71. Schmoll, H., Ramboiu, S., Platt, D., Herndon, J. G., Kessler, C. & Popa-Wagner, A. (2005). Age influences the expression of GAP-43 in the rat hippocampus following seizure. *Gerontology* **51**, 215-24.

72. Felgenhauer, K. (1974). Protein size and cerebrospinal fluid composition. *Klin Wochenschr* **52**, 1158-64.
73. Bock, E. (1973). Quantitation of plasma proteins in cerebrospinal fluid. *Scand J Immunol Suppl* **1**, 111-7.
74. Sadoul, K., Meyer, A., Low, M. G. & Schachner, M. (1986). Release of the 120 kDa component of the mouse neural cell adhesion molecule N-CAM from cell surfaces by phosphatidylinositol-specific phospholipase C. *Neurosci Lett* **72**, 341-6.
75. Bock, E., Edvardsen, K., Gibson, A., Linnemann, D., Lyles, J. M. & Nybroe, O. (1987). Characterization of soluble forms of NCAM. *FEBS Lett* **225**, 33-6.
76. Siman, R., McIntosh, T. K., Soltesz, K. M., Chen, Z., Neumar, R. W. & Roberts, V. L. (2004). Proteins released from degenerating neurons are surrogate markers for acute brain damage. *Neurobiol Dis* **16**, 311-20.
77. Minagar, A. & Alexander, J. S. (2003). Blood-brain barrier disruption in multiple sclerosis. *Mult Scler* **9**, 540-9.
78. Dhib-Jalbut, S. (2007). Pathogenesis of myelin/oligodendrocyte damage in multiple sclerosis. *Neurology* **68**, S13-21; discussion S43-54.
79. Serafini, B., Rosicarelli, B., Magliozzi, R., Stigliano, E. & Aloisi, F. (2004). Detection of ectopic B-cell follicles with germinal centers in the meninges of patients with secondary progressive multiple sclerosis. *Brain Pathol* **14**, 164-74.
80. Prineas, J. W., Barnard, R. O., Kwon, E. E., Sharer, L. R. & Cho, E. S. (1993). Multiple sclerosis: remyelination of nascent lesions. *Ann Neurol* **33**, 137-51.
81. Barkhof, F., Bruck, W., De Groot, C. J., Bergers, E., Hulshof, S., Geurts, J., Polman, C. H. & van der Valk, P. (2003). Remyelinated lesions in multiple sclerosis: magnetic resonance image appearance. *Arch Neurol* **60**, 1073-81.
82. Ozawa, K., Suchanek, G., Breitschopf, H., Bruck, W., Budka, H., Jellinger, K. & Lassmann, H. (1994). Patterns of oligodendroglia pathology in multiple sclerosis. *Brain* **117 (Pt 6)**, 1311-22.
83. Rodriguez, M. & Scheithauer, B. (1994). Ultrastructure of multiple sclerosis. *Ultrastruct Pathol* **18**, 3-13.
84. Pryce, G., O'Neill, J. K., Croxford, J. L., Amor, S., Hankey, D. J., East, E., Giovannoni, G. & Baker, D. (2005). Autoimmune tolerance eliminates relapses but fails to halt progression in a model of multiple sclerosis. *J Neuroimmunol* **165**, 41-52.
85. Coles, A. J., Cox, A., Le Page, E., Jones, J., Trip, S. A., Deans, J., Seaman, S., Miller, D. H., Hale, G., Waldmann, H. & Compston, D. A. (2006). The window of therapeutic opportunity in multiple sclerosis: evidence from monoclonal antibody therapy. *J Neurol* **253**, 98-108.
86. Franklin, R. J. & Ffrench-Constant, C. (2008). Remyelination in the CNS: from biology to therapy. *Nat Rev Neurosci* **9**, 839-55.
87. Stys, P. K. (2005). General mechanisms of axonal damage and its prevention. *J Neurol Sci* **233**, 3-13.
88. Lo, A. C., Saab, C. Y., Black, J. A. & Waxman, S. G. (2003). Phenytoin protects spinal cord axons and preserves axonal conduction and neurological function in a model of neuroinflammation in vivo. *J Neurophysiol* **90**, 3566-71.
89. Joosten, E. A. (1997). Corticospinal tract regrowth. *Prog Neurobiol* **53**, 1-25.

90. Group, B. D. W. (2001). Biomarkers and surrogate endpoints: preferred definitions and conceptual framework. *Clin Pharmacol Ther* **69**, 89-95.
91. Bielekova, B. & Martin, R. (2004). Development of biomarkers in multiple sclerosis. *Brain* **127**, 1463-78.
92. Lassere, M. N., Johnson, K. R., Boers, M., Tugwell, P., Brooks, P., Simon, L., Strand, V., Conaghan, P. G., Ostergaard, M., Maksymowych, W. P., Landewe, R., Bresnihan, B., Tak, P. P., Wakefield, R., Mease, P., Bingham, C. O., 3rd, Hughes, M., Altman, D., Buyse, M., Galbraith, S. & Wells, G. (2007). Definitions and validation criteria for biomarkers and surrogate endpoints: development and testing of a quantitative hierarchical levels of evidence schema. *J Rheumatol* **34**, 607-15.
93. Cohn, J. N. (2004). Introduction to surrogate markers. *Circulation* **109**, IV20-1.
94. Katz, R. (2004). Biomarkers and surrogate markers: an FDA perspective. *NeuroRx* **1**, 189-95.
95. Miller, D. H., Albert, P. S., Barkhof, F., Francis, G., Frank, J. A., Hodgkinson, S., Lublin, F. D., Paty, D. W., Reingold, S. C. & Simon, J. (1996). Guidelines for the use of magnetic resonance techniques in monitoring the treatment of multiple sclerosis. US National MS Society Task Force. *Ann Neurol* **39**, 6-16.
96. Schmierer, K., Scaravilli, F., Altmann, D. R., Barker, G. J. & Miller, D. H. (2004). Magnetization transfer ratio and myelin in postmortem multiple sclerosis brain. *Ann Neurol* **56**, 407-15.
97. Sorensen, P. S., Gjerris, F., Ibsen, S. & Bock, E. (1983). Low cerebrospinal fluid concentration of brain-specific protein D2 in patients with normal pressure hydrocephalus. *J Neurol Sci* **62**, 59-65.
98. Strekalova, H., Buhmann, C., Kleene, R., Eggers, C., Saffell, J., Hemperly, J., Weiller, C., Muller-Thomsen, T. & Schachner, M. (2006). Elevated levels of neural recognition molecule L1 in the cerebrospinal fluid of patients with Alzheimer disease and other dementia syndromes. *Neurobiol Aging* **27**, 1-9.
99. Todaro, L., Puricelli, L., Gioseffi, H., Guadalupe Pallotta, M., Lastiri, J., Bal de Kier Joffe, E., Varela, M. & Sacerdote de Lustig, E. (2004). Neural cell adhesion molecule in human serum. Increased levels in dementia of the Alzheimer type. *Neurobiol Dis* **15**, 387-93.
100. Massaro, A. R. (1998). Are there indicators of remyelination in blood or CSF of multiple sclerosis patients? *Mult Scler* **4**, 228-31.
101. Ottervald, J., Franzen, B., Nilsson, K., Andersson, L. I., Khademi, M., Eriksson, B., Kjellstrom, S., Marko-Varga, G., Vegvari, A., Harris, R. A., Laurell, T., Miliotis, T., Matusevicius, D., Salter, H., Ferm, M. & Olsson, T. (2010). Multiple sclerosis: Identification and clinical evaluation of novel CSF biomarkers. *J Proteomics* **73**, 1117-32.
102. van Kammen, D. P., Poltorak, M., Kelley, M. E., Yao, J. K., Gurklis, J. A., Peters, J. L., Hemperly, J. J., Wright, R. D. & Freed, W. J. (1998). Further studies of elevated cerebrospinal fluid neuronal cell adhesion molecule in schizophrenia. *Biol Psychiatry* **43**, 680-6.
103. Poltorak, M., Wright, R., Hemperly, J. J., Torrey, E. F., Issa, F., Wyatt, R. J. & Freed, W. J. (1997). Monozygotic twins discordant for schizophrenia are discordant for N-CAM and L1 in CSF. *Brain Res* **751**, 152-4.
104. Poltorak, M., Khoja, I., Hemperly, J. J., Williams, J. R., el-Mallakh, R. & Freed, W. J. (1995). Disturbances in cell recognition molecules (N-CAM

and L1 antigen) in the CSF of patients with schizophrenia. *Exp Neurol* **131**, 266-72.

105. Vawter, M. P., Usen, N., Thatcher, L., Ladenheim, B., Zhang, P., VanderPutten, D. M., Conant, K., Herman, M. M., van Kammen, D. P., Sedvall, G., Garver, D. L. & Freed, W. J. (2001). Characterization of human cleaved N-CAM and association with schizophrenia. *Exp Neurol* **172**, 29-46.
106. Vawter, M. P., Hemperly, J. J., Freed, W. J. & Garver, D. L. (1998). CSF N-CAM in neuroleptic-naive first-episode patients with schizophrenia. *Schizophr Res* **34**, 123-31.
107. Vawter, M. P., Frye, M. A., Hemperly, J. J., VanderPutten, D. M., Usen, N., Doherty, P., Saffell, J. L., Issa, F., Post, R. M., Wyatt, R. J. & Freed, W. J. (2000). Elevated concentration of N-CAM VASE isoforms in schizophrenia. *J Psychiatr Res* **34**, 25-34.
108. Poltorak, M., Frye, M. A., Wright, R., Hemperly, J. J., George, M. S., Pazzaglia, P. J., Jerrels, S. A., Post, R. M. & Freed, W. J. (1996). Increased neural cell adhesion molecule in the CSF of patients with mood disorder. *J Neurochem* **66**, 1532-8.
109. Sjogren, M., Davidsson, P., Gottfries, J., Vanderstichele, H., Edman, A., Vanmechelen, E., Wallin, A. & Blennow, K. (2001). The cerebrospinal fluid levels of tau, growth-associated protein-43 and soluble amyloid precursor protein correlate in Alzheimer's disease, reflecting a common pathophysiological process. *Dement Geriatr Cogn Disord* **12**, 257-64.
110. Sjogren, M., Minthon, L., Davidsson, P., Granerus, A. K., Clarberg, A., Vanderstichele, H., Vanmechelen, E., Wallin, A. & Blennow, K. (2000). CSF levels of tau, beta-amyloid(1-42) and GAP-43 in frontotemporal dementia, other types of dementia and normal aging. *J Neural Transm* **107**, 563-79.
111. Teunissen, C. E., Dijkstra, C. D., Jasperse, B., Barkhof, F., Vanderstichele, H., Vanmechelen, E., Polman, C. H. & Bo, L. (2006). Growth-associated protein 43 in lesions and cerebrospinal fluid in multiple sclerosis. *Neuropathol Appl Neurobiol* **32**, 318-31.
112. Kim, J., Schafer, J. & Ming, G. L. (2006). New directions in neuroregeneration. *Expert Opin Biol Ther* **6**, 735-8.
113. Mueller, B. K., Mueller, R. & Schoemaker, H. (2009). Stimulating neuroregeneration as a therapeutic drug approach for traumatic brain injury. *Br J Pharmacol* **157**, 675-85.
114. Rolls, A., Shechter, R. & Schwartz, M. (2009). The bright side of the glial scar in CNS repair. *Nat Rev Neurosci* **10**, 235-41.
115. Giovannoni, G., Lai, M., Kidd, D., Thorpe, J. W., Miller, D. H., Thompson, A. J., Keir, G., Feldmann, M. & Thompson, E. J. (1997). Daily urinary neopterin excretion as an immunological marker of disease activity in multiple sclerosis. *Brain* **120 (Pt 1)**, 1-13.
116. Garde, A. H., Hansen, A. M., Kristiansen, J. & Knudsen, L. E. (2004). Comparison of uncertainties related to standardization of urine samples with volume and creatinine concentration. *Ann Occup Hyg* **48**, 171-9.
117. Lee, J. W. & Hall, M. (2009). Method validation of protein biomarkers in support of drug development or clinical diagnosis/prognosis. *J Chromatogr B Analyt Technol Biomed Life Sci* **877**, 1259-71.
118. Romeo, M. J., Espina, V., Lowenthal, M., Espina, B. H., Petricoin, E. F., 3rd & Liotta, L. A. (2005). CSF proteome: a protein repository for potential biomarker identification. *Expert Rev Proteomics* **2**, 57-70.

119. Nandapalan, V., Watson, I. D. & Swift, A. C. (1996). Beta-2-transferrin and cerebrospinal fluid rhinorrhoea. *Clin Otolaryngol Allied Sci* **21**, 259-64.
120. Kohn, M. I., Tanna, N. K., Herman, G. T., Resnick, S. M., Mozley, P. D., Gur, R. E., Alavi, A., Zimmerman, R. A. & Gur, R. C. (1991). Analysis of brain and cerebrospinal fluid volumes with MR imaging. Part I. Methods, reliability, and validation. *Radiology* **178**, 115-22.
121. Doherty, P. & Walsh, F. S. (1992). Cell adhesion molecules, second messengers and axonal growth. *Curr Opin Neurobiol* **2**, 595-601.
122. Palser, A. L., Norman, A. L., Saffell, J. L. & Reynolds, R. (2009). Neural cell adhesion molecule stimulates survival of premyelinating oligodendrocytes via the fibroblast growth factor receptor. *J Neurosci Res* **87**, 3356-68.
123. Kiss, J. Z. & Muller, D. (2001). Contribution of the neural cell adhesion molecule to neuronal and synaptic plasticity. *Rev Neurosci* **12**, 297-310.
124. Gerrow, K. & El-Husseini, A. (2006). Cell adhesion molecules at the synapse. *Front Biosci* **11**, 2400-19.
125. Jorgensen, O. S. & Bock, E. (1974). Brain specific synaptosomal membrane proteins demonstrated by crossed immunoelectrophoresis. *J Neurochem* **23**, 879-80.
126. Barbas, J. A., Chaix, J. C., Steinmetz, M. & Goridis, C. (1988). Differential splicing and alternative polyadenylation generates distinct NCAM transcripts and proteins in the mouse. *EMBO J* **7**, 625-32.
127. Murray, B. A., Owens, G. C., Prediger, E. A., Crossin, K. L., Cunningham, B. A. & Edelman, G. M. (1986). Cell surface modulation of the neural cell adhesion molecule resulting from alternative mRNA splicing in a tissue-specific developmental sequence. *J Cell Biol* **103**, 1431-9.
128. Noble, M., Albrechtsen, M., Moller, C., Lyles, J., Bock, E., Goridis, C., Watanabe, M. & Rutishauser, U. (1985). Glial cells express N-CAM/D2-CAM-like polypeptides in vitro. *Nature* **316**, 725-8.
129. Oltmann-Norden, I., Galuska, S. P., Hildebrandt, H., Geyer, R., Gerardy-Schahn, R., Geyer, H. & Muhlenhoff, M. (2008). Impact of the polysialyltransferases ST8SiaII and ST8SiaIV on polysialic acid synthesis during postnatal mouse brain development. *J Biol Chem* **283**, 1463-71.
130. Santoni, M. J., Barthels, D., Vopper, G., Boned, A., Goridis, C. & Wille, W. (1989). Differential exon usage involving an unusual splicing mechanism generates at least eight types of NCAM cDNA in mouse brain. *EMBO J* **8**, 385-92.
131. Krog, L., Olsen, M., Dalseg, A. M., Roth, J. & Bock, E. (1992). Characterization of soluble neural cell adhesion molecule in rat brain, CSF, and plasma. *J Neurochem* **59**, 838-47.
132. Dickson, G., Gower, H. J., Barton, C. H., Prentice, H. M., Elsom, V. L., Moore, S. E., Cox, R. D., Quinn, C., Putt, W. & Walsh, F. S. (1987). Human muscle neural cell adhesion molecule (N-CAM): identification of a muscle-specific sequence in the extracellular domain. *Cell* **50**, 1119-30.
133. Vawter, M. P. (2000). Dysregulation of the neural cell adhesion molecule and neuropsychiatric disorders. *Eur J Pharmacol* **405**, 385-95.
134. Vawter, M. P., Cannon-Spoor, H. E., Hemperly, J. J., Hyde, T. M., VanderPutten, D. M., Kleinman, J. E. & Freed, W. J. (1998). Abnormal expression of cell recognition molecules in schizophrenia. *Exp Neurol* **149**, 424-32.

135. Vawter, M. P., Hemperly, J. J., Hyde, T. M., Bachus, S. E., VanderPutten, D. M., Howard, A. L., Cannon-Spoor, H. E., McCoy, M. T., Webster, M. J., Kleinman, J. E. & Freed, W. J. (1998). VASE-containing N-CAM isoforms are increased in the hippocampus in bipolar disorder but not schizophrenia. *Exp Neurol* **154**, 1-11.
136. Chang, H., Bartlett, E. S., Patterson, B., Chen, C. I. & Yi, Q. L. (2005). The absence of CD56 on malignant plasma cells in the cerebrospinal fluid is the hallmark of multiple myeloma involving central nervous system. *Br J Haematol* **129**, 539-41.
137. Jaques, G., Auerbach, B., Pritsch, M., Wolf, M., Madry, N. & Havemann, K. (1993). Evaluation of serum neural cell adhesion molecule as a new tumor marker in small cell lung cancer. *Cancer* **72**, 418-25.
138. Lehmann, J. M., Riethmuller, G. & Johnson, J. P. (1989). MUC18, a marker of tumor progression in human melanoma, shows sequence similarity to the neural cell adhesion molecules of the immunoglobulin superfamily. *Proc Natl Acad Sci U S A* **86**, 9891-5.
139. Todaro, L., Christiansen, S., Varela, M., Campodonico, P., Pallotta, M. G., Lastiri, J., Sacerdote de Lustig, E., Bal de Kier Joffe, E. & Puricelli, L. (2007). Alteration of serum and tumoral neural cell adhesion molecule (NCAM) isoforms in patients with brain tumors. *J Neurooncol* **83**, 135-44.
140. Zocchi, M. R., Vidal, M. & Poggi, A. (1993). Involvement of CD56/N-CAM molecule in the adhesion of human solid tumor cell lines to endothelial cells. *Exp Cell Res* **204**, 130-5.
141. Zoltowska, A., Stepinski, J., Lewko, B., Serkies, K., Zamorska, B., Roszkiewicz, A., Izycka-Swieszewska, E. & Kruszewski, W. J. (2001). Neural cell adhesion molecule in breast, colon and lung carcinomas. *Arch Immunol Ther Exp (Warsz)* **49**, 171-4.
142. Olsen, M., Krog, L., Edvardsen, K., Skovgaard, L. T. & Bock, E. (1993). Intact transmembrane isoforms of the neural cell adhesion molecule are released from the plasma membrane. *Biochem J* **295 (Pt 3)**, 833-40.
143. Jorgensen, O. S. (1982). Fetal neural tube defects detected by rocket-on-line immunoelectrophoresis of amniotic fluids. *Clin Chim Acta* **124**, 179-86.
144. Nybroe, O., Linnemann, D. & Bock, E. (1989). Heterogeneity of soluble neural cell adhesion molecule. *J Neurochem* **53**, 1372-8.
145. Hinkle, C. L., Diestel, S., Lieberman, J. & Maness, P. F. (2006). Metalloprotease-induced ectodomain shedding of neural cell adhesion molecule (NCAM). *J Neurobiol* **66**, 1378-95.
146. Massaro, A. R. (2006). Serum and cerebrospinal fluid levels of neural cell adhesion molecule in multiple sclerosis. *Multiple Sclerosis Journal* **12**, S1-S228.
147. Massaro, A. R., De Pascalis, D., Carnevale, A. & Carbone, G. (2009). The neural cell adhesion molecule (NCAM) present in the cerebrospinal fluid of multiple sclerosis patients is unsialylated. *Eur Rev Med Pharmacol Sci* **13**, 397-9.
148. Massaro, A. R. (2002). The role of NCAM in remyelination. *Neurol Sci* **22**, 429-35.
149. Kapoor, R., Furby, J., Hayton, T., Smith, K. J., Altmann, D. R., Brenner, R., Chataway, J., Hughes, R. A. & Miller, D. H. (2010). Lamotrigine for neuroprotection in secondary progressive multiple sclerosis: a randomised, double-blind, placebo-controlled, parallel-group trial. *Lancet Neurol* **9**, 681-8.

150. Crowther, J. R. (2000). *The ELISA Guidebook* 2nd Revised Edition edit. Methods in Molecular Biology, 149, Humana Press.
151. Drake, P. M., Nathan, J. K., Stock, C. M., Chang, P. V., Muench, M. O., Nakata, D., Reader, J. R., Gip, P., Golden, K. P., Weinhold, B., Gerardy-Schahn, R., Troy, F. A., 2nd & Bertozzi, C. R. (2008). Polysialic acid, a glycan with highly restricted expression, is found on human and murine leukocytes and modulates immune responses. *J Immunol* **181**, 6850-8.
152. Langley, O. K., Aletsee-Ufrecht, M. C., Grant, N. J. & Gratzl, M. (1989). Expression of the neural cell adhesion molecule NCAM in endocrine cells. *J Histochem Cytochem* **37**, 781-91.
153. Langley, O. K. & Aunis, D. (1984). Ultrastructural immunocytochemical demonstration of D2-protein in adrenal medulla. *Cell Tissue Res* **238**, 497-502.
154. Moore, S. E. & Walsh, F. S. (1985). Specific regulation of N-CAM/D2-CAM cell adhesion molecule during skeletal muscle development. *EMBO J* **4**, 623-30.
155. Roth, J., Taatjes, D. J., Bitter-Suermann, D. & Finne, J. (1987). Polysialic acid units are spatially and temporally expressed in developing postnatal rat kidney. *Proc Natl Acad Sci U S A* **84**, 1969-73.
156. Diestel, S., Hinkle, C. L., Schmitz, B. & Maness, P. F. (2005). NCAM140 stimulates integrin-dependent cell migration by ectodomain shedding. *J Neurochem* **95**, 1777-84.
157. Hubschmann, M. V., Skladchikova, G., Bock, E. & Berezin, V. (2005). Neural cell adhesion molecule function is regulated by metalloproteinase-mediated ectodomain release. *J Neurosci Res* **80**, 826-37.
158. Thomaidou, D., Coquillat, D., Meintanis, S., Noda, M., Rougon, G. & Matsas, R. (2001). Soluble forms of NCAM and F3 neuronal cell adhesion molecules promote Schwann cell migration: identification of protein tyrosine phosphatases zeta/beta as the putative F3 receptors on Schwann cells. *J Neurochem* **78**, 767-78.
159. Thoulouze, M. I., Lafage, M., Schachner, M., Hartmann, U., Cremer, H. & Lafon, M. (1998). The neural cell adhesion molecule is a receptor for rabies virus. *J Virol* **72**, 7181-90.
160. Waksman, B. H. (1989). Multiple sclerosis. *Curr Opin Immunol* **1**, 733-9.
161. Reynolds, R., Roncaroli, F., Nicholas, R., Radotra, B., Gveric, D. & Howell, O. (2011). The neuropathological basis of clinical progression in multiple sclerosis. *Acta Neuropathol* **122**, 155-70.
162. Jadasz, J. J., Aigner, L., Rivera, F. J. & Kury, P. (2012). The remyelination Philosopher's Stone: stem and progenitor cell therapies for multiple sclerosis. *Cell Tissue Res* **349**, 331-47.
163. Huang, J. K. & Franklin, R. J. (2011). Regenerative medicine in multiple sclerosis: identifying pharmacological targets of adult neural stem cell differentiation. *Neurochem Int* **59**, 329-32.
164. Tomassini, V., Johansen-Berg, H., Jbabdi, S., Wise, R. G., Pozzilli, C., Palace, J. & Matthews, P. M. (2012). Relating Brain Damage to Brain Plasticity in Patients With Multiple Sclerosis. *Neurorehabil Neural Repair* **26**, 581-93.
165. Ronn, L. C., Pedersen, N., Jahnsen, H., Berezin, V. & Bock, E. (1997). Brain plasticity and the neural cell adhesion molecule (NCAM). *Adv Exp Med Biol* **429**, 305-22.

166. Povlsen, G. K., Ditlevsen, D. K., Berezin, V. & Bock, E. (2003). Intracellular signaling by the neural cell adhesion molecule. *Neurochem Res* **28**, 127-41.
167. Horstkorte, R., Schachner, M., Magyar, J. P., Vorherr, T. & Schmitz, B. (1993). The fourth immunoglobulin-like domain of NCAM contains a carbohydrate recognition domain for oligomannosidic glycans implicated in association with L1 and neurite outgrowth. *J Cell Biol* **121**, 1409-21.
168. Hubschmann, M. V. & Skladchikova, G. (2010). The role of ATP in the regulation of NCAM function. *Adv Exp Med Biol* **663**, 81-91.
169. Schmitt-Ulms, G., Legname, G., Baldwin, M. A., Ball, H. L., Bradon, N., Bosque, P. J., Crossin, K. L., Edelman, G. M., DeArmond, S. J., Cohen, F. E. & Prusiner, S. B. (2001). Binding of neural cell adhesion molecules (N-CAMs) to the cellular prion protein. *J Mol Biol* **314**, 1209-25.
170. Vutskits, L., Djebbara-Hannas, Z., Zhang, H., Paccaud, J. P., Durbec, P., Rougon, G., Muller, D. & Kiss, J. Z. (2001). PSA-NCAM modulates BDNF-dependent survival and differentiation of cortical neurons. *Eur J Neurosci* **13**, 1391-402.
171. Cao, J. P., Wang, H. J., Yu, J. K., Yang, H., Xiao, C. H. & Gao, D. S. (2008). Involvement of NCAM in the effects of GDNF on the neurite outgrowth in the dopamine neurons. *Neurosci Res* **61**, 390-7.
172. Nielsen, J., Gotfryd, K., Li, S., Kulahin, N., Soroka, V., Rasmussen, K. K., Bock, E. & Berezin, V. (2009). Role of glial cell line-derived neurotrophic factor (GDNF)-neural cell adhesion molecule (NCAM) interactions in induction of neurite outgrowth and identification of a binding site for NCAM in the heel region of GDNF. *J Neurosci* **29**, 11360-76.
173. Zhang, H., Vutskits, L., Calaora, V., Durbec, P. & Kiss, J. Z. (2004). A role for the polysialic acid-neural cell adhesion molecule in PDGF-induced chemotaxis of oligodendrocyte precursor cells. *J Cell Sci* **117**, 93-103.
174. Povlsen, G. K., Berezin, V. & Bock, E. (2008). Neural cell adhesion molecule-180-mediated homophilic binding induces epidermal growth factor receptor (EGFR) down-regulation and uncouples the inhibitory function of EGFR in neurite outgrowth. *J Neurochem* **104**, 624-39.
175. Cremer, H., Lange, R., Christoph, A., Plomann, M., Vopper, G., Roes, J., Brown, R., Baldwin, S., Kraemer, P., Scheff, S. & et al. (1994). Inactivation of the N-CAM gene in mice results in size reduction of the olfactory bulb and deficits in spatial learning. *Nature* **367**, 455-9.
176. Rolf, B., Bastmeyer, M., Schachner, M. & Bartsch, U. (2002). Pathfinding errors of corticospinal axons in neural cell adhesion molecule-deficient mice. *J Neurosci* **22**, 8357-62.
177. Loers, G., Aboul-Enein, F., Bartsch, U., Lassmann, H. & Schachner, M. (2004). Comparison of myelin, axon, lipid, and immunopathology in the central nervous system of differentially myelin-compromised mutant mice: a morphological and biochemical study. *Mol Cell Neurosci* **27**, 175-89.
178. Karpus, W. J. (2013). Inflammatory macrophage migration in experimental autoimmune encephalomyelitis. *Methods Mol Biol* **1013**, 161-9.
179. Wujek, J. R., Bjartmar, C., Richer, E., Ransohoff, R. M., Yu, M., Tuohy, V. K. & Trapp, B. D. (2002). Axon loss in the spinal cord determines permanent neurological disability in an animal model of multiple sclerosis. *J Neuropathol Exp Neurol* **61**, 23-32.

180. Kornek, B., Storch, M. K., Weissert, R., Wallstroem, E., Stefferl, A., Olsson, T., Linington, C., Schmidbauer, M. & Lassmann, H. (2000). Multiple sclerosis and chronic autoimmune encephalomyelitis: a comparative quantitative study of axonal injury in active, inactive, and remyelinated lesions. *Am J Pathol* **157**, 267-76.
181. Raine, C. S. & Wu, E. (1993). Multiple sclerosis: remyelination in acute lesions. *J Neuropathol Exp Neurol* **52**, 199-204.
182. Kerschensteiner, M., Bareyre, F. M., Buddeberg, B. S., Merkler, D., Stadelmann, C., Bruck, W., Misgeld, T. & Schwab, M. E. (2004). Remodeling of axonal connections contributes to recovery in an animal model of multiple sclerosis. *J Exp Med* **200**, 1027-38.
183. Diemel, L. T., Wolswijk, G., Jackson, S. J. & Cuzner, M. L. (2004). Remyelination of cytokine- or antibody-demyelinated CNS aggregate cultures is inhibited by macrophage supplementation. *Glia* **45**, 278-86.
184. Loughlin, A. J., Copelman, C. A., Hall, A., Armer, T., Young, B. C., Landon, D. N. & Cuzner, M. L. (1997). Myelination and remyelination of aggregate rat brain cell cultures enriched with macrophages. *J Neurosci Res* **47**, 384-92.
185. Loers, G. & Schachner, M. (2007). Recognition molecules and neural repair. *J Neurochem* **101**, 865-82.
186. Loughlin, A. J., Honegger, P., Woodroofe, M. N., Comte, V., Matthieu, J. M. & Cuzner, M. L. (1994). Myelin basic protein content of aggregating rat brain cell cultures treated with cytokines and/or demyelinating antibody: effects of macrophage enrichment. *J Neurosci Res* **37**, 647-53.
187. Jackson, S. J., Baker, D., Cuzner, M. L. & Diemel, L. T. (2004). Cannabinoid-mediated neuroprotection following interferon-gamma treatment in a three-dimensional mouse brain aggregate cell culture. *Eur J Neurosci* **20**, 2267-75.
188. Confavreux, C. & Vukusic, S. (2006). Age at disability milestones in multiple sclerosis. *Brain* **129**, 595-605.
189. Kremenchutzky, M., Rice, G. P., Baskerville, J., Wingerchuk, D. M. & Ebers, G. C. (2006). The natural history of multiple sclerosis: a geographically based study 9: observations on the progressive phase of the disease. *Brain* **129**, 584-94.
190. Papadopoulos, D., Pham-Dinh, D. & Reynolds, R. (2006). Axon loss is responsible for chronic neurological deficit following inflammatory demyelination in the rat. *Exp Neurol* **197**, 373-85.
191. Berry, M. & Riches, A. C. (1974). An immunological approach to regeneration in the central nervous system. *Br Med Bull* **30**, 135-40.
192. Xu, G., Nie, D. Y., Chen, J. T., Wang, C. Y., Yu, F. G., Sun, L., Luo, X. G., Ahmed, S., David, S. & Xiao, Z. C. (2004). Recombinant DNA vaccine encoding multiple domains related to inhibition of neurite outgrowth: a potential strategy for axonal regeneration. *J Neurochem* **91**, 1018-23.
193. Reynolds, R., Cenci di Bello, I., Dawson, M. & Levine, J. (2001). The response of adult oligodendrocyte progenitors to demyelination in EAE. *Prog Brain Res* **132**, 165-74.
194. Zwiers, H., Schotman, P. & Gispen, W. H. (1980). Purification and some characteristics of an ACTH-sensitive protein kinase and its substrate protein in rat brain membranes. *J Neurochem* **34**, 1689-99.

195. Jacobson, R. D., Virag, I. & Skene, J. H. (1986). A protein associated with axon growth, GAP-43, is widely distributed and developmentally regulated in rat CNS. *J Neurosci* **6**, 1843-55.
196. Fishman, M. C. (1996). GAP-43: putting constraints on neuronal plasticity. *Perspect Dev Neurobiol* **4**, 193-8.
197. Kristjansson, G. I., Zwiers, H., Oestreicher, A. B. & Gispen, W. H. (1982). Evidence that the synaptic phosphoprotein B-50 is localized exclusively in nerve tissue. *J Neurochem* **39**, 371-8.
198. Oestreicher, A. B., Zwiers, H., Schotman, P. & Gispen, W. H. (1981). Immunohistochemical localization of a phosphoprotein (B-50) isolated from rat brain synaptosomal plasma membranes. *Brain Res Bull* **6**, 145-53.
199. Oestreicher, A. B., Dekker, L. V. & Gispen, W. H. (1986). A radioimmunoassay for the phosphoprotein B-50: distribution in rat brain. *J Neurochem* **46**, 1366-9.
200. Benowitz, L. I., Perrone-Bizzozero, N. I., Finklestein, S. P. & Bird, E. D. (1989). Localization of the growth-associated phosphoprotein GAP-43 (B-50, F1) in the human cerebral cortex. *J Neurosci* **9**, 990-5.
201. Benowitz, L. I., Apostolides, P. J., Perrone-Bizzozero, N., Finklestein, S. P. & Zwiers, H. (1988). Anatomical distribution of the growth-associated protein GAP-43/B-50 in the adult rat brain. *J Neurosci* **8**, 339-52.
202. Coleman, P. D., Kazee, A. M., Lapham, L., Eskin, T. & Rogers, K. (1992). Reduced GAP-43 message levels are associated with increased neurofibrillary tangle density in the frontal association cortex (area 9) in Alzheimer's disease. *Neurobiol Aging* **13**, 631-9.
203. de la Monte, S. M., Ng, S. C. & Hsu, D. W. (1995). Aberrant GAP-43 gene expression in Alzheimer's disease. *Am J Pathol* **147**, 934-46.
204. Perrone-Bizzozero, N. I., Sower, A. C., Bird, E. D., Benowitz, L. I., Ivins, K. J. & Neve, R. L. (1996). Levels of the growth-associated protein GAP-43 are selectively increased in association cortices in schizophrenia. *Proc Natl Acad Sci U S A* **93**, 14182-7.
205. Yuan, Q., Hu, B., Su, H., So, K. F., Lin, Z. & Wu, W. (2009). GAP-43 expression correlates with spinal motoneuron regeneration following root avulsion. *J Brachial Plex Peripher Nerve Inj* **4**, 18.
206. Fernandes, K. J., Fan, D. P., Tsui, B. J., Cassar, S. L. & Tetzlaff, W. (1999). Influence of the axotomy to cell body distance in rat rubrospinal and spinal motoneurons: differential regulation of GAP-43, tubulins, and neurofilament-M. *J Comp Neurol* **414**, 495-510.
207. Kobayashi, N. R., Fan, D. P., Giehl, K. M., Bedard, A. M., Wiegand, S. J. & Tetzlaff, W. (1997). BDNF and NT-4/5 prevent atrophy of rat rubrospinal neurons after cervical axotomy, stimulate GAP-43 and Talpha1-tubulin mRNA expression, and promote axonal regeneration. *J Neurosci* **17**, 9583-95.
208. Madsen, J. R., MacDonald, P., Irwin, N., Goldberg, D. E., Yao, G. L., Meiri, K. F., Rimm, I. J., Stieg, P. E. & Benowitz, L. I. (1998). Tacrolimus (FK506) increases neuronal expression of GAP-43 and improves functional recovery after spinal cord injury in rats. *Exp Neurol* **154**, 673-83.
209. Schreyer, D. J. & Skene, J. H. (1991). Fate of GAP-43 in ascending spinal axons of DRG neurons after peripheral nerve injury: delayed accumulation and correlation with regenerative potential. *J Neurosci* **11**, 3738-51.

210. Mercken, M., Lubke, U., Vandermeeren, M., Gheuens, J. & Oestreicher, A. B. (1992). Immunocytochemical detection of the growth-associated protein B-50 by newly characterized monoclonal antibodies in human brain and muscle. *J Neurobiol* **23**, 309-21.
211. Oestreicher, A. B., van Duin, M., Zwiers, H. & Gispen, W. H. (1984). Cross-reaction of anti-rat B-50: characterization and isolation of a "B-50 phosphoprotein" from bovine brain. *J Neurochem* **43**, 935-43.
212. Chang, W. S., Friedman, C. H., Iqbal, M. A. & Neff, N. T. (1991). An ELISA assay for GAP-43. *J Neurosci Methods* **36**, 71-6.
213. Liu, Y. C., Chapman, E. R. & Storm, D. R. (1991). Targeting of neuromodulin (GAP-43) fusion proteins to growth cones in cultured rat embryonic neurons. *Neuron* **6**, 411-20.
214. Zuber, M. X., Strittmatter, S. M. & Fishman, M. C. (1989). A membrane-targeting signal in the amino terminus of the neuronal protein GAP-43. *Nature* **341**, 345-8.
215. Futatsumori-Sugai, M. & Tsumoto, K. (2010). Signal peptide design for improving recombinant protein secretion in the baculovirus expression vector system. *Biochem Biophys Res Commun* **391**, 931-5.
216. Bland, J. M. & Altman, D. G. (1986). Statistical methods for assessing agreement between two methods of clinical measurement. *Lancet* **1**, 307-10.
217. Oestreicher, A. B., De Graan, P. N., Gispen, W. H., Verhaagen, J. & Schrama, L. H. (1997). B-50, the growth associated protein-43: modulation of cell morphology and communication in the nervous system. *Prog Neurobiol* **53**, 627-86.
218. Strittmatter, S. M., Vartanian, T. & Fishman, M. C. (1992). GAP-43 as a plasticity protein in neuronal form and repair. *J Neurobiol* **23**, 507-20.
219. Schreyer, D. J., Andersen, P. L., Williams, K., Kosatka, I. & Truong, T. N. (1997). Quantitative analysis of GAP-43 expression by neurons in microcultures using cell-ELISA. *J Neurosci Methods* **72**, 137-45.
220. van der Neut, R., Oestreicher, A. B., Gispen, W. H. & Bar, P. R. (1990). The expression of B-50/GAP-43 during development of rat spinal neurons in culture is regulated by interneuronal contact. *Neurosci Lett* **109**, 36-41.
221. Walter, P., Gilmore, R. & Blobel, G. (1984). Protein translocation across the endoplasmic reticulum. *Cell* **38**, 5-8.
222. Zwiers, H., Verhaagen, J., van Dongen, C. J., de Graan, P. N. & Gispen, W. H. (1985). Resolution of rat brain synaptic phosphoprotein B-50 into multiple forms by two-dimensional electrophoresis: evidence for multisite phosphorylation. *J Neurochem* **44**, 1083-90.
223. Zakharov, V. V. & Mosevitsky, M. I. (2010). Oligomeric structure of brain abundant proteins GAP-43 and BASP1. *J Struct Biol* **170**, 470-83.
224. Kage, M., Ikemoto, A., Akiguchi, I., Kimura, J., Matsumoto, S., Kimura, H. & Tooyama, I. (1998). Primary structure of GAP-43 mRNA expressed in the spinal cord of ALS patients. *Neuroreport* **9**, 1403-6.
225. Barter, P. J., Caulfield, M., Eriksson, M., Grundy, S. M., Kastelein, J. J., Komajda, M., Lopez-Sendon, J., Mosca, L., Tardif, J. C., Waters, D. D., Shear, C. L., Revkin, J. H., Buhr, K. A., Fisher, M. R., Tall, A. R. & Brewer, B. (2007). Effects of torcetrapib in patients at high risk for coronary events. *N Engl J Med* **357**, 2109-22.
226. Thompson, I. M., Pauler, D. K., Goodman, P. J., Tangen, C. M., Lucia, M. S., Parnes, H. L., Minasian, L. M., Ford, L. G., Lippman, S. M.,

Crawford, E. D., Crowley, J. J. & Coltman, C. A., Jr. (2004). Prevalence of prostate cancer among men with a prostate-specific antigen level < or =4.0 ng per milliliter. *N Engl J Med* **350**, 2239-46.

227. Ahmed, A. A. & Brenton, J. D. (2005). Microarrays and breast cancer clinical studies: forgetting what we have not yet learnt. *Breast Cancer Res* **7**, 96-9.
228. Altman, D. G. & Lyman, G. H. (1998). Methodological challenges in the evaluation of prognostic factors in breast cancer. *Breast Cancer Res Treat* **52**, 289-303.
229. Panteghini, M. (2001). Recent approaches in standardization of cardiac markers. *Clin Chim Acta* **311**, 19-25.
230. Riley, R. D., Abrams, K. R., Sutton, A. J., Lambert, P. C., Jones, D. R., Heney, D. & Burchill, S. A. (2003). Reporting of prognostic markers: current problems and development of guidelines for evidence-based practice in the future. *Br J Cancer* **88**, 1191-8.
231. Jurewicz, A., Matysiak, M., Raine, C. S. & Selmaj, K. (2007). Soluble Nogo-A, an inhibitor of axonal regeneration, as a biomarker for multiple sclerosis. *Neurology* **68**, 283-7.
232. Lindsey, J. W., Crawford, M. P. & Hatfield, L. M. (2008). Soluble Nogo-A in CSF is not a useful biomarker for multiple sclerosis. *Neurology* **71**, 35-7.
233. Kuhle, J., Pohl, C., Mehling, M., Edan, G., Freedman, M. S., Hartung, H. P., Polman, C. H., Miller, D. H., Montalban, X., Barkhof, F., Bauer, L., Dahms, S., Lindberg, R., Kappos, L. & Sandbrink, R. (2007). Lack of association between antimyelin antibodies and progression to multiple sclerosis. *N Engl J Med* **356**, 371-8.
234. Baker, M. (2005). In biomarkers we trust? *Nat Biotechnol* **23**, 297-304.
235. Wilkins, M. R., Appel, R. D., Van Eyk, J. E., Chung, M. C., Gorg, A., Hecker, M., Huber, L. A., Langen, H., Link, A. J., Paik, Y. K., Patterson, S. D., Pennington, S. R., Rabilloud, T., Simpson, R. J., Weiss, W. & Dunn, M. J. (2006). Guidelines for the next 10 years of proteomics. *Proteomics* **6**, 4-8.
236. Blennow, K., Hampel, H., Weiner, M. & Zetterberg, H. (2010). Cerebrospinal fluid and plasma biomarkers in Alzheimer disease. *Nat Rev Neurol* **6**, 131-44.
237. Vincent, A. (1999). Antibodies to ion channels in paraneoplastic disorders. *Brain Pathol* **9**, 285-91.
238. Teunissen, C. E., Petzold, A., Bennett, J. L., Berven, F. S., Brundin, L., Comabella, M., Franciotta, D., Frederiksen, J. L., Fleming, J. O., Furlan, R., Hintzen, R. Q., Hughes, S. G., Johnson, M. H., Krasulova, E., Kuhle, J., Magnone, M. C., Rajda, C., Rejdak, K., Schmidt, H. K., van Pesch, V., Waubant, E., Wolf, C., Giovannoni, G., Hemmer, B., Tumani, H. & Deisenhammer, F. (2009). A consensus protocol for the standardization of cerebrospinal fluid collection and biobanking. *Neurology* **73**, 1914-22.
239. McShane, L. M., Altman, D. G., Sauerbrei, W., Taube, S. E., Gion, M. & Clark, G. M. (2006). REporting recommendations for tumor MARKer prognostic studies (REMARK). *Breast Cancer Res Treat* **100**, 229-35.
240. Bossuyt, P. M., Reitsma, J. B., Bruns, D. E., Gatsonis, C. A., Glasziou, P. P., Irwig, L. M., Lijmer, J. G., Moher, D., Rennie, D. & de Vet, H. C. (2003). Towards complete and accurate reporting of studies of diagnostic accuracy: The STARD Initiative. *Ann Intern Med* **138**, 40-4.

241. Schulz, K. F., Altman, D. G. & Moher, D. (2010). CONSORT 2010 statement: updated guidelines for reporting parallel group randomized trials. *Ann Intern Med* **152**, 726-32.
242. Bast, R. C., Jr., Lilja, H., Urban, N., Rimm, D. L., Fritsche, H., Gray, J., Veltri, R., Klee, G., Allen, A., Kim, N., Gutman, S., Rubin, M. A. & Hruszkewycz, A. (2005). Translational crossroads for biomarkers. *Clin Cancer Res* **11**, 6103-8.
243. Ioannidis, J. P. & Panagiotou, O. A. (2011). Comparison of effect sizes associated with biomarkers reported in highly cited individual articles and in subsequent meta-analyses. *JAMA* **305**, 2200-10.
244. Vandenbroucke, J. P. (2009). STREGA, STROBE, STARD, SQUIRE, MOOSE, PRISMA, GNOSIS, TREND, ORION, COREQ, QUOROM, REMARK... and CONSORT: for whom does the guideline toll? *J Clin Epidemiol* **62**, 594-6.
245. Seki, T. & Arai, Y. (1991). Expression of highly polysialylated NCAM in the neocortex and piriform cortex of the developing and the adult rat. *Anat Embryol (Berl)* **184**, 395-401.
246. Ng, S. C., de la Monte, S. M., Conboy, G. L., Karns, L. R. & Fishman, M. C. (1988). Cloning of human GAP-43: growth association and ischemic resurgence. *Neuron* **1**, 133-9.
247. Meiri, K. F., Pfenninger, K. H. & Willard, M. B. (1986). Growth-associated protein, GAP-43, a polypeptide that is induced when neurons extend axons, is a component of growth cones and corresponds to pp46, a major polypeptide of a subcellular fraction enriched in growth cones. *Proc Natl Acad Sci U S A* **83**, 3537-41.
248. Scalfari, A., Neuhaus, A., Degenhardt, A., Rice, G. P., Muraro, P. A., Daumer, M. & Ebers, G. C. The natural history of multiple sclerosis: a geographically based study 10: relapses and long-term disability. *Brain* **133**, 1914-29.
249. Doherty, P., Fruns, M., Seaton, P., Dickson, G., Barton, C. H., Sears, T. A. & Walsh, F. S. (1990). A threshold effect of the major isoforms of NCAM on neurite outgrowth. *Nature* **343**, 464-6.
250. Honegger, P. (1985). *biochemical differentiation in serum-free aggregating brain cell cultures*. Cell Culture in Neurosciences (Bollenstein, J. E. S., G., Ed.), Plenum Press, New York.